PASSIVE MICROWAVE ALGORITHM DEVELOPMENT AND EVALUATION

NASA GRANT NAGW-3944

ANNUAL REPORT

Year 1: April 1994–March 1995

Prepared 15 March 1995

PRINCIPAL INVESTIGATOR: Grant W. Petty
Department of Earth and Atmospheric Sciences
1397 CIVL Bldg.
Purdue University
West Lafayette, IN 47907
(317) 494-2544

NASA TECHNICAL MONITOR: Dr. James C. Dodge
Code YD
National Aeronautics and Space Administration
Washington, D.C. 20546

Scientific Objectives

(1) Thoroughly evaluate, both theoretically and empirically, and on identical terms, all available SSM/I retrieval algorithms for column water vapor, column liquid water, and surface wind speed. (2) Where both appropriate and feasible, develop, validate, and document satellite passive microwave retrieval algorithms that offer significantly improved performance compared with currently available algorithms. (3) Refine and validate a novel physical inversion scheme for retrieving rain rate over the ocean.

1. Progress Report

This report summarizes work accomplished or in progress during the first year of a three year grant.

1.1 Precipitation retrievals

The emphasis during the first year has been on the validation and refinement of the rain rate algorithm published by Petty (1994a,b) and on the analysis of independent data sets that can be used to help evaluate the performance of rain rate algorithms over remote areas of the ocean. The following summarizes relevant activities and results.

1.1.1 Individual validation efforts

Following both the 2nd Algorithm Intercomparison Project (AIP-2) and the WetNet 1st Precipitation Intercomparison Project (PIP-1), various aspects of the global performance of our over-ocean rain rate algorithm were further evaluated against a variety of sources, and any unambiguous problems we were able to detect were corrected.

In particular, we first verified that our screening procedures for classifying pixels as no-rain or possible-rain yielded realistic global distributions of precipitation frequency, as compared with surface ship-derived frequencies of precipitation. Surprisingly, the liquid water threshold we had previously specified on an ad hoc basis proved to be nearly optimal for reproducing climatological frequencies of light precipitation; therefore no adjustment was deemed necessary.

We recently extended the comparison with our ship-derived climatology to include all 10 algorithms for which latitude-time products had been submitted to the WetNet PIP-1 project. We found that, whereas most algorithms yielded acceptable distributions in the tropics and subtropics, only the Petty submission and the Olson submission (which was also based on the normalized polarization and scattering indices defined by Petty 1994) successfully reproduced the rather high frequency of light precipitation at latitudes poleward of 45°. This study, a preliminary draft of which is appended to this report, is now being written up for submission to a journal.

In addition, we tuned various details of the algorithm so as to eliminate the factor-of-two bias observed during PIP-1 in the monthly rainfall retrievals relative to the atoll gage totals. Because the apparent bias varied with the minimum number of atolls per 2.5° box that were included in the sample, a completely unambiguous bias determination and correction was not possible. Performance of the final tuned algorithm is summarized in Table 1.

Further validation work completed during the past year included comparison of instantaneous rain rate estimates with near-coincident over water radar data from Hualien, Taiwan. This intercomparison yielded several results of interest, many of which did not speak well for the usefulness of the radar data as "truth". On the positive side, instantaneous correlations over a long time period (10 July 1987 - 31 March 1988) were as high as 0.85 when the maximum range of the radar data used was restricted to 100 km (Fig. 1).

1.1.2 Participation in PIP-2

The latest in the PIP series is the 2nd Precipitation Intercomparison Project, which focused on instantaneous rain rate retrievals in over 100 swaths of SSM/I imagery, representing a variety of storm cases from around the world. As of this writing, analysis of the results is not complete, but preliminary tables of validation statistics relative to each of the individual swaths have been released.

Two products were submitted by the PI; one based on the full physical inversion ("Petty-1") and another based strictly on the scattering-based "first-guess" rain rate field ("Petty-2"). Fig. 2 depicts the number of over water cases (out of 56) for which each participating algorithm yielded a correlation coefficient of better than 0.5 with respect to the available validation data. Although the meaningfulness of the precise ranking is doubtful, on account of the very mixed quality of the validation data, it is noteworthy that the Petty submissions were among the top performers by this particular measure, suggesting that they were unusually successful in extracting instantaneous spatial patterns of rain rate from the SSM/I brightness temperatures.

1.1.3 Participation in AIP-3

The 3d Algorithm Intercomparison Project (AIP-3) is also now in its final analysis phase. This intercomparison focused on validation of algorithms against ship weather radar over the tropical Pacific during TOGA-COARE. Preliminary results have already been made available. As seen in Table 2, the Petty physical algorithm (PE1) exhibited the overall best correlation coefficient ($r = 0.757$) with respect to instantaneous rain rates pooled over all cruises and a common set of swaths, out of 47 submissions (including IR and mixed IR/microwave algorithms, as well as SSM/I only). This result again appears to confirm that the Petty algorithm does unusually well at responding directly to temporal and spatial variations in rainfall intensity in the tropics, which has been one of the principle aims of our algorithm development work.

Reliable evaluation of competing algorithms' absolute calibration in AIP-3 (and thus of RMS errors and biases) is proving to be less straightforward. 19 out of 47 submissions (including IR, SSM/I, and mixed, and including the Petty physical algorithm) yielded ratios of satellite to radar rain rate falling in the narrow interval 1.8–2.2, whereas only 4 had ratios near unity. This suggests that either the radar calibration is off by a factor of about two, or else there is an inexplicable tendency for 19 distinct algorithms, some of which have a long history of being tuned to gauges, to be out of calibration by almost exactly the same amount. Unless this question is clearly resolved in favor of the radar, we are reluctant to attribute much significant to the RMS differences or ratios computed in AIP-3.

are reluctant to attribute much significant to the RMS differences or ratios computed in AIP-3.

1.2 Other SSM/I Retrievals

In addition to the refinement and validation of the Petty rain rate algorithms, the objectives of the project include intercomparing and, where applicable, improving algorithms retrieving other variables from SSM/I data. To this end, 5-year sequences of global ship and island radiosonde data and of surface buoy winds have recently been purchased and are now being processed. These will be matched with SSM/I brightness temperatures to aid in a detailed empirical and theoretical exploration of the performance of a variety of retrieval techniques. In addition, new Ph.D. student Nitin Gautam intends to further explore applications of SSM/I retrievables (e.g., precipitable water, surface wind speed, etc.) to studies of air-sea interaction and the local global water cycle.

2. Highlights of project-related professional activities

- Seven journal publications were published or accepted for publication during the project year, three of which acknowledge major support from the present NASA grant or its immediate predecessor (NAGW-2984). An eighth manuscript, also supported by this grant, is nearing completion.
- M.S. student David R. Stettner (initially supported by NASA Grant NAGW-2984, subsequently by NAGW-3944) completed thesis entitled *Evaluation of an Over-Water Rain Rate Retrieval Algorithm for the SSM/I* (August, 1994). Excerpts of this thesis will be submitted for journal publication upon completion of AIP-3 and PIP-2 activities.
- Attended the 7th AMS Conference on Satellite Meteorology and Oceanography, in Monterey, June 1994, accompanied by the PI's three graduate students (Douglas K. Miller, Mark D. Conner, and David R. Stettner) Five conference papers were presented, four of which describe research supported by the present grant. Also served as Program Committee member and Session Chair for this conference.
- Appointed conference Co-Chair for the upcoming AMS 8th Conference on Satellite Meteorology and Oceanography (Atlanta, January 1996).
- Appointed to a 2-year term on the scientific advisory team for the WMO World Climate Research Program (WCRP) Global Precipitation Climatology Project (GPCP)
- Appointed to Steering Committee, NASA WetNet 3d Precipitation [Algorithm] Intercomparison Project (PIP-3).
- Participated in the NASA WetNet 2nd Precipitation Intercomparison Project (PIP-2).
- Participated in the GPCP 3d Algorithm Intercomparison Project (AIP-3); will attend the GPCP AIP-3 Results workshop in Melbourne, Australia; 27–30 March 1995.
- Participated in the NASA WetNet Workshop in Durham, NH, 13–15 February 1995.

3. NASA-supported publications during project year

3.1 Refereed

Petty, G.W., 1994: Physical retrievals of over-ocean rain rate from multichannel microwave imagery. Part I: Theoretical characteristics of normalized polarization and scattering indices. *Meteorol. Atmos. Phys.*, **54**, 79–100

Petty, G.W., 1994: Physical retrievals of over-ocean rain rate from multichannel microwave imagery. Part II: Algorithm implementation. *Meteorol. Atmos. Phys.*, **54**, 101–122

Wilheit, T., R. Adler, S. Avery, E. Barrett, P. Bauer, W. Berg, A. Chang, J. Ferriday, N. Grody, S. Goodman, C. Kidd, D. Kniveton, C. Kummerow, A. Mugnai, W. Olson, G. Petty, A. Shibata, E. Smith, R. Spencer, 1994: Algorithms for the retrieval of rainfall from passive microwave measurements. *Remote Sens. Rev.*, **11**, 163–194

Barrett, E.C., R.F. Adler, K. Arpe, P. Bauer, W. Berg, A. Chang, R. Ferraro, J. Ferriday, S. Goodman, Y. Hong, J. Janowiak, C. Kidd, D. Kniveton, M. Morrissey, W. Olson, G. Petty, B. Rudolf, A. Shibata, E. Smith, R. Spencer, 1994: The first WetNet Precipitation Intercomparison Project: Interpretation of results. *Remote Sens. Rev.*, **11**, 303–373

Petty, G.W., 1995: The status of satellite-based rainfall estimation over land. *Remote Sens. Environ.* **51**, 125–137

Petty, G.W., and D.K. Miller, 1995: Satellite microwave observations of precipitation correlated with intensification rate in extratropical oceanic cyclones. *Mon. Wea. Rev.* (to appear in May issue)

Petty, G.W., 1995: Frequencies and characteristics of global oceanic precipitation from shipboard present-weather reports. *Bull. Amer. Meteor. Soc.* (to appear in September issue)

Petty, G.W., 1995: An Intercomparison of Oceanic Precipitation Frequencies from 10 SSM/I Rain Rate Algorithms and Shipboard Present-Weather Reports. (in preparation for submission to *J. Appl. Meteor.*; draft enclosed)

3.2 Conference Papers

Petty, G.W., and D.R. Stettner, 1994: A new inversion-based algorithm for retrieval of over-water rain rate from SSM/I multichannel imagery. *7th Conference on Satellite Meteorology and Oceanography*, Monterey, California, 6–10 June.

Petty, G.W., A. Mugnai, and E.A. Smith, 1994: Reverse Monte Carlo simulations of microwave radiative transfer in realistic 3-D rain clouds. *7th Conference on Satellite Meteorology and Oceanography*, Monterey, California, 6–10 June.

Petty, G.W., 1994: Some regional characteristics of oceanic rainfall and their implications for satellite rainfall retrievals. *7th Conference on Satellite Meteorology and Oceanography*, Monterey, California, 6–10 June.

Petty, G.W., and M.D. Conner, 1994: Identification and classification of transient signatures in over-land SSM/I imagery. *7th Conference on Satellite Meteorology and Oceanography*, Monterey, California, 6–10 June.

Petty, G.W., and D.K. Miller, 1994: SSM/I rainfall indices correlated with deepening rate in extratropical cyclones. *7th Conference on Satellite Meteorology and Oceanography*, Monterey, California, 6–10 June. (invited paper)

Table 1. Comparison between Petty physical algorithm ocean rain rate retrievals, over 2.5° boxes, and tropical atoll monthly rainfall totals (from Stettner 1994, M.S. Thesis, Purdue University).

Min. Atolls	N	$\bar{R}_{atoll}$ (mm/month)	$\bar{R}_{est}$ (mm/month)	Ratio	r	RMS Diff.
			August, 1987			
1	35	228	204	0.893	0.769	119
2	9	271	256	0.944	0.790	103
3	6	256	277	1.08	0.940	69
			September, 1987			
1	31	179	152	0.816	0.815	76
2	9	221	193	0.861	0.926	62
3	6	242	197	0.813	0.948	71
			October, 1987			
1	37	213	191	0.788	0.752	101
2	10	272	227	0.835	0.759	111
3	6	253	241	0.952	0.951	59
			November, 1987			
1	37	232	189	0.814	0.712	101
2	10	236	181	0.767	0.656	113
3	6	163	158	0.969	0.872	77
			Pooled 4 Month Period			
1	143	221	181	0.833	0.766	102
2	38	251	214	0.852	0.776	100
3	24	228	218	0.955	0.912	69

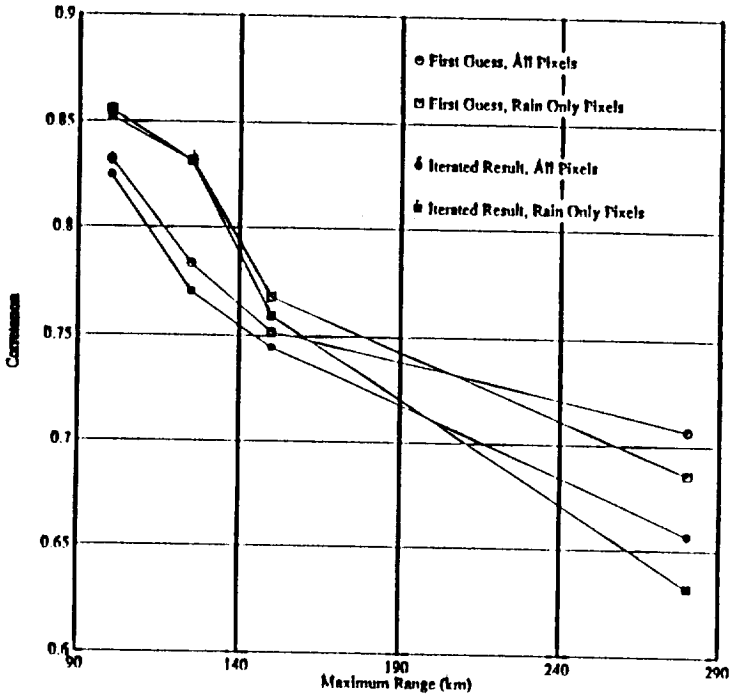

Figure 1. Correlation coefficients of satellite derived rain rate versus Hualien radar derived rain rate as function of maximum range, for 0.25° grid boxes. Total sample size varies from $N = 1669$ at $R_{max} = 100$ km to $N = 13030$ at $R_{max} = 280$. Corresponding rain only sample sizes are $N = 90$ and $N = 756$, respectively. Note steady increase in correlation coefficient as range limit becomes small. Note also decreasing difference in correlation for First Guess versus Iterated Result. (from Stettner 1994, M.S. Thesis, Purdue University).

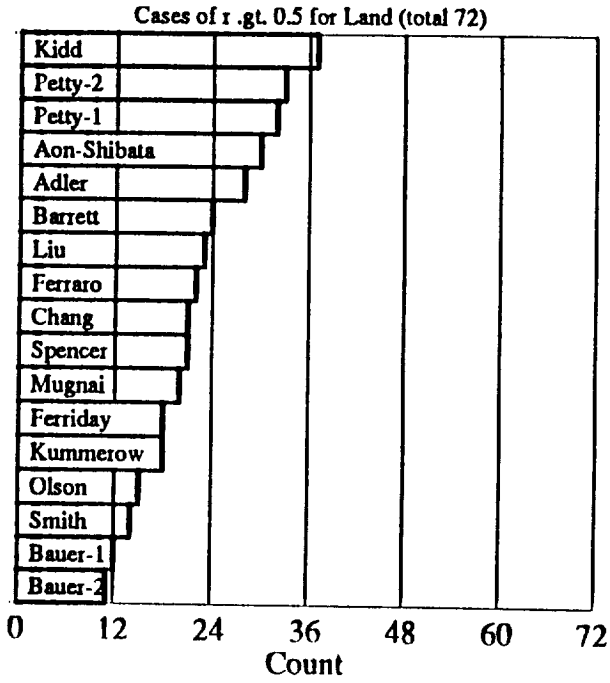

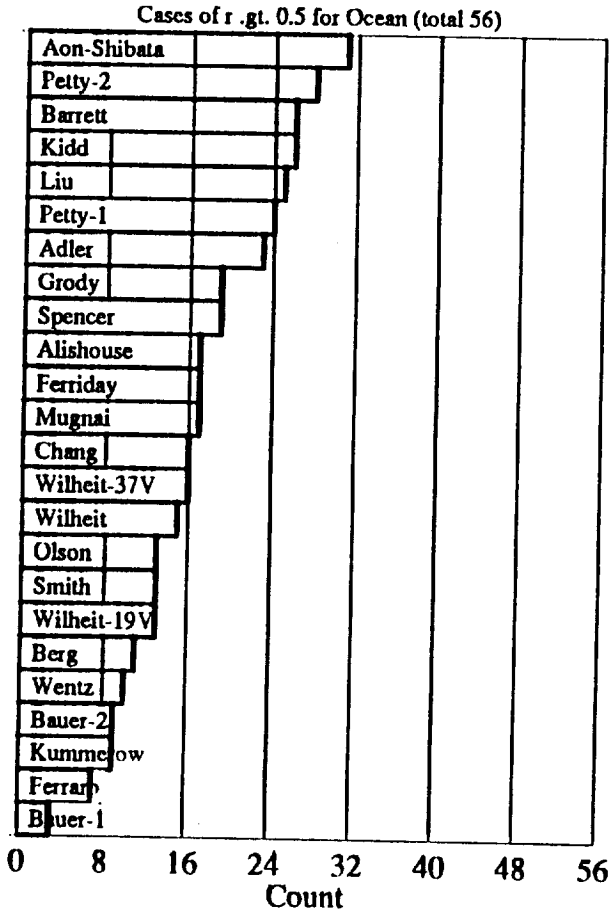

Figure 2. Preliminary correlation results for algorithms competing in PIP-2. Count represents the number of cases in each class (land or ocean) for which a given algorithm achieved a correlation coefficient $r > 0.5$ with validation data. Precise rankings should not be taken literally, because of wide variations in the quality of the validation data, as well as uneven representation of geographic regions and precipitation types.

Table 2. Preliminary validation results from AIP-3. Validation data is derived from shipboard radar in TOGA-COARE (Western Tropical Pacific). The Petty physical algorithm is identified as PE1.

Validation of Instantaneous Rainfall Rates - All Cruises, Common Set of Swaths

algo-rithm	correlation coeff.	slope	inter-cept (mm/h)	slope thru origin	Chi square	prob. distrs equal	POD	FAR	Heidke skill score	ratio diag-onals
GMS algorithms:										
AD5	0.520	1.181	0.133	1.268	2.840	1.000	0.278	0.052	0.182	0.533
AD6	0.504	1.174	0.156	1.276	3.480	1.000	0.276	0.050	0.182	0.533
AR1	0.484	0.996	0.331	1.214	2.197	1.000	0.461	0.157	0.213	0.504
AR2	0.484	0.664	0.221	0.809	0.781	1.000	0.461	0.157	0.210	0.504
AR3	0.521	0.797	0.159	0.902	0.686	1.000	0.350	0.078	0.206	0.530
GA1	0.536	1.286	0.369	1.529	8.603	1.000	0.790	0.614	0.112	0.317
GA2	0.543	1.317	0.345	1.545	8.487	1.000	0.752	0.543	0.129	0.347
HO1	0.473	0.402	0.080	0.456	0.022	1.000	0.681	0.412	0.193	0.455
KR1	0.567	2.270	0.594	2.661	43.238	0.056	0.757	0.509	0.149	0.363
KR2	0.516	1.200	0.386	1.454	1.398	1.000	0.618	0.301	0.186	0.437
MA1	0.329	0.865	0.301	1.063	8.644	1.000	0.528	0.236	0.182	0.459
MA2	0.311	0.447	0.157	0.550	0.602	1.000	0.424	0.140	0.183	0.492
MA3	0.310	0.456	0.156	0.559	0.332	1.000	0.424	0.140	0.183	0.492
MA4	0.324	0.660	0.229	0.811	2.050	1.000	0.528	0.236	0.182	0.460
MO1	0.457	0.716	0.265	0.891	1.487	1.000	0.444	0.155	0.187	0.487
Mixed GMS / SSM/I algorithms:										
AD2	0.487	1.359	0.113	1.433	58.321	0.002	0.177	0.014	0.147	0.535
AD3	0.531	1.129	0.131	1.215	2.066	1.000	0.320	0.075	0.198	0.533
AD4	0.508	1.212	0.120	1.291	10.680	1.000	0.301	0.056	0.189	0.533
BE2	0.539	0.725	0.176	0.841	0.173	1.000	0.427	0.139	0.202	0.503
BE3	0.535	1.003	0.271	1.181	0.639	1.000	0.550	0.248	0.188	0.457
JO1	0.423	1.308	0.099	1.373	27.069	0.620	0.195	0.019	0.146	0.530
KM2	0.511	0.821	0.182	0.940	0.751	1.000	0.370	0.085	0.214	0.532
KM4	0.502	1.116	0.112	1.189	6.746	1.000	0.301	0.056	0.189	0.534
SH1	0.562	1.212	0.043	1.245	10.141	1.000	0.420	0.284	0.124	0.456
SSM/I algorithms:										
AD1	0.601	2.061	-0.009	2.055	7.525	1.000	0.186	0.005	0.177	0.549
BA0	0.526	1.527	0.249	1.689	14.743	0.991	0.595	0.078	0.326	0.567
BA1	0.623	1.473	0.095	1.534	6.770	1.000	0.287	0.023	0.242	0.571
BA2	0.714	1.621	0.088	1.679	5.445	1.000	0.480	0.048	0.323	0.591
BA3	0.631	1.976	0.235	2.129	35.163	0.237	0.553	0.077	0.311	0.566
BA4	0.697	2.045	0.213	2.184	13.295	0.996	0.726	0.341	0.314	0.536
BA5	0.584	4.150	0.334	4.368	49.193	0.015	0.736	0.235	0.321	0.540
BE1	0.705	1.488	0.076	1.539	4.861	1.000	0.209	0.010	0.205	0.562
CH1	0.737	0.690	0.055	0.726	0.010	1.000	0.492	0.047	0.322	0.582
FE1	0.685	1.918	-0.016	1.908	6.534	1.000	0.282	0.009	0.245	0.581
FE2	0.625	2.214	0.030	2.233	3.961	1.000	0.343	0.019	0.274	0.578
FE3	0.644	1.629	0.092	1.689	24.228	0.762	0.335	0.013	0.279	0.577
FR1	0.598	1.974	0.206	2.107	49.417	0.014	0.427	0.042	0.294	0.578
IA1	0.730	3.545	0.615	3.944	51.603	0.008	0.902	0.607	0.135	0.321
IA2	0.739	3.644	0.578	4.018	63.475	0.000	0.873	0.611	0.120	0.309
KM1	0.609	1.535	0.037	1.559	3.090	1.000	0.339	0.016	0.252	0.567
LI1	0.674	1.238	-0.009	1.233	4.676	1.000	0.287	0.010	0.224	0.563
PE1	0.757	2.079	-0.004	2.076	12.615	0.998	0.376	0.018	0.295	0.590
PE2	0.716	2.054	0.043	2.083	25.099	0.720	0.362	0.017	0.279	0.583
PR1	0.495	2.351	0.190	2.474	24.357	0.756	0.699	0.145	0.347	0.573
SM1	0.368	0.876	0.150	0.974	10.326	1.000	0.377	0.027	0.278	0.579
SC1	0.634	1.352	0.052	1.385	1.361	1.000	0.571	0.093	0.323	0.571
WI1	0.621	0.877	0.013	0.886	1.187	1.000	0.169	0.009	0.174	0.552

To appear in Bull. Amer. Meteor. Soc.
~September 1995 issue

Frequencies and Characteristics of Global Oceanic Precipitation from Shipboard Present-Weather Reports

Grant W. Petty*

Purdue University
West Lafayette, Indiana

Abstract

Ship reports of present-weather obtained from the Comprehensive Ocean-Atmosphere Data Set (COADS) are analyzed for the period 1958–1991 in order to elucidate regional and seasonal variations in the climatological frequency, phase, intensity, and character of oceanic precipitation. Specific findings of note include the following:

(1) The frequency of thunderstorm reports, relative to all precipitation reports, is a strong function of location, with thunderstorm activity being favored within 1000–3000 km of major tropical and subtropical land masses, while being quite rare at other locations, even within the ITCZ.

(2) The latitudinal frequency of precipitation over the southern oceans increases steadily toward the Antarctic continent and shows relatively little seasonal variation. The frequency of convective activity, however, shows considerable seasonal variability, with sharp winter maxima occurring near 38° latitude in both hemispheres.

(3) Drizzle is the preferred form of precipitation in a number of regions, most of which coincide with known regions of persistent marine stratus and stratocumulus in the subtropical highs. Less well documented is the high relative frequency of drizzle in the vicinity of the equatorial sea surface temperature front in the Eastern Pacific.

(4) Regional differences in the temporal scale of precipitation events (e.g., transient showers vs. steady precipitation) are clearly depicted by way of the ratio of the frequency of precipitation at the observation time to the frequency of all precipitation reports, including precipitation during the previous hour.

The results of this study suggest that many current satellite rainfall estimation techniques may substantially underestimate the fractional coverage or frequency of precipitation poleward of 50° latitude and in the subtropical dry zones. They also draw attention to the need to carefully account for regional differences in the physical and spatial properties of rainfall when developing calibration relationships for satellite algorithms.

*Corresponding Author Address: Grant W. Petty, Earth and Atmospheric Sciences Dept., West Lafayette, IN, 47907-1397

1 Introduction

The need for an accurate global precipitation climatology over the ocean has been recognized for many decades, owing to the key role played by oceanic precipitation in the general circulation of the atmosphere and in the global hydrological and geochemical cycles. Because it is the average precipitation *rate* (or average monthly precipitation accumulation) that is of greatest direct importance for studies of atmospheric energetics and moisture budgets, most research to date has focused on the estimation of this variable by various means. Until recently, the only data available for this purpose was qualitative shipboard observations of present-weather, sometimes combined with rainfall measurements from nearby coastal and island sites.

A review of early efforts to develop a precipitation climatology over the ocean is given by Tucker (1961); these efforts generally involved highly indirect estimates based on extrapolation from nearby continents and on observations of sea surface salinity. Tucker proposed to estimate rainfall more directly from coded shipboard present-weather observations. He assigned calibrated weights (based on land station observations in the UK) to various categories of codes representing precipitation and analyzed 5 years of ocean weather ship observations to derive patterns of precipitation amount over the North Atlantic.

Later authors (Reed 1979; Reed and Elliott 1979; Dorman and Bourke 1979, 1981) refined and extended Tucker's method, emphasizing the correction of systematic regional differences in the average precipitation intensity associated with various reported present weather codes. Jaeger (1983) used a different approach, basing his estimates of monthly precipitation accumulation over the ocean in part on precipitation frequency estimates extracted from the *U.S. Navy Marine Climatic Atlas of the World* (U.S. Navy 1974–1979). These in turn were based on shipboard present-weather reports compiled for the period 1854–1978. Legates and Willmott (1990) have contributed the most recent oceanic precipita-

tion climatology, based partly on a synthesis of techniques and data from Dorman and Bourke (1979; 1981) and Jaeger (1983).

Regardless of the method used, all of the above authors recognized that the estimation of quantitative precipitation amounts from the qualitative weather reports transmitted by ships of opportunity is a task fraught with uncertainties. Even for well-trained observers, the visual classification of precipitation intensity and character by shipboard weather observers is an inherently subjective task, notwithstanding comprehensive reporting rules published by the World Meteorological Organization (e.g., WMO 1974) and other agencies overseeing the collection of synoptic reports. As pointed out in the *U.S. Navy Marine Climatic Atlas*, precipitation is "one of [the elements] most subject to error in interpretation. This derives from a number of causes such as coding practices, observers' preference for certain present-weather codes and other biases."

Furthermore, even if quantitative criteria could be rigorously adhered to in the reporting of rain intensity, the three conventional classifications "slight", "moderate", and "heavy" — bounded by nominal thresholds of 2.5 and 7.5 mm h^{-1} (0.1 and 0.3 inch h^{-1}) (FMH 1978) — are inadequate to characterize the wide range of observed precipitation intensities. For example, instantaneous rain rates in the tropics may regularly exceed 150 mm h^{-1}, or about twenty times the minimum intensity for classification as "heavy". Moreover, most of the operational present-weather codes transmitted in shipboard synoptic weather reports do not even distinguish between moderate and heavy precipitation; thus, intensity is classified only as "slight" or as "moderate or heavy". Clearly, the derivation of climatological rain rates from routine ship reports alone is impossible without recourse to rather sweeping assumptions (either explicit or implicit) concerning the underlying rain rate probability distribution function and its homogeneity in time and space.

Finally, the sampling density afforded by ships of opportunity is extremely poor, especially over the majority of the southern oceans. While the sampling may be adequate to derive climatological averages of certain precipitation properties (the focus of this paper), it is often inadequate for studying shorter-term variability in precipitation patterns over all but the most densely sampled areas.

Because of these and other problems with conventional reports over the ocean, there is now tremendous interest in extracting quantitative estimates of precipitation from satellite observations of the atmosphere. Already, operational visible, infrared, and microwave sensors are being utilized to derive experimental estimates of monthly precipitation over the global oceans, and considerable effort is being devoted to the validation and improvement of the respective algorithms (e.g., Arkin and Xie 1994; Barrett et al. 1994a). A Tropical Rainfall Measuring Mission (TRMM; Simpson et al. 1988), scheduled for launch in 1997, will be the first satellite mission dedicated primarily to the task of developing a rainfall climatology, in this case within the latitude belt between 30°N and 30°S.

While the quest for satellite-derived rainfall climatologies is propelled by the reasonable belief that satellites should eventually be able to provide information superior to that obtainable from sparse and mostly qualitative surface observations alone, the fact remains that competing satellite algorithms applied to the same sensor data continue to yield rather large (factor of two or more) differences in precipitation estimates; furthermore, the differences are regionally and latitudinally dependent (Barrett et al. 1994b). This observation suggests, among other things, that further calibration and validation of algorithms over a variety of regions, as well as improvements to the underlying retrieval strategies, may be necessary before satellite estimates of oceanic precipitation totals can be regarded as reliable everywhere. Unfortunately, the same lack of calibrated ocean surface rainfall data which motivates the development of satellite techniques also hampers their global calibration and validation.

The lack of surface rainfall measurements for calibrating satellite-derived rainfall totals is well-known and will undoubtedly remain a serious problem for some time to come; it is perhaps less widely recognized that current published satellite retrieval algorithms continue to differ markedly even in the retrieved *frequency* (or, equivalently, average fractional coverage) of precipitation over various regions. Given that passive microwave techniques in particular are often billed as "physically direct", the ability of these techniques to correctly classify a pixel as raining or not raining might be regarded as an even more fundamental measure of performance than the area-averaged magnitude of the retrieved rainfall.

Also, an unavoidable source of uncertainty in current-generation satellite estimates of global precipitation is that the techniques used are inherently sensitive to the macro- and microphysical characteristics of the precipitating cloud system — e.g., whether it is spatially extensive or localized, whether it is convective or stratiform, and whether it is warm-cloud precipitation dominated by colli-

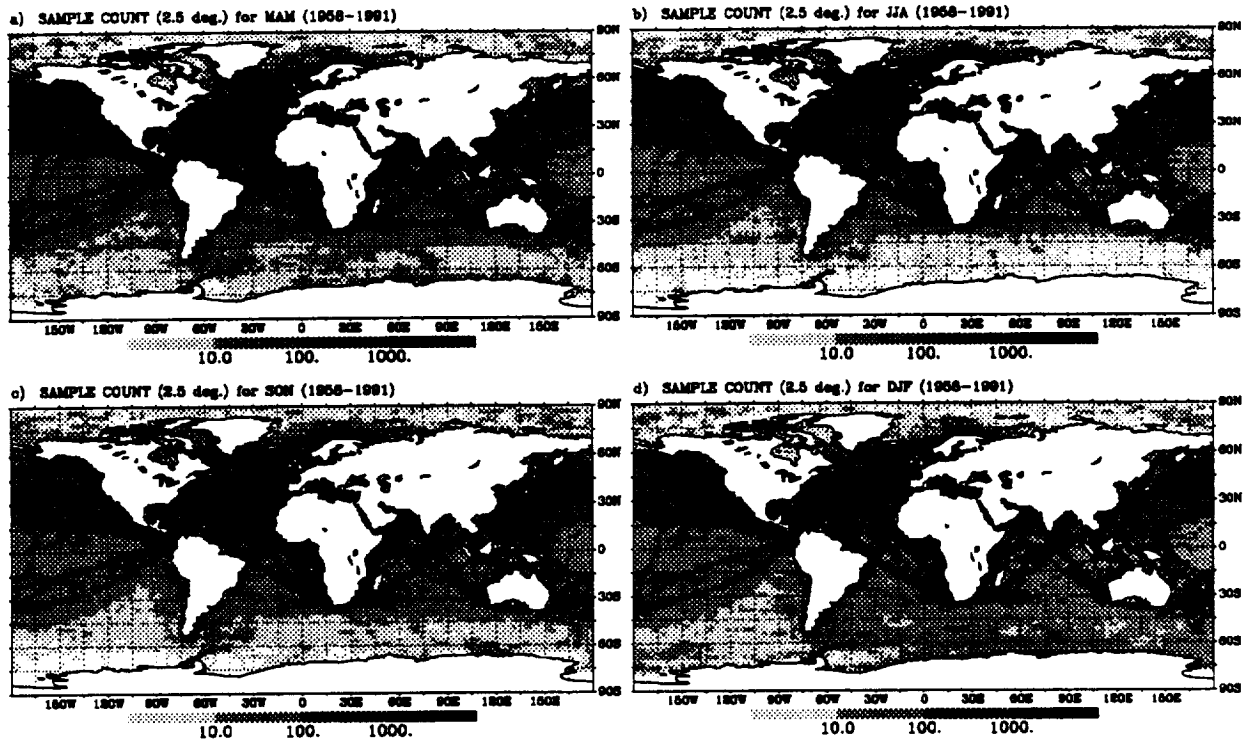

Fig. 1: Count per 2.5° latitude-longitude grid box of ship reports utilized in the analysis.

sion/coalescence of liquid water droplets or cold-cloud precipitation dominated by mixed-phase microphysics (Wilheit 1986). However, because relatively little is known about the spatial and seasonal variability of these characteristics over the global oceans, the actual potential for regionally or seasonally dependent biases in precipitation estimates has never been adequately assessed.

Thirdly, while liquid-equivalent precipitation *rate* is undoubtedly the variable of greatest interest for many purposes, other characteristics of precipitation over the ocean, such as frequency, phase, and physical character (e.g., convective vs stratiform) may be of considerable climatological interest in their own right, not least because of what they tell us about regional differences in the physical and dynamic processes of the atmosphere.

Motivated by all three of the considerations cited above, we have undertaken a statistical analysis of the present-weather codes reported by ships of opportunity over a 34 year period (1958–1991). The result of this analysis may be the most detailed global climatology to date of the frequency of occurrence and, especially, the general physical properties of global oceanic precipitation.

The surface precipitation frequencies derived herein should thus provide the first solid basis for evaluating the ability of satellite techniques to correctly estimate average fractional coverage by precipitation over remote ocean areas. Furthermore, the precipitation characteristics presented below should provide new insight into the regional and seasonal variability of precipitation properties to which satellite techniques are sensitive. Finally, it is felt that some characteristics of global precipitation elucidated in this analysis are indeed noteworthy from a purely climatological point of view.

2 COADS

The recent availability of the Comprehensive Ocean-Atmosphere Data Set (COADS; Woodruff et al. 1987) in digital form has made it convenient to analyze a long time series of global ship reports for the purpose of extracting climatological statistics. In this study, we employ the Compressed Marine Reports (CMR.5) format COADS product. The CMR record format provides for the archival of much of the same information as is contained in the standard ship synoptic code, including air and sea surface temperature, dewpoint, wind speed and direction, cloud coverage and type, and present-weather

Table 1: Definitions of present-weather codes pertaining to precipitation.

PW Code	Intensity, Phase, Char.	Description
Codes 00 to 49 indicate no precipitation at the station (e.g., ship) at time of observation.		
13	003	lightning visible, no thunder heard
14	200	precipitation within sight, not reaching the surface of the sea
15	000	precipitation within sight, reaching the surface of the sea, but more than 5 kilometers from the station
16	000	precipitation within sight, reaching the surface of the sea, near to, but not at the station
17	003	thunderstorm, but no precipitation at time of observation
18	003	squalls at or within sight of the station during the preceding hour or at time of observation
19	003	funnel cloud or waterspout at or within sight of the station during the preceding hour or at time of observation
Codes 20 to 29 refer to phenomena that occurred at the station during the preceding hour but not at time of observation.		
20	100	drizzle (not freezing) or snow grains
21	011	rain (not freezing)
22	021	snow
23	031	rain and snow or ice pellets, type (a)
24	031	freezing drizzle or freezing rain
25	012	shower of rain
26	022	shower of snow, or of rain and snow
27	003	shower of hail (ice pellets, type (b), snow pellets), or of rain and hail
29	003	thunderstorm (with or without precipitation)
Codes 50 to 99 indicate precipitation at the station at time of observation.		
50	111	drizzle, not freezing, intermittent, slight at time of observation
51	111	drizzle, not freezing, continuous, slight at time of observation
52	111	drizzle, not freezing, intermittent, moderate at time of observation
53	111	drizzle, not freezing, continuous, moderate at time of observation
54	111	drizzle, not freezing, intermittent, heavy (dense) at time of observation
55	111	drizzle, not freezing, continuous, heavy (dense) at time of observation
56	131	drizzle, freezing, slight
57	131	drizzle, freezing, moderate or heavy (dense)
58	211	drizzle and rain, slight
59	311	drizzle and rain, moderate or heavy
60	211	rain, not freezing, intermittent, slight at time of observation
61	211	rain, not freezing, continuous, slight at time of observation
62	311	rain, not freezing, intermittent, moderate at time of observation
63	311	rain, not freezing, continuous, moderate at time of observation
64	311	rain, not freezing, intermittent, heavy at time of observation
65	311	rain, not freezing, continuous, heavy at time of observation
66	231	rain, freezing, slight
67	331	rain, freezing, moderate or heavy

68	231	rain or drizzle and snow, slight
69	331	rain or drizzle and snow, moderate or heavy
70	221	intermittent fall of snowflakes, slight at time of observation
71	221	continuous fall of snowflakes, slight at time of observation
72	321	intermittent fall of snowflakes, moderate at time of observation
73	321	continuous fall of snowflakes, moderate at time of observation
74	321	intermittent fall of snowflakes, heavy at time of observation
75	321	continuous fall of snowflakes, heavy at time of observation
76	121	ice prisms (with or without fog)
77	121	snow grains (with or without fog)
78	121	isolated star-like snow crystals (with or without fog)
79	030	ice pellets, type (a) (sleet, U.S. definition)
80	212	rain shower, slight
81	312	rain shower, moderate or heavy
82	313	rain shower, violent
83	232	shower of rain and snow mixed, slight
84	332	shower of rain and snow mixed, moderate or heavy
85	222	snow shower, slight
86	322	snow shower, moderate or heavy
87	202	slight showers of snow pellets or ice pellets, type (b), with or without rain or rain and snow mixed
88	302	moderate or heavy showers of snow pellets or ice pellets, type (b), with or without rain or rain and snow mixed
89	303	slight showers of hail, with or without rain or rain and snow mixed, not associated with thunder
90	303	moderate or heavy showers of hail, with or without rain or rain and snow, mixed, not associated with thunder
91	213	slight rain at time of observation, thunderstorm during preceding hour but not at time of observation
92	313	moderate or heavy rain at time of observation, thunderstorm during preceding hour but not at time of observation
93	203	slight snow, or rain and snow mixed, or hail, at time of observation with thunderstorm during the preceding hour but not at time of observation
94	303	moderate or heavy snow, or rain and snow mixed, or hail, at time of observation with thunderstorm during the preceding hour but not at time of observation
95	303	thunderstorm, slight or moderate, without hail, but with rain and/or snow at time of observation
96	303	thunderstorm, slight or moderate, with hail at time of observation
97	303	thunderstorm, heavy, without hail but with rain and/or snow at time of observation
98	303	thunderstorm combined with dust storm or sandstorm at time of observation
99	303	thunderstorm, heavy, with hail at time of observation

codes. In addition, quality control flags are included which indicate whether certain variables fall within the normal climatological range associated with the time and location of the report. Details of the COADS record formats and archive contents may be found in the document *Comprehensive Ocean-Atmosphere Data Set: Release 1* (ERL 1985).

For the purpose of this study, the present-weather code is the variable of primary interest. Other variables are employed here strictly for screening purposes.

The majority of records contained in the COADS data set are derived from routine marine synoptic reports of observations taken at the standard times of 00, 06, 12, and 18 UTC. A smaller number are taken at intermediate 3-hourly intervals, or at other non-standard times. Some COADS reports are derived from unmanned sources (e.g., buoys), but these constitute a small fraction of the total and play no role in this study owing to the absence of present-weather information.

Table 2: Precipitation intensity, phase, and character class definitions.

Code		Description
	Intensity Classes	
0	=	indeterminate
1	=	extremely light (e.g., drizzle) intensity
2	=	light
3	=	moderate/heavy
	Phase Classes	
0	=	indeterminate, or hail
1	=	liquid
2	=	snow
3	=	transition (mixed phase or freezing precipitation, or sleet)
	Character Classes	
0	=	indeterminate
1	=	steady/intermittent
2	=	showery
3	=	strong convection/thunderstorm

2.1 Present-Weather Codes

The synoptic present-weather (PW) element of a COADS record consists of a two-digit code ranging from 00 to 99. The selection of a single unique code to represent observed conditions at a particular time and place is accomplished via a well-defined set of criteria and priorities published by the World Meteorological Organization (WMO 1974). Of the 100 possible PW codes, 66 are associated — either explicitly or by strong implication — with precipitation. For clarity and convenience in the following discussion, the definitions of these 66 codes are reproduced in Table 1.

Table 3: Precipitation PW code groups.

Group	Intensity, Phase, Char.	PW Codes
1	000	15,16
2	003	13,17,18,19,27,29
3	011	21
4	012	25
5	021	22
6	022	26
7	030	79
8	031	23,24
9	100	20
10	111	50,51,52,53,54,55
11	121	76,77,78
12	131	56,57
13	200	14
14	202	87
15	203	89,93
16	211	58,60,61
17	212	80
18	213	91
19	221	70,71
20	222	85
21	231	66,68
22	232	83
23	302	88
24	303	90,94,95,96,97,98,99
25	311	59,62,63,64,65
26	312	81
27	313	82,92
28	321	72,73,74,75
29	322	86
30	331	67,69
31	332	84

If the specific conditions represented by more than one PW code are consistent with the observed conditions, it is generally the PW code with the higher numerical value that must be reported. This implies that, for example, the reporting of fog at the station (codes 40–49) would take precedence over the reporting of past precipitation (codes 20–29) or of precipitation and related phenomena observed in the vicinity of, but not necessarily at, the station at the time of observation (codes 13–19). Also, the reporting of current precipitation in any form (codes

50 and greater) takes precedence of the reporting of past or nearby thunderstorm or lightning activity. The potential for minor statistical biases arising from these rules of precedence should be kept in mind throughout the remainder of this paper.

Many of the PW code definitions differ in rather subtle respects from one another. For the sake of determining the gross climatological characteristics of over-ocean precipitation, the 66 codes were therefore grouped according to precipitation intensity, phase, and character. Within each of these three categories, each PW code was assigned to one of four possible classes, the definitions of which appear in Table 2.

The results of this classification are summarized in Table 3. Note that while a total of 64 combinations of intensity, phase, and character codes are theoretical possible, only 31 of these are actually represented by the available PW codes. For example, there are no "1X2" or "1X3" categories (where "X" here implies a "wild card" value) because no PW code has been assigned to the nonexistent case of drizzle-intensity precipitation having a showery or strongly convective character.

Most PW codes receiving an intensity classification of "0" ("indeterminate") correspond to precipitation within sight of but not at the station at the time of observation or else precipitation observed at the station during the hour preceding the observation time but not at the time of observation.

In a departure from the above rule, PW code 14 (virga) was assigned a nominal intensity classification of "2", since the precipitation must be intense enough to be visible to a surface observer yet light enough to evaporate before reaching the surface. As the sole PW code in Table 1 which is clearly unassociated with *surface* precipitation, its occurrence is not considered in the statistics presented in this paper. However, virga does represent the end product of precipitation processes, and its occurrence has therefore been tabulated here together with the other forms of precipitation for possible use in future studies.

2.2 Study Sample

A 34-year period of COADS data was analyzed for this study, covering the years 1958 through 1991. Although the COADS archive extends as far back as 1854, the starting year of 1958 was subjectively chosen so as to minimize uncertainties associated with nonstandard or variable reporting procedures during earlier periods (Reed 1979).

The total sample count of usable ship reports per 2.5° latitude/longitude box is depicted graphically in Fig. 1 for each season. Major shipping lanes are clearly delineated by large sample counts; by contrast, large areas of the southern hemisphere, particularly the southeastern Pacific, were only rarely sampled. In particular, during the southern hemisphere winter, ship reports south of 45°S are remarkably scarce, with a great many gridboxes having never been sampled at all during the entire 34-year period.

A small number of reports (generally no more than ~1 per grid box) in the COADS data base were found to be associated with landlocked locations (not depicted in Fig. 1). As discussed by Warren et al. (1988), these reports, along with a comparable number of those appearing over the north polar ice cap, presumably reflect errors in the coding or transmission of the ship's location. Assuming that such spurious reports are scattered more or less uniformly over the globe, it seems likely that a similar number of the over-water reports within in any given gridbox are likely to be mislocated as well. This in turn implies that statistics may not be reliable unless the total sample size in the grid box is much greater than the random contribution from mislocated reports.

2.3 Data Limitations

In past studies, considerable attention has been given to the so-called "fair weather bias" (Quayle 1974), attributed to the tendency of ships to avoid foul weather and/or take fewer observations during periods of foul weather. A partially counteracting "foul weather bias" may arise from the tendency of certain ships that report weather only intermittently to do so mainly when the weather is deemed significant. Another foul weather bias is hypothesized to result from ships slowing down in rough seas and thus spending more time within the stormy region. Warren et al. (1988) examined the above fair/foul weather biases primarily from the standpoint of cloud observations and found that the fair weather bias appears to prevail but is small.

With respect to the present-weather statistics derived in this study, the following additional biases are felt by the author to be of similar potential importance:

(1) Systematic misclassification of precipitation type by inadequately trained observers — e.g., drizzle reported as rain, or vice versa; intermittent stratiform rain reported as rain showers; ice pellets reported as hail, etc. In particular, characterizations of precipitation intensity are undoubtedly made in the field at least partly by reference to what the

crew member has commonly experienced in the past. For example, observers accustomed to heavy tropical downpours may be more likely to classify as "light" a rain intensity which would earn the classification "moderate" from an observer accustomed to conditions in the North Atlantic.

(2) Day/night bias — fewer observations are made at night, and those observations submitted may be less reliable, particularly as regards present-weather codes requiring visual identification — e.g., virga (code 14) or precipitation within sight of but not at the station (codes 15 and 16). However, distant lightning (code 13) is probably reported more frequently at night. Partly because of the difficulty of accurately accounting for day/night biases, this study does not attempt to examine diurnal variations in the reporting of various PW codes (see, however, Hahn et al. 1994, who did calculate the diurnal phase and amplitude of the frequency of local precipitation reports from ships and found a relative day-night difference on the order of 6% globally).

(3) Mislocations — in data sparse regions such as the far southern oceans, a significant fraction of the available data may consist of mislocated reports from more densely sampled regions.

In this study, no attempt is made to account for any of the above possible errors, mainly because there is still no reliable, globally applicable basis for doing so. The practice of arbitrarily including past precipitation reports (i.e., precipitation during the past hour but not at the time of observation) in previous climatologies of precipitation frequency (e.g., U.S. Navy, 1974–1979) in order to offset the perceived underreporting of precipitation is difficult to justify, since the statistical occurrence of such reports, relative to present precipitation reports, is highly variable according to region and reflects real differences in the temporal character of the precipitation (see Section 4d). There is no reason to expect that the artificial (and variable) increase in apparent precipitation frequency obtained in this way is correlated in any way with the true reporting bias.

While some effort has been made to screen out obviously faulty or unreliable reports, based in part on other reported variables, all frequencies presented below should be interpreted in light of the potential for the above noted biases.

3 Processing

The initial phase of the analysis of the 34-year COADS data set entailed the simple tabulation of PW classes within each 2.5° latitude/longitude gridbox over the entire globe for each of the 12 calendar months, resulting in a $144 \times 72 \times 12 \times 31$ histogram of raw counts. Also computed was the corresponding $144 \times 72 \times 12$ array containing the total count of valid PW reports.

In order for a report to be included in the above tabulation, two criteria had to be met. First, the total cloud amount reported had to be a legitimate non-missing value (0–8 for oktas of the celestial covered by cloud, or 9 for sky obscured). This limits the sample to reports made by human observers taking visual observations of sky and weather conditions and thus mitigates an important ambiguity in the interpretation of a missing value for the PW code ("//" in the original synoptic report). According to new WMO rules implemented in 1982, a missing PW code can imply either (1) that no present-weather observation was possible (as is the case for all buoy reports) or (2) that the present-weather was observed by a human observer but that it involved no reportable meteorological phenomena and that sky cover development over time was not determined (note: after 1985, a station/weather indicator code was added to the WMO code form for ships to distinguish between the two cases; unfortunately this indicator is not available in the COADS CMR data record format). The requirement that the total cloud cover be reported in some form largely eliminates reports of the first type from the sample, thus reducing the likelihood of a significant low bias in computed precipitation frequencies.

The second condition was that the sea surface temperature quality flag in the COADS record have a value less than or equal to zero. This criterion eliminated reports in which the reported sea surface temperature deviates by more than 2.8σ from the smoothed median sea surface temperature for that month and region, where σ is the smoothed upper or lower median deviation (for details, see Supplement C in the COADS Release 1 documentation - ERL 1985). The intent of this screening procedure was to reduce the number of mislocated reports in the data set, since the reported sea surface temperature in many such cases will be inconsistent with the reported location. Undoubtedly, a few valid reports are also discarded on this basis; however, it is assumed that the potential bias introduced by discarding occasional valid reports is likely to be much smaller than that contributed by the inadvertent inclusion of grossly mislocated reports.

Once gridded histograms of PW groups are derived, absolute and relative frequencies of various classes of precipitation reports may be examined in detail. In general, two types of statistics are considered here: (1) the frequency of certain classes of pre-

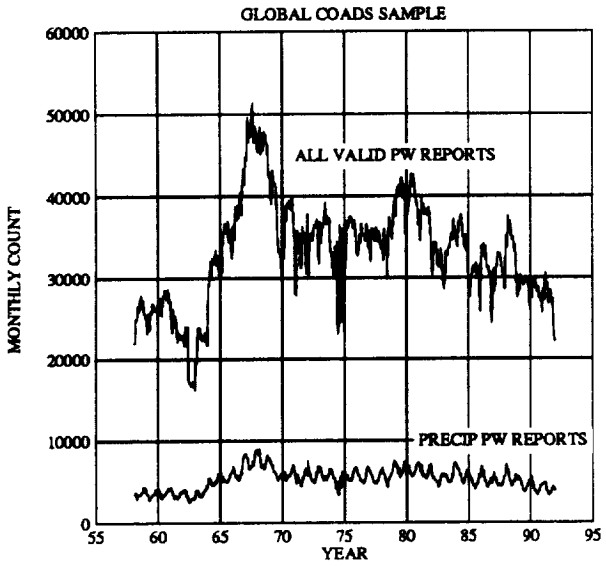

Fig. 2: Monthly count of global shipboard present-weather reports and precipitation reports utilized in the analysis.

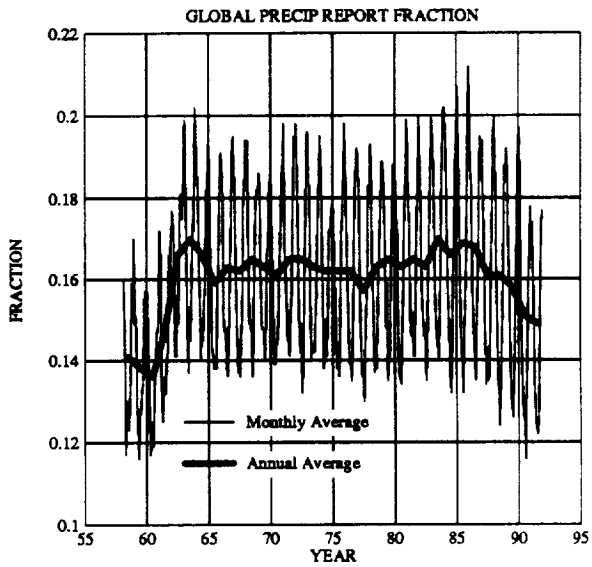

Fig. 3: Global fraction of valid present-weather reports indicating precipitation.

cipitation reports relative to all valid PW reports; and (2) the frequency of certain classes of precipitation reports relative to a more general class of precipitation. The first type of statistic may be interpreted as an absolute climatological frequency of a certain class of precipitation, while the second type may be interpreted as the predominance of a certain class of precipitation (e.g. snow) conditioned on the occurrence of a broader class (e.g., all precipitation).

4 Results

4.1 Global Statistics

4.1.1 Reporting of precipitation

The 34-year period of data analyzed yielded a total of 13.45×10^6 valid present-weather reports over the entire globe, of which 2.16×10^6, or 16.0%, corresponded to one of the 66 precipitation codes appearing in Table 1. A time series of absolute counts per month is depicted graphically in Fig. 2. Of note here are substantial (up to a factor of $\sim$2) fluctuations in the total sample size, with a minimum near 1963 and a maximum near 1967.

Figure 3 depicts the temporal dependence of the global fraction of PW reports representing precipitation. On a monthly basis, a pronounced annual cycle is seen which peaks in December and January and reaches a minimum in July. The magnitude and

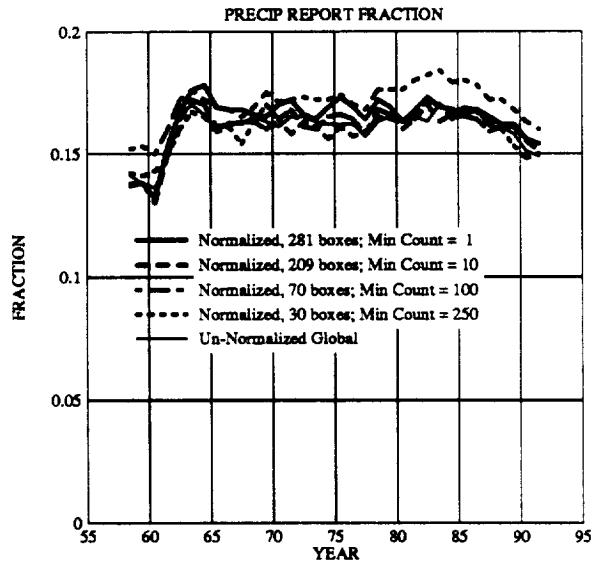

Fig. 4: Global fraction of valid present-weather reports indicating precipitation, calculated first as averages over season and over 10° latitude-longitude boxes and then combined to yield yearly global averages. Each curve corresponds to a different minimum seasonal sample size required in order for a latitude-longitude box to be included in the global average. The non-normalized global fraction is reproduced from Fig. 3 for comparison.

phase of this cycle is chiefly due to the overwhelming predominance of ship reports from the North Atlantic and North Pacific oceans, so that the unnormalized precipitation frequencies appearing in Fig. 3 reflect mainly the seasonal cycle of precipitation in the northern middle latitudes.

An unexpected feature in Fig. 3 is a sharp increase (from ~0.14 to ~0.16) in the yearly average reporting of precipitation between 1960 and 1963 and a general downward trend again after about 1986. Candidate explanations for these differences include (1) systematic changes with time in the geographic or seasonal distribution of ship reports, (2) changes in shipboard present-weather reporting habits or procedures, (3) variations in the procedures for subsequent processing and reformating of weather reports taken from ship logs, and/or (4) actual long-term trends in precipitation frequency. While the last of these hypotheses cannot be dismissed out of hand, it seemed prudent to first seek an explanation among the first three.

To examine the first possibility, separate time series of precipitation frequency were computed for each 10° latitude-longitude box that always yielded a specified minimum number of reports per season over the entire 34 year period. These were then averaged both in space and over the annual cycle so as to yield an area-normalized yearly average precipitation frequency. The resulting frequency curves (Fig. 4) do not differ appreciably from the unnormalized precipitation frequency, implying that large-scale geographic or seasonal shifts in the distribution of reports cannot be responsible for the sharp changes in the frequency of precipitation reports.

As regards (2), the only official change in reporting requirements known to the author to have been implemented during the period in question occurred in 1982, after which present weather could be coded as "missing" if there was no reportable weather. This year does not appear to be associated with a significant change in the reported frequency depicted in Fig. 4, though the downward trend beginning near 1987 might reflect a belated response by shipboard observers to the new rules. As noted earlier, an attempt was made to minimize the impact of the rule change by including only reports for which cloud information was reported.

Alternative (3) seems to be the most plausible of the possible explanations for the behavior of the precipitation frequency prior to 1964, as that year coincides with establishment of the International Maritime Meteorological exchange of ship logbook data in standardized formats under WMO Resolution 35. Earlier data were obtained in card decks

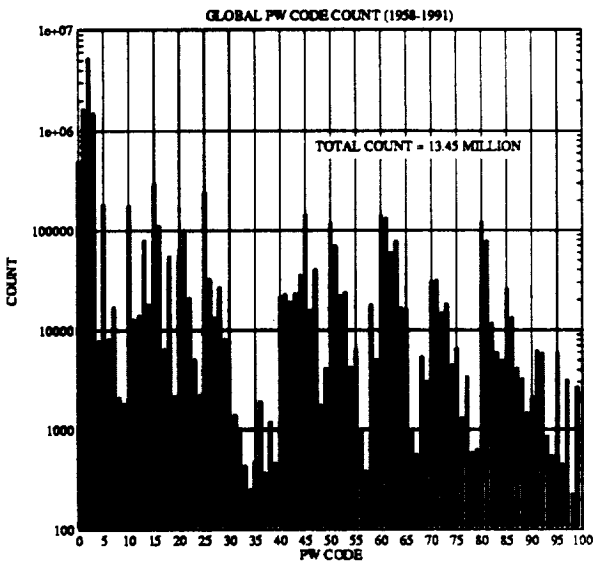

Fig. 5: Global histogram of all present-weather codes reported by ships during the period 1958–1991.

in non-standard formats from various countries and sources. Therefore, the apparent bias could possibly be an artifact of variations in processing and reformatting of original data to fit into the original card decks, or subsequent reprocessing to consolidate all the original card decks into the merged data set that eventually was incorporated into COADS. An in-depth study of the data in each deck, and any surviving documentation, would probably be required to help answer this question more definitively (S. Woodruff and J. Elms, pers. comm.).

The total relative uncertainty that the apparent bias, averaged over the full period, introduces into our results is of the order of 2%. Consequently, the option of restricting the analysis to the shorter, but more homogeneous, period from 1964 to 1988 was rejected in favor of retaining the larger sample offered by the original 34 year period.

4.1.2 Reporting of PW codes and categories

Figures 5 and 6, respectively, depict the total counts of each PW code (including non-precipitating codes) and of each precipitation group encountered in this period. Apart from codes 1–3, which imply the absence of any significant weather and which account for 61% of the total reports, the single most common code is 15 (precipitation observed at a distance but not at the station at the time of the observation; 2.98×10^5 reports or 2.2% of the total) followed

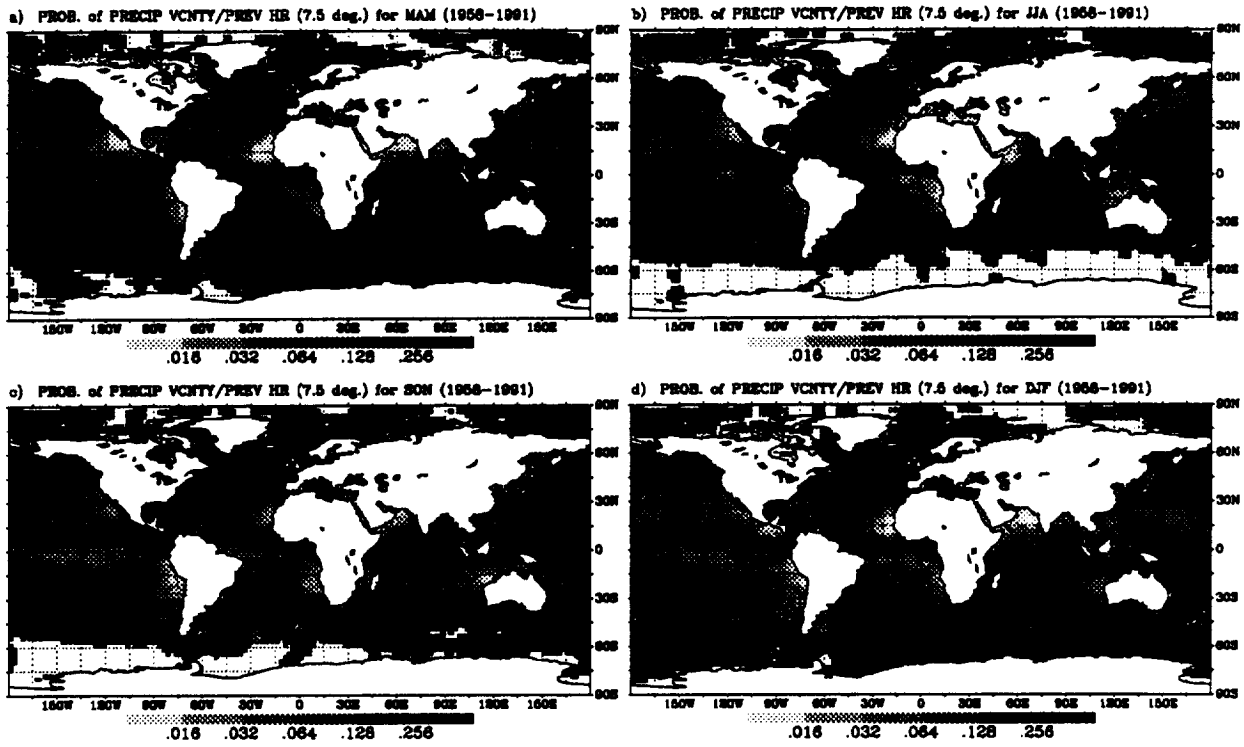

Fig. 7: Fraction of PW reports indicating some form of surface precipitation, either near or at the ship at the time of the observation or during the preceding hour. Displayed values at any geographic point are computed from ship reports within 7.5° boxes centered on the point.

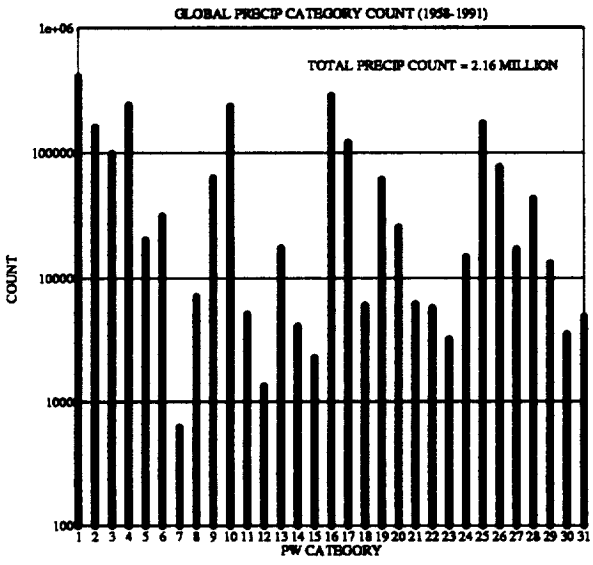

Fig. 6: Global histogram of the 31 present-weather categories defined in Table 3.

closely by code 25 (rain at the station during the preceding hour but not at the actual time of observation; 2.41×10^5 reports or 1.8%). The least common code, with a mere 222 reports, is code 98, which represents the rare combination (at sea at least) of a thunderstorm and a dust storm or sandstorm at time of observation.

Of the precipitation groups defined in Table 3, the most common, representing 18.8% of all precipitation-related reports, is group 1 (Fig. 6). This group consists of all reports of precipitation within sight of, but not at, the station. Next, with 13.3%, is group 16, which consists of reports of light and steady or intermittent rainfall at the time of the observation. Group 4, corresponding to PW code 25 (rain during the preceding hour), and group 10 (drizzle) follow with 11.2% and 11.0%, respectively. Least common is group 7 (only 620 reports), representing sleet (PW code 79).

Combining groups based on intensity, character, or phase, it is found (for example) that 14.2% of the global precipitation reports correspond to drizzle-intensity precipitation (intensity class 1), while 16.1% correspond to moderate to heavy pre-

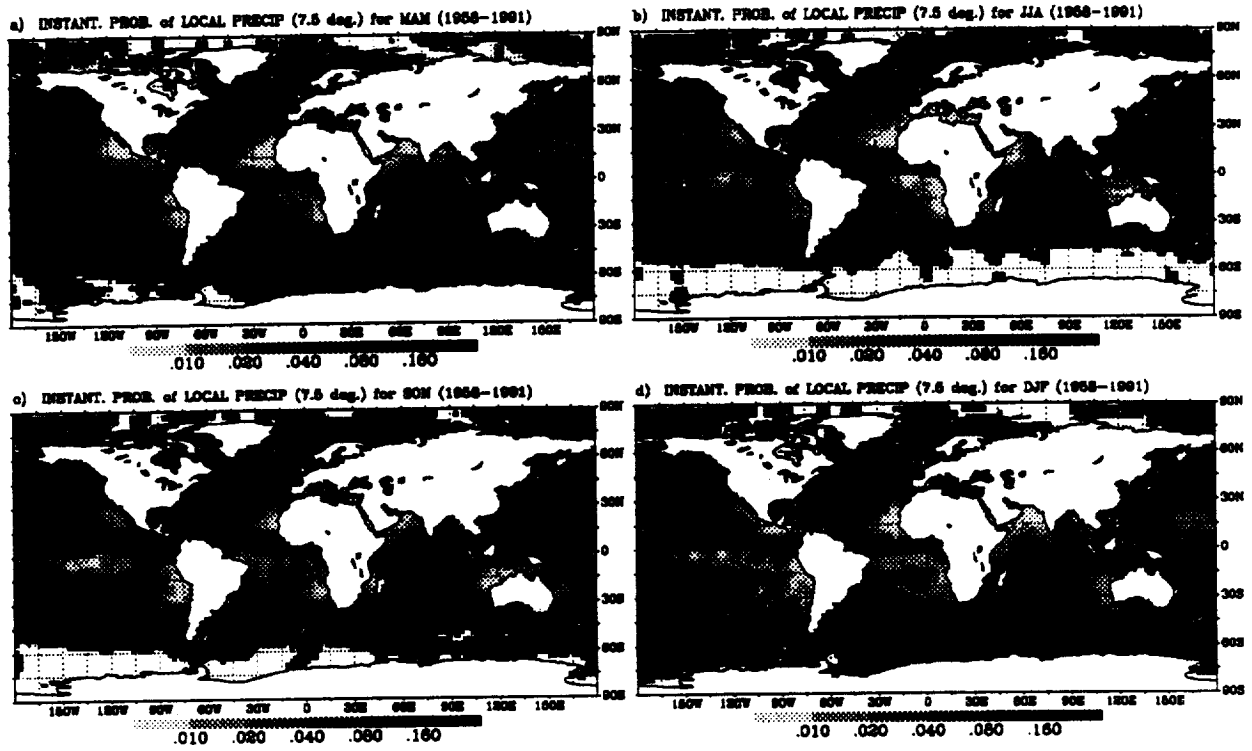

Fig. 8: Same as Fig. 7, but fraction of PW reports indicating some form of surface precipitation occurring locally and at the actual time of the observation.

cipitation (intensity class 3). A total of 9.3% of the reports indicate snowfall in some form (phase class 2).

Finally, 9.2% of the precipitating reports represent PW codes indicative of thunderstorm activity or at least strong convection (character class 3), of which more than 1/3 (3.6% of the total) are contributed by code 13 (lightning observed at a distance; no thunder) while another 1/4 (2.5% of the total) are contributed by "squalls at or within sight of the station during the preceding hour or at time of observation" (code 18 — note that the PW code definition does not make clear what constitutes a "squall" within this context; we have relied here on the "common nautical definition", as cited in Huschke (1959), of "a severe local storm considered as a whole, that is winds and cloud mass and [if any] precipitation, thunder and lightning." The more narrow technical definition of a squall as a strong wind with sudden onset that persists for at most a few minutes seems inconsistent with the "within sight" aspect of the PW code definition, since wind speed and duration cannot be reliably estimated at a distance by a shipboard observer).

4.2 Regional Frequencies of Precipitation

In this subsection, global maps of the absolute frequencies of occurrence of various classes of precipitation relative to all valid PW reports are presented. Although frequencies were tabulated at 2.5° resolution, fields have been subsequently smoothed to 7.5° resolution (or greater where indicated) for presentation purposes in order to reduce statistical noise in regions where the sampling is sparser. An unwanted side effect of this smoothing is of course that very localized features in the precipitation frequency, such as the Intertropical Convergence Zone (ITCZ), appear somewhat flatter and more diffuse than they are in reality.

Fig. 7 depicts the combined frequency of the 30 PW code groups representing precipitation activity observed (or implied) at the surface; only group 13, virga, is excluded. Since this includes those codes representing precipitation occurring during the previous hour but not at the time of observation and those indicating precipitation within sight of the station, this figure may be loosely viewed as a map of the 1-hour probability of precipitation at, or in the vicinity of, the station (note, however, that there are no PW codes corresponding to precipitation ob-

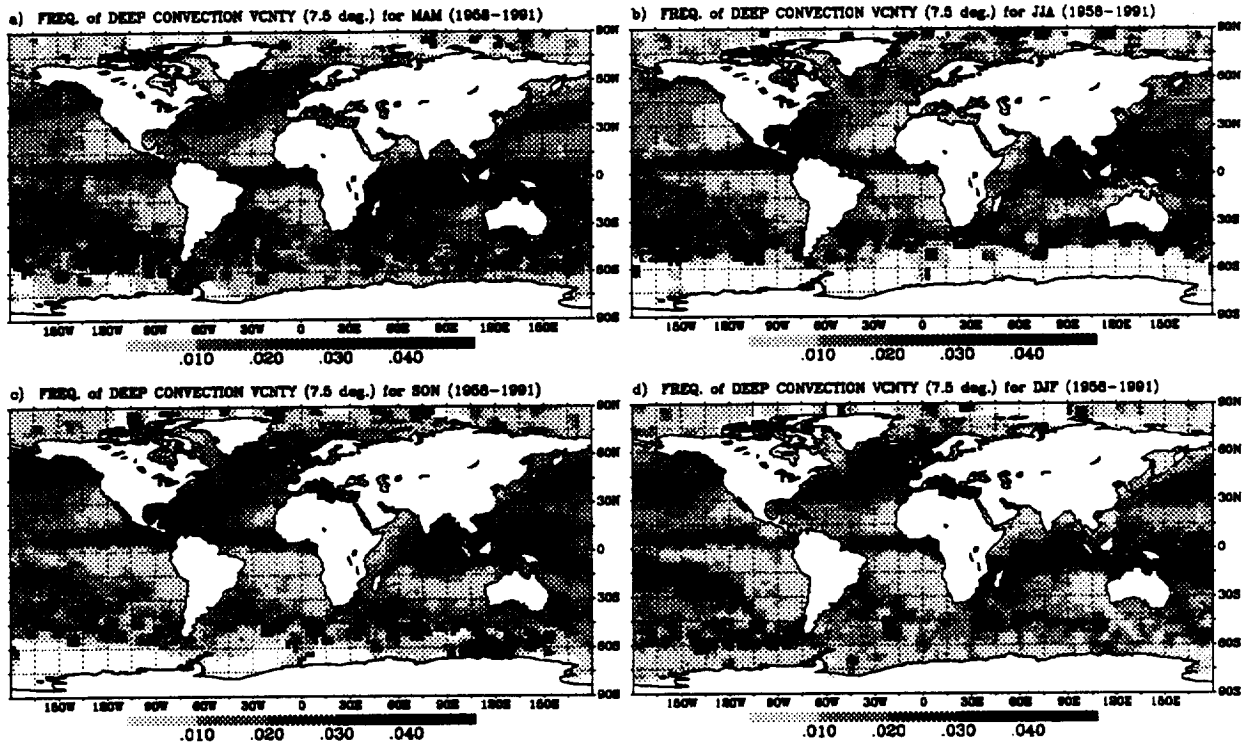

Fig. 9: Same as Fig. 7, but fraction of PW reports indicating some form of strong convective activity (character class 3 in Table 2 and Table 3).

served near the station during the previous hour). These frequencies range from less that 1.6% in certain portions of the subtropical dry zones to the west of the major land masses to more than 25% in portions of the ITCZ, the South Pacific Convergence Zone (SPCZ), and at high latitudes. The monsoonal cycle is clearly evident in the Arabian Sea and the Bay of Bengal, as is a dramatic wintertime increase in precipitation frequency over the northern Pacific and Atlantic oceans. During June-July-August, so few ship reports were received from the far southern latitudes that reliable frequencies could not be computed for much of this region.

Limiting the sample to the set of reports indicating precipitation actually observed at the station at the time of the observation (groups 7, 10–12, and 14–31), we obtain maps depicted in Fig. 8, which may be interpreted as depicting the approximate climatological frequency of precipitation at a single point in time and space. It is seen that the ITCZ is a less rainy place, at least in terms of precipitation *frequency* averaged over a 7.5° gridbox, than the far southern latitudes.

Not surprisingly, the instantaneous local precipitation frequencies in Fig. 8 are generally lower than the frequencies of nearby and/or recent precipitation depicted in Fig. 7. The fact that the ratio is regionally dependent is of some interest and will be considered again in the next subsection.

The patterns of rainfall frequency in Fig. 8 show some interesting differences from recent climatologies of annual or seasonal rainfall accumulation. For example, the map of mean annual precipitation by Legates and Willmott (1990) (not shown) depicts a very prominent 1500 km-diameter "bulls-eye" of greater than 12 mm day^{-1} embedded in the Pacific ITCZ near 140°W. No analogous feature is observed in Fig. 8. Spencer (1993), too, noted that this feature in the Legates and Willmott climatology was inconsistent with his own 14 year rainfall climatology based on Microwave Sounding Unit (MSU) observations. He attributed the discrepancy to the sparseness of surface ship data employed at that location in the Legates and Willmott analysis.

On the other hand, while the Spencer MSU-derived climatology (not shown) agrees quite well with Fig. 8 in the placement and shape of the ITCZ, there are important differences in the higher latitudes. In particular, the Spencer climatology depicts very pronounced, narrow "storm tracks" of en-

hanced rainfall extending eastward and slightly poleward across each of the midlatitude oceans. While the equatorward boundaries of his storm tracks have counterparts in Fig. 8, the poleward boundaries and the local maxima at the track centers do not. Rather, the COADS precipitation frequencies consistently increase more or less monotonically toward higher latitudes. As will be further discussed in Section 4.d, such differences between rainfall frequency patterns and mean rainfall accumulation can be reconciled only if it is assumed that there is a drastic reduction in the average precipitation intensity, within precipitation, poleward of the storm tracks.

Figure 9 depicts the climatological frequency of PW reports indicating strong convective activity and/or thunderstorms (character class 3 in Table 2; PW groups 2, 15, 18, 24, and 27). Not surprisingly, the highest frequencies are concentrated in the tropics and subtropics along the ITCZ and SPCZ. Less expected, perhaps, are the relatively high frequencies (>4%) appearing in the middle and high northern latitudes during Fall and Winter seasons. It will be shown in a later subsection that the relatively high level of convective activity reported at high latitudes appears less dramatic when considered as a percentage of all precipitation reports.

4.3 Zonal Averages

Figure 10 depicts the latitude-averaged frequency of all reports indicating "local or nearby surface precipitation" (i.e., all PW categories excepting 13, as in Fig. 7). Averages were obtained by first calculating seasonal frequencies on 2.5° gridboxes and then averaging over longitude for ocean gridboxes containing a minimum of 5 valid reports. Similar calculations (Figs. 11–14, respectively) were done for "local precipitation at the time of observation" (groups 7, 10–12, and 14–31; as in Fig. 8), "local precipitation of greater than drizzle intensity" (PW groups 7, 14–31), "local precipitation of moderate or heavy intensity" (groups 23–31), and "deep convection in the vicinity" (groups 2, 15, 18, 24, 27).

One interesting aspect of Figs. 11–13 is the very high reported frequency of precipitation at high latitudes, with total instantaneous precipitation frequencies (Fig. 11) exceeding ~20% at latitudes poleward of 60°. Even precipitation of moderate to heavy intensity (Fig. 13) is more likely to be reported north of 40°N during the winter months than anywhere else over the ocean, including the ITCZ belt. The latter statistic is perhaps less reliable than the first, however, since it depends on the ability of shipboard observers not only to note the occurrence of precipitation but also to classify its intensity according to reasonably consistent criteria. As discussed in section 2c, the subjective perception of intensity by an observer in any given instance may perhaps be biased by "typical" intensities experienced in a given climate zone.

Between the equator and 15°N, the latitudinal distribution of precipitation is nearly identical for both the DJF and MAM periods; the JJA and SON periods are likewise very similar. Among other things, these results suggest that, *at a given latitude* between 5° and 15°N, the annual cycle in oceanic rainfall peaks near August and September and is at a minimum near February and March, consistent with the expected influence of the monsoonal dry and rainy seasons over a substantial fraction of the tropical oceans. North of 35°N, on the other hand, distributions are nearly identical for the fall and spring seasons, while the summer and winter seasons, not unexpectedly, represent opposite extremes in precipitation frequency.

In contrast to both of the above results, virtually no seasonal cycle in precipitation frequency is observed throughout most of the southern hemisphere. Hahn et al. (1995) found a similar lack of seasonal cycle in southern hemispheric cloud cover over the ocean, especially for daytime observations. While it is expected that the predominance of ocean area in the southern hemisphere would tend to moderate seasonal changes in baroclinicity relative to those in the northern hemisphere, there are nevertheless large seasonal variations in the mean air temperature over the Antarctic continent (and thus in the meridional temperature gradient offshore) as well as in the latitudinal extent of contiguous coverage by sea ice. That the reported precipitation frequency does not respond more markedly to these environmental differences is noteworthy.

Figure 14 depicts the frequency of reports suggestive of deep convective activity in the vicinity of the ship (PW groups 2, 15, 18, 24, and 27; as in Fig. 9). Unlike the precipitation frequencies discussed above, the frequency of deep convection tends to fall off toward high latitudes, though not as rapidly as one might expect. Frequencies in and near the ITCZ are only slightly higher (~5%) than those reported at 35–40° during DJF (4.4%). Also, in contrast to the precipitation frequency, there is significant seasonal variability in the frequency of convective activity in the southern tropical and middle latitudes. Interestingly, a sharp maximum is found in both hemispheres at identical latitudes (37.5–40°) during the respective winter seasons; the same latitudes are associated with a local *minimum* in convective activity

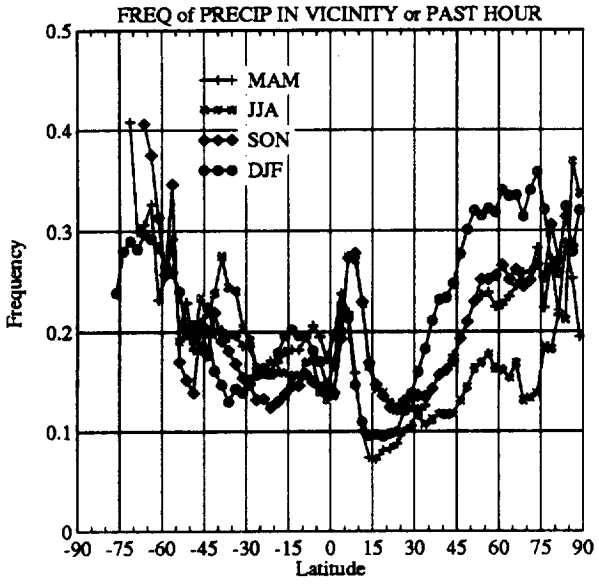

Fig. 10: Zonally averaged seasonal frequencies of reports indicating some form of surface precipitation, either near or at the ship at the time of the observation or during the preceding hour.

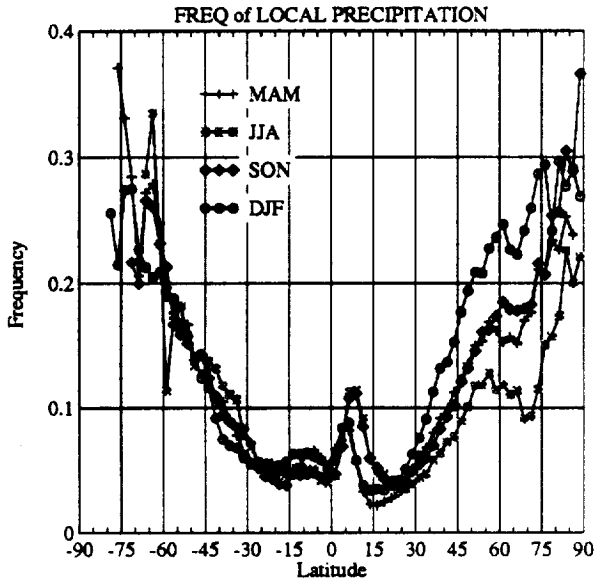

Fig. 11: Same as Fig. 10, but only PW reports indicating some form of surface precipitation occurring locally and at the actual time of the observation.

during the summer seasons.

4.4 Comparison with research ship observations

As already noted, one notable aspect of the zonal average statistics computed above is the very high frequency of precipitation reported in the far southern latitudes. In particular, Fig. 11 shows average frequencies of local precipitation increasing monotonically from ~7% near 30°S to ~30% near 75°S.

Published climatologies of mean annual precipitation accumulation tend to show a zonal maximum on the order of 1000 mm yr^{-1} near 50°S, with a decrease to approximately ~500 mm yr^{-1} (Legates and Willmott 1990) or even as little as ~250 mm yr^{-1} (Jaeger 1983) in the vicinity of 70°S. In order for the frequency statistics presented here to be consistent with those climatologies, there would have to be a very sharp decrease toward the Antarctic coast in the average precipitation rate within precipitation. For example, if one accepts the Jaeger (1983) values, one must assume an average precipitation rate, within areas of precipitation, of ~0.9 mm h^{-1} at 50°S, whereas the corresponding value at 70°S would only be ~0.1 mm h^{-1}.

However, even the frequency of moderate to heavy precipitation derived from the COADS reports increases sharply toward Antarctica (Fig. 13), with values as high as ~6% in the vicinity of 70°S. If one

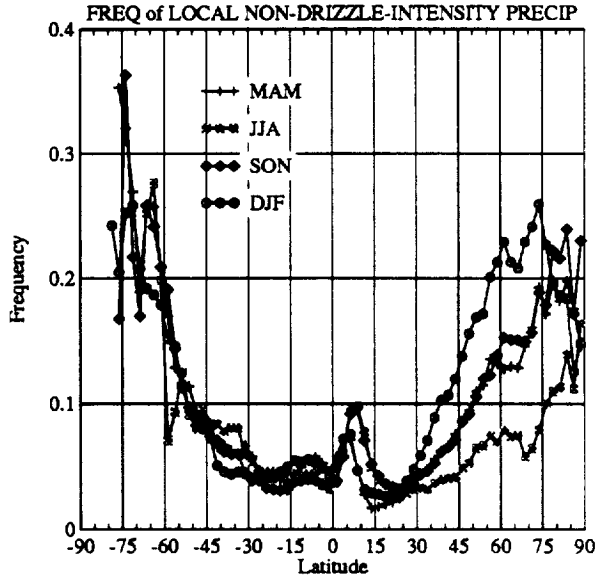

Fig. 12: Same as Fig. 11, but excluding precipitation of "drizzle" intensity (intensity class 1 in Table 2 and Table 3).

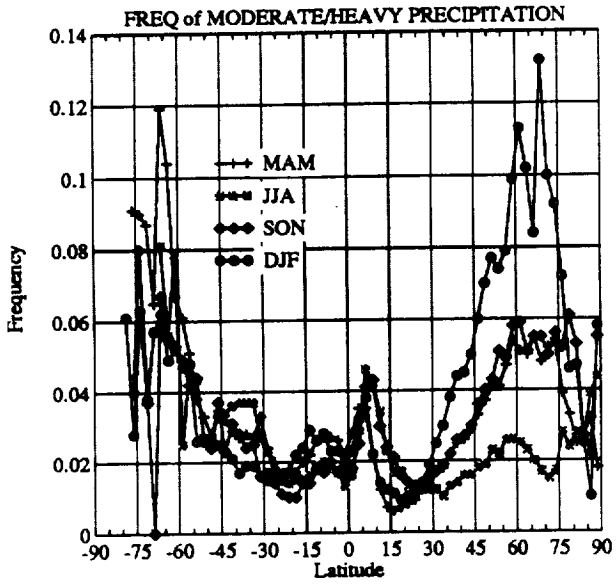

Fig. 13: Same as Fig. 11, but including only precipitation of moderate or heavy intensity (intensity class 3 in Table 2 and Table 3).

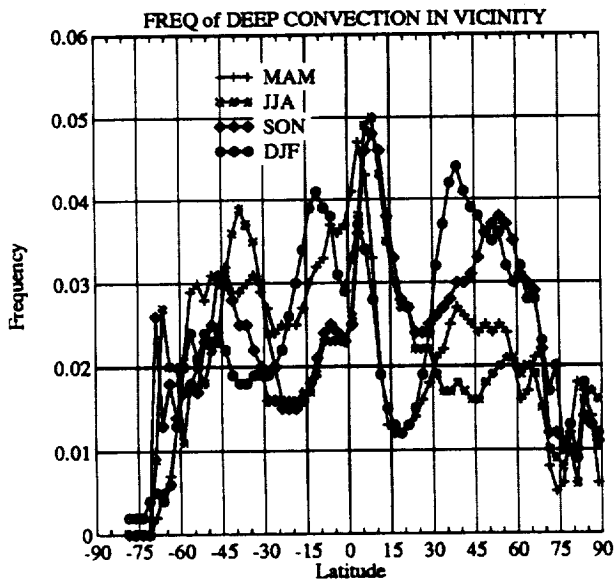

Fig. 14: Zonally averaged seasonal frequencies of reports indicating strong convective activity (character class 3 in Table 2 and Table 3).

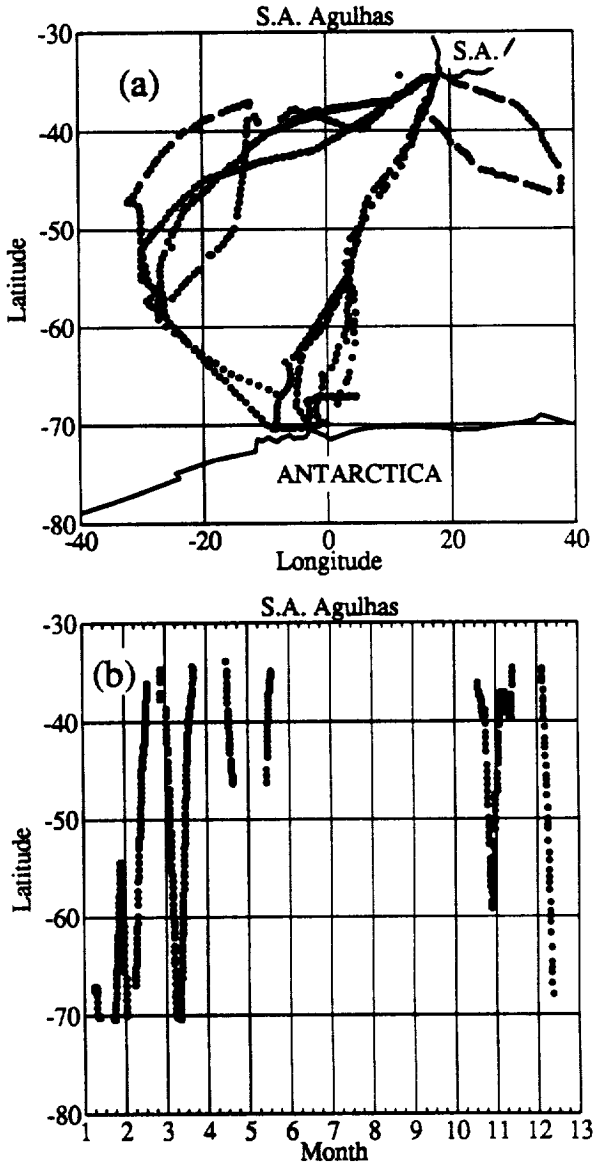

Fig. 15: Location and timing (with respect to time of year) of 3-hourly weather observations obtained from the South African research ship S.A. Agulhas. (a) geographic location; (b) latitude vs. time of year.

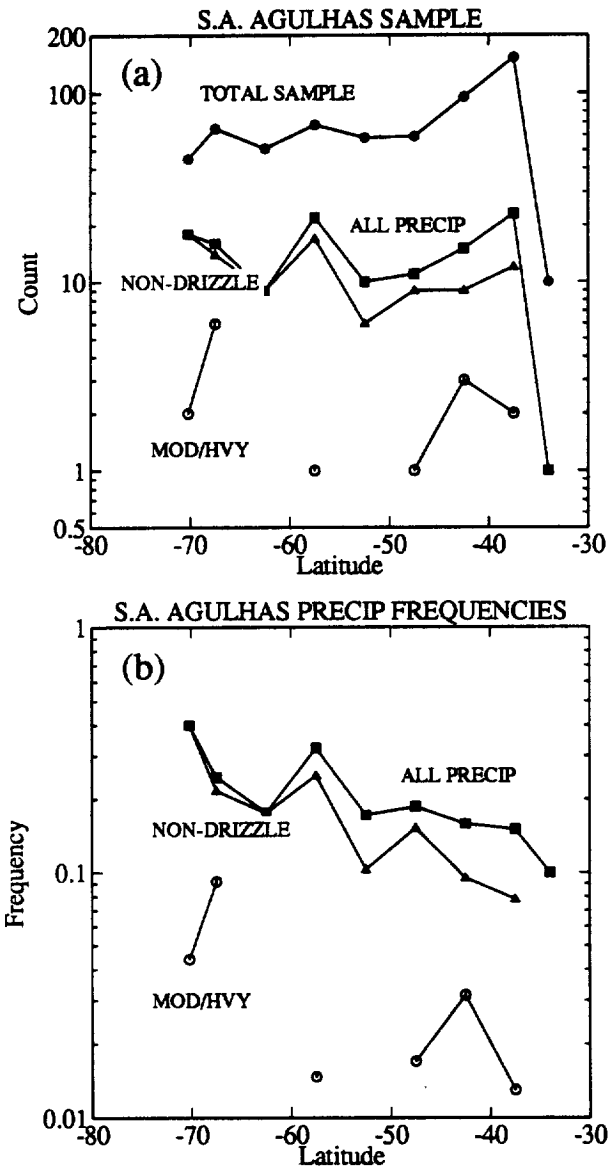

Fig. 16: Precipitation statistics derived from the S.A. Agulhas. (a) Total counts of PW reports falling in various intensity categories; (b) normalized frequencies derived from the counts in (a).

conservatively assumes a minimum intensity of ~1.0 mm h^{-1} (equivalent to ~1 cm h^{-1} snow accumulation) associated with this class of report *and* one ignores the contribution from light precipitation, the resulting lower bound on the mean annual precipitation at that latitude is still ~500 mm or greater. Including the contribution from light snow and/or using a threshold for moderate precipitation more in line with the nominal threshold of 2.5 mm h^{-1} would significantly increase the total.

One must therefore either conclude that total precipitation is more abundant in the far southern latitudes than is indicated in previously published climatologies or else that there are large systematic biases in the reporting of precipitation frequency and/or intensity at those latitudes by ships of opportunity. In order to investigate the latter possibility, weather logs were obtained from a South African scientific research vessel, the S.A. Agulhas, which made several transits between South Africa and an Antarctic coastal station during January 1991 - May 1993. The locations and seasonal timing of the Agulhas' weather observations are indicated in Fig. 15.

It is expected that weather observations taken regularly at three hour intervals on board a scientific research vessel are less likely to suffer from systematic reporting biases of the type discussed in section 2c than are the sometimes intermittent observations from the merchant or fishing vessels that constitute the majority of COADS reports. It is therefore noteworthy that the summary statistics of the S.A. Agulhas' precipitation present-weather reports for 5° latitude intervals (Fig. 16) are in excellent agreement with the corresponding COADS statistics presented in Figs. 11-13, notwithstanding significant statistical uncertainties in the Agulhas' precipitation frequencies (esp. for moderate/heavy precipitation) due to the small sample. There thus appears to be no immediate basis for discounting as biased the rather high COADS-derived precipitation frequency statistics for this latitude belt.

4.5 Regional Characteristics of Precipitation

When absolute frequencies of various types of oceanic precipitation are globally mapped as in section 4b, only relatively subtle variations in global patterns can be discerned, since the shapes of these patterns are all dominated by the rather dramatic differences in overall precipitation frequency that distinguish the subtropical highs from the ITCZ, SPCZ, and midlatitude storm tracks. New spatial patterns, and new insight into the regional *characteristics* of precipitation, emerge when the frequency

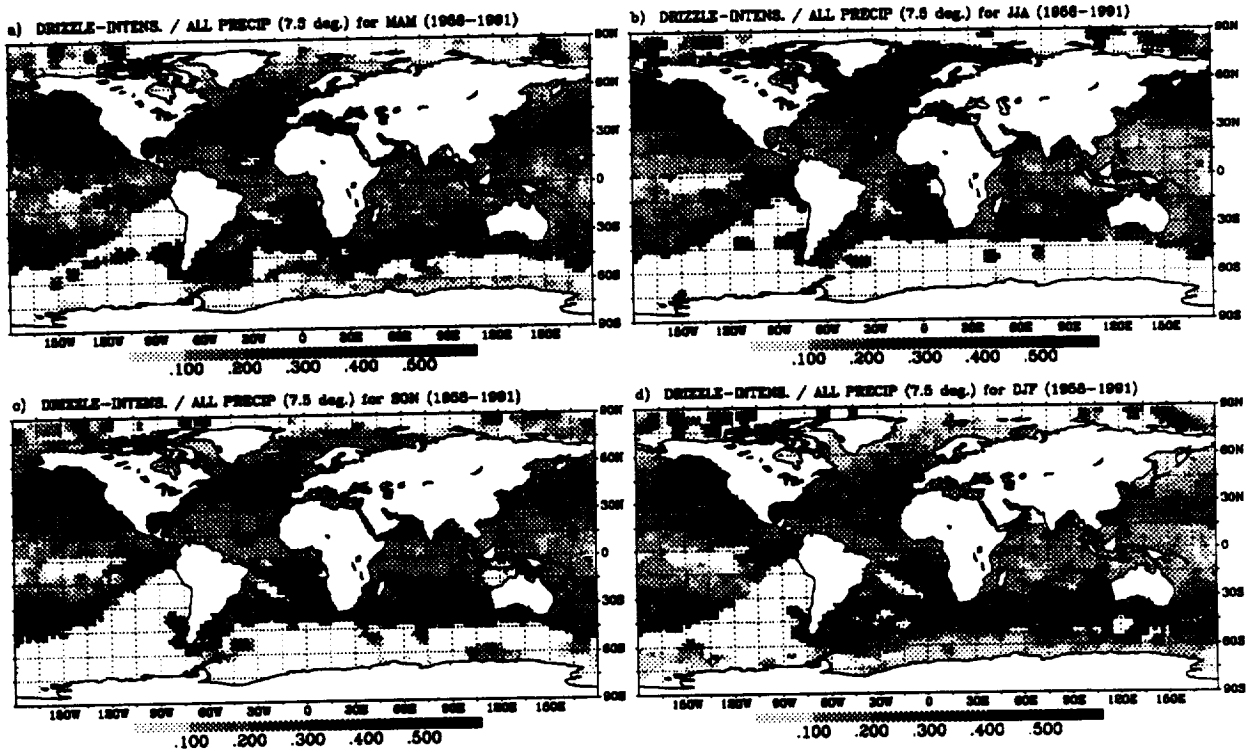

Fig. 17: Fraction of all surface precipitation reports specifically associated with "drizzle" intensity precipitation (intensity class 1 in Table 2 and Table 3).

of a selected class of precipitation report is expressed as a fraction of the frequency of a more general class that includes the first class as a subset.

There is a very large number of possible combinations of groups that can be considered; space permits only a few of the more interesting examples to be presented here.

4.5.1 Intensity

Figure 17 depicts the fraction of all surface precipitation reports, excluding those of indefinite intensity (i.e., intensity code '0' in Table 3), that specifically indicate precipitation of extremely light or "drizzle" intensity (groups 9–12 only). Globally, a typical value for this ratio is approximately 20–30%; slightly smaller values prevail throughout much of the tropical belt.

A few regions, however, show a decided preference (>50%) for drizzle-intensity precipitation relative to other forms. One prominent region encompasses most of the Pacific north of 30°N during June–August. Others correspond to known regions of persistent coastal marine stratocumulus clouds arising from a combination of cool sea surface temperatures and subsiding air within the subtropical high pressure belts; the most prominent of these are found off the west coasts of North America and South Africa.

Less well documented is a narrow but pronounced tongue of high drizzle fraction appearing just south of the equator and west of South America during the months of June–November. Both the seasonality and location of this climatological feature is consistent with low stratocumulus formation as air blows northward over the tongue of cooler sea surface temperatures on the south side of the equatorial front (Deser et al. 1993).

The very low drizzle fraction (<15%) appearing at very high latitudes probably reflects the fact that even extremely light frozen precipitation is more likely to be reported as light snow (codes 70 and 71) than as ice prisms (code 76), snow grains (codes 77), or isolated snow crystals (code 78).

Figure 18 depicts the frequency of moderate or heavy precipitation (intensity class 3) conditioned on the occurrence of precipitation of at least light intensity (intensity classes 2 and 3 combined). The frequency of drizzle intensity precipitation is not included in the denominator of this ratio, because true drizzle is normally produced by meteorological and

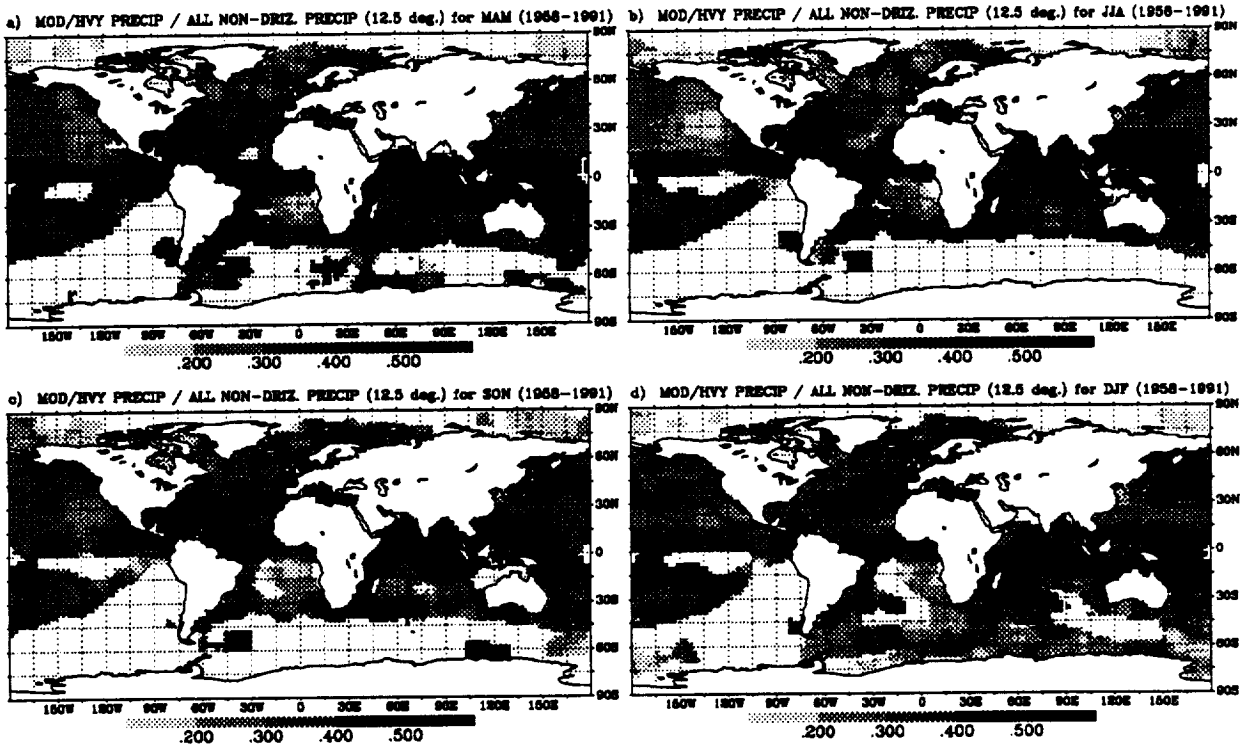

Fig. 18: Fraction of all surface precipitation reports specifically associated with "moderate or heavy" intensity precipitation (intensity class 3 in Table 2 and Table 3). Displayed fractions are calculated from reports within 12.5° latitude-longitude windows centered on each 2.5° grid box.

microphysical processes quite distinct from those responsible for the other forms of precipitation.

As before, significant regional differences are apparent, though the details of these differences are more difficult to relate to known climatological features. For example, there is a decided tendency (>50%) for precipitation to be reported as moderate to heavy in intensity in the vicinity of Indonesia, near the southwest coast of North Africa, and between Africa and Madagascar, even relative to other tropical areas. A similar tendency exists during the spring and summer months over the northern Indian Ocean.

By contrast, less than 20% of rain reports in regions near the California and West South Africa coasts are classified as moderate to heavy. While this may partly reflect a genuine predominance of light rain, when rain occurs, the geographic distribution raises the possibility that many of the nominal light rain reports in these areas actually represent misclassified drizzle (cf. Fig. 17).

4.5.2 Phase

Figure 19 depicts the frequency of snow reports (phase category 2) expressed as a fraction of all precipitation reports for which phase is indicated. The seasonal shift in the snow line is clearly discernible in the northern hemisphere, while it is considerably less dramatic in the southern hemisphere. Indeed, the northernmost boundary of occasional snowfall at approximately 30°W longitude appears to be fixed very close to 45°S latitude, irrespective of season.

In addition to shedding light on the seasonal boundaries between predominantly liquid and predominantly solid surface precipitation, the qualitative reasonableness and smoothness of the patterns, even in data sparse regions, would appear to rule out a significant contribution to the statistics by mislocated reports. The only apparent anomalies are a number of non-zero values for snow fraction appearing at certain low-latitude locations, especially along the African, Arabian, and Indian coasts. One preferred location is at the intersection of the Equator and Greenwich Meridian, suggesting that zeroes have been substituted for the correct latitude and longitude in a number of reports. Other anomalies,

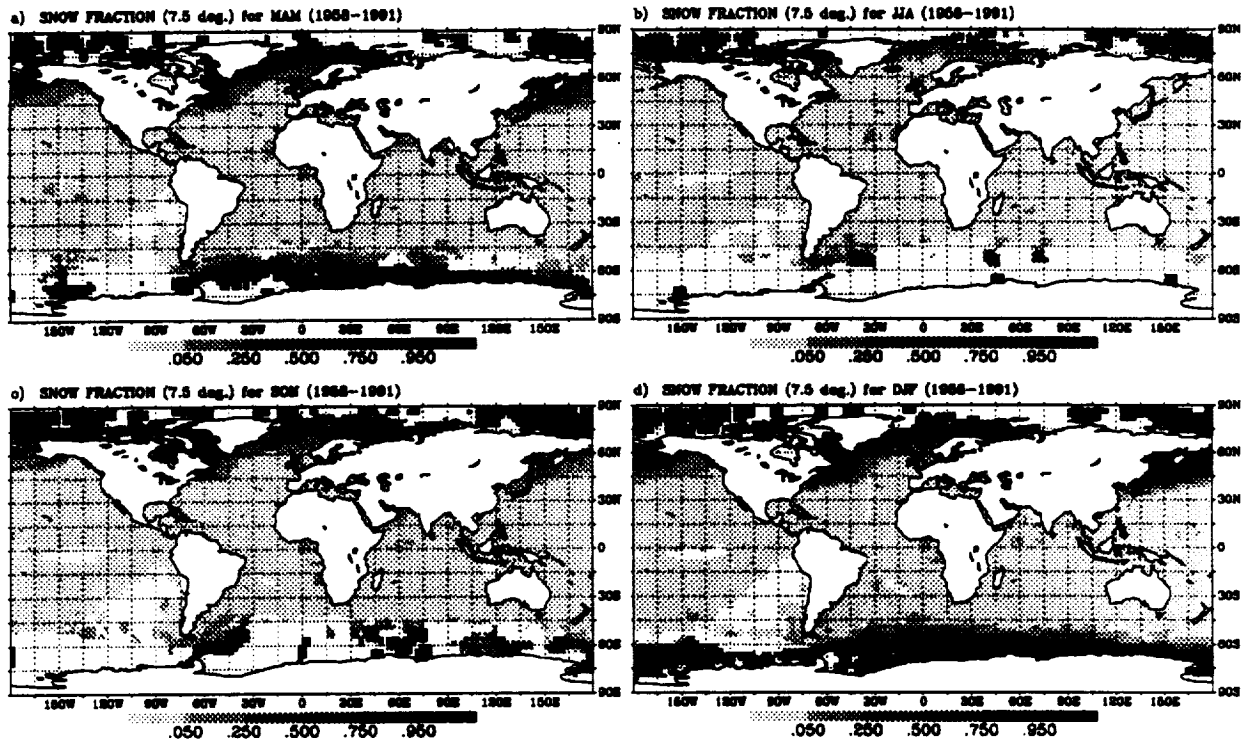

Fig. 19: Fraction of all surface precipitation reports specifically associated with "snow" (phase class 2 in Table 2 and Table 3).

such as those at the mouth of the Persian Gulf and at 15°S, 15°E in MAM and SON, are harder to explain, especially given the relatively high density of legitimate ship reports at those locations.

4.5.3 Strong Convection and Thunderstorms

Figure 20 depicts the frequency of PW reports indicative of thunderstorms or strong convective activity (character class 3) expressed as a fraction of the frequency of all reports of precipitation, excluding intensity class 1 (drizzle). This depiction of the relative predominance of strong convective activity reveals some surprisingly pronounced regional variations.

In particular, the highest rates of thunderstorm or squall activity appear to be confined to several well defined zones in which such reports constitute >24% of the total non-drizzle precipitation reports, as contrasted with roughly half that value at many other locations in the tropics and subtropics. Furthermore, these zones of high activity appear to be closely tied to the continents and to vary only in relatively minor ways from one season to the next. Even within the Atlantic and Pacific ITCZ, the tendency for thunderstorms, lightning, or squalls to be reported depends rather strongly on proximity to land.

Some similarities are apparent between the reported patterns of thunderstorm/squall activity and the tendency for heavier rainfall to be reported (cf. Fig. 18) — both maps, for example, are fairly consistent in depicting higher fractions near Indonesia, over the northern Indian Ocean, and near Central America and West Africa. However, the regions of high reported convective activity in Fig. 20 appear more coherent and sharply delineated.

As noted in Section 4a, the inclusion of "squalls at or within sight of the station" (PW code 18) introduces some uncertainty in the meteorological interpretation of the above statistics, since this code contributes a significant fraction of the global reports falling in character class 3, yet its reporting criteria are probably among the least well-understood by shipboard observers (based in part on the author's own experience as a shipboard observer in the U.S. Navy). In order to specifically examine the relative frequency of thunderstorm activity, the COADS data set was reanalyzed, this time restricting the analysis to PW codes explicitly indicating

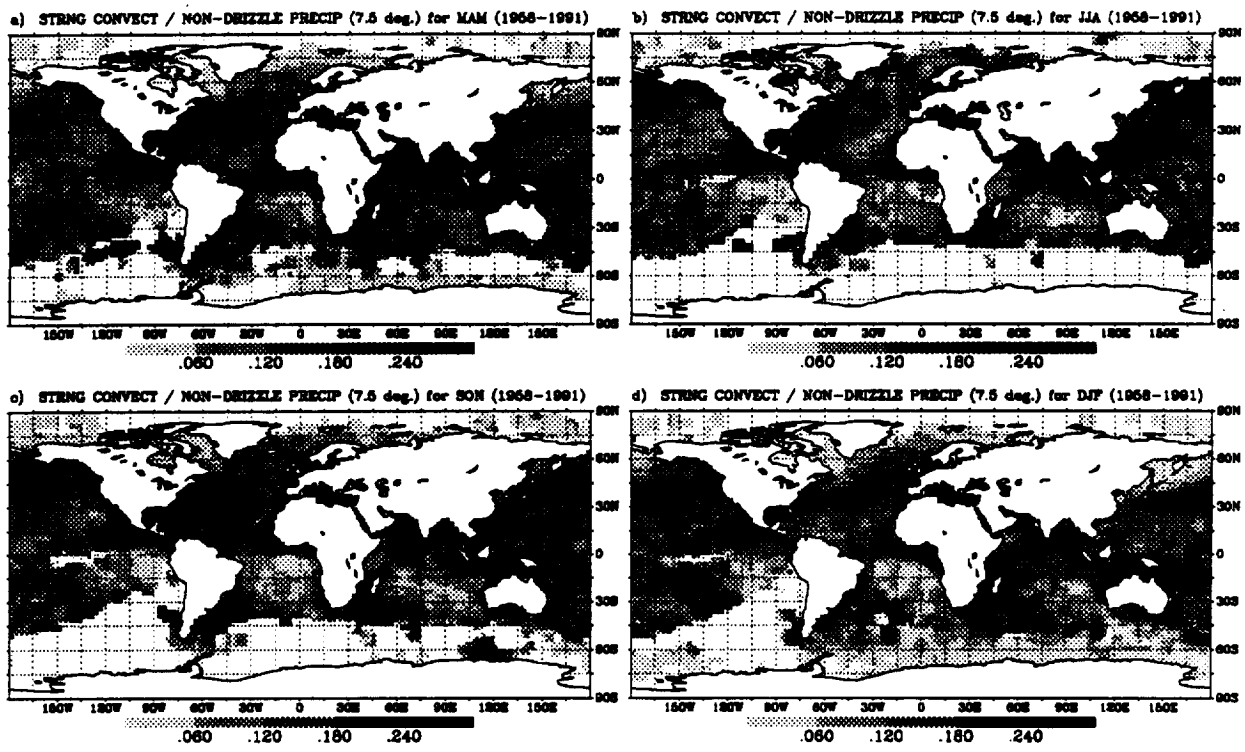

Fig. 20: Fraction of all non-drizzle surface precipitation reports (i.e., excluding intensity class 1) specifically associated with strong convection or thunderstorms (character class 3 in Table 2 and Table 3).

that lightning was seen or thunder heard (PW codes 13, 17, 29, and 91–99), expressed as a fraction of all non-drizzle precipitation reports. The results, presented in Fig. 21, show an even more dramatic regional variation than was the case for Fig. 20 (note the introduction of a logarithmic scale in the shading scheme).

Clearly, the climatological tendency of precipitation to be accompanied by thunderstorms is highly nonuniform, even throughout the tropics, with the preferred regions for thunderstorm occurrence apparently tied closely to the major land masses. Within those preferred regions, ~10–25% of all non-drizzle PW reports indicate thunderstorm activity, whereas the fraction is as low as ~3% or less over much of the remaining ocean area, including some areas of the so-called "warm pool" of the Western Tropical Pacific. Interestingly, the SPCZ provides a modest exception to this generalization, with thunderstorm reports comprising approximately 8% of all precipitation-related reports in the December–May seasons, a significantly higher fraction than is found in much of the Pacific ITCZ. This apparent anomaly may perhaps be related to the relatively large number of islands scattered throughout the SPCZ region, notwithstanding the very small total fractional area covered by land.

PW code 13 (lightning observed at a distance from the station; no thunder heard) constitutes almost one-half of the total thunderstorm reports. Furthermore, the conditions under which distant lightning may be observed are likely to vary widely between different climate zones. For example, it has been the author's experience that lightning associated with isolated thunderstorm cells or clusters can frequently be observed ~100 km away at night in the tropics and subtropics, while over the middle latitude oceans, the viewing of distant lightning is often hampered by more widespread cloudiness and precipitation.

In view of this additional ambiguity in the interpretation of Fig. 21, the raw COADS data were again reanalyzed, this time excluding PW code 13 and thus restricting the analysis to PW codes indicating that a thunderstorm actually occurred (i.e., thunder was heard) at the ship's location at or just prior to the observation time. It was found, however, that this modification does not greatly alter the general spatial patterns of thunderstorm activity described above, though it does reduce the overall

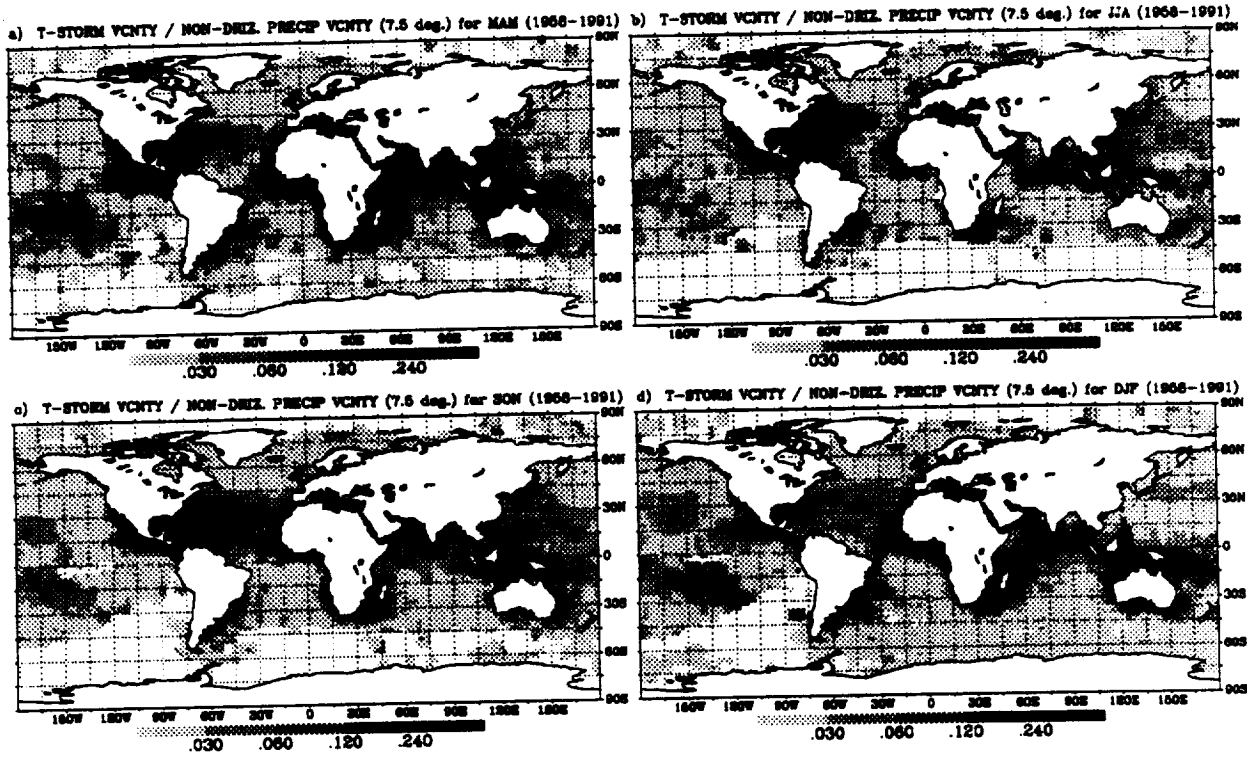

Fig. 21: Same as Fig. 20, but excluding PW code 18. Note use of logarithmic scale.

frequencies.

4.5.4 Persistence of precipitation

As indicated earlier, some PW codes refer to precipitation observed during the preceding hour but not at the actual time of the observation, while others refer to precipitation at the station at the time of the observation. The relative frequencies of the two groups of PW codes contain information on the temporal scale, or persistence, of individual precipitation events. For example, if all precipitation received at a location is contributed by extremely brief showers, then the likelihood of recording precipitation during the preceding hour can be considerably higher than the likelihood of recording precipitation at the actual time of the observation. If, on the other hand, precipitation events consist of relatively long periods of continuous precipitation, then precipitation occurring during the previous hour is less likely to end before the nominal observation time; hence the relative frequency of reports of precipitation at the time of the observation increases.

Figure 22 depicts the ratio of the frequency of reports indicating non-drizzle-intensity precipitation at the time of the observation (i.e., the climatological "instantaneous" probability of non-drizzle precipitation) to that of all reports of non-drizzle precipitation at the station, including precipitation observed during the preceding hour (i.e., the climatological 1-hour probability of precipitation). Throughout most of the high latitudes, the ratio exceeds 0.7–0.8, consistent with the expectation that high latitude precipitation is largely stratiform in character and is thus associated with relatively persistent precipitation. In the subtropical high pressure zones, on the other hand, the ratio is often less that 0.5, confirming the expectation that precipitation there is associated with more transient or localized precipitation events, such as trade wind cumulus showers. Interestingly, ratios are generally somewhat higher in the northern hemisphere subtropics than in the southern hemisphere subtropics, except during the northern hemisphere summer.

Other minor features are apparent whose explanation is less obvious. For example, in all but the DJF season, the maximum ratio (>0.7) for the tropics and subtropics is consistently found within the short segment of Pacific ITCZ between 120°W and 135°W, suggesting that, climatologically, this region is somewhat anomalous as regards the occurrence of longer-lived and/or more stratiform precipitation events.

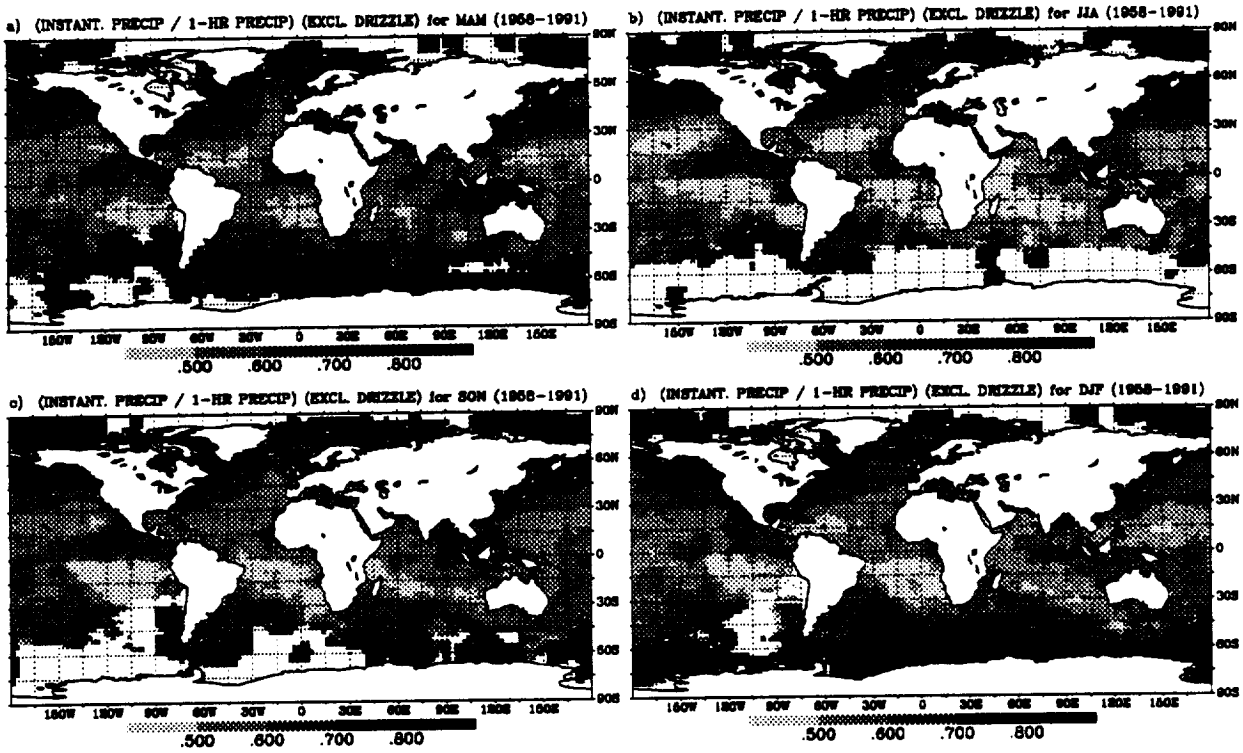

Fig. 22: Frequency of local non-drizzle precipitation occurring at the time of the observation, expressed as a fraction of all non-drizzle precipitation reports, including precipitation during the preceding hour. Low values of the ratio imply a predominance of transient precipitation events; values approaching 1 imply a predominance of long-lived precipitation events. Displayed fractions are calculated from reports within 12.5° latitude-longitude windows centered on each 2.5° grid box.

5 Conclusions

One of the primary motivations behind the present study was the need to develop an objective, if obviously incomplete, basis for predicting or assessing the general performance of satellite rainfall estimation algorithms over remote areas of the global oceans. Several results of the COADS-derived present-weather statistics are significant in this context:

(1) Precipitation frequencies are apparently quite high (~10–20+%) in the far southern latitudes and increase monotonically toward the Antarctic coast. This observation runs counter to the results yielded by the majority of the satellite microwave algorithms submitted to the First Precipitation [Algorithm] Intercomparison Project (PIP-1; Barrett et al. 1994a), most of which produced very low (~1%) frequencies of precipitation at 50°S and/or decreasing frequencies toward Antarctica. The striking disparity between satellite and surface observations suggests that the passive microwave detection of lighter, shallower and/or frozen precipitation typical of the polar environment (viz. Fig. 19) is an area requiring additional attention. Similar differences were noted between the general patterns of precipitation frequency in Fig. 8 and the MSU-derived rainfall climatology of Spencer (1993). However, in the latter case, the differences could be reconciled if the Spencer method is correctly seeing a significant decrease in mean precipitation intensity (within precipitation) poleward of the storm track axes.

(2) The subtropical high pressure zones west of South America and Africa are comparatively dry, but are not completely devoid of precipitation. Indeed, climatological frequencies of non-drizzle precipitation as high as 1–4% are found in some regions where most PIP-1 submissions failed to detect any precipitation at all over a 4-month period (August–November 1987). Infrared-based algorithms (e.g., Arkin and Janowiak 1993) also consistently yield extremely low (much less than 0.5 mm/day) rainfall amounts throughout rather large regions of the subtropical oceans. In order for these estimates to be compatible with the frequencies derived here, av-

erage rainfall intensities within rain events would have to fall well below ~0.6 mm h^{-1}. (A preliminary analysis by the author of ship reports for only the 4-month PIP-1 period appears to rule out the alternative explanation that this period simply coincided with much drier than average conditions in the regions in question.)

Based on the ratio of 1-hour frequencies to instantaneous frequencies (Fig. 22), it seems likely that precipitation of greater intensity does occur with some regularity in much of the subtropical dry zone, but that it takes the form of scattered, transient showers which are too small to be detected with the 12–25 km resolution of the SSM/I and which have tops too warm to be detected by IR threshold techniques. Since there is no obvious way to overcome either difficulty using currently operational sensors, it could prove impossible for any satellite technique to give reliable rainfall estimates within these regions until such time as active microwave sensors and/or higher resolution passive microwave sensors become available in the latter part of this decade.

(3) In general, the results presented in Figs. 17–22 suggest that the spatial scale and microphysical character of precipitation varies strongly with location and season, even within a given latitude belt. Since satellite rainfall algorithms are known to be sensitive to some of these properties, it seems unlikely that any satellite technique can be made to yield unbiased results globally without the benefit of careful region-by-region calibration. In this context, it should perhaps be of concern that many of the low latitude radar sites most widely used for overwater calibration of satellite algorithms (e.g., U.S. Gulf and Atlantic coastal sites; Darwin, Australia) appear to be located in regions of anomalously high thunderstorm activity relative to the overall occurrence of precipitation.

On the other hand, ship-derived precipitation statistics of the type presented in this paper may be of some value for segmenting the global oceans into zones of relatively homogeneous precipitation properties. Within such zones, a satellite retrieval technique might perhaps be expected to respond in a more consistent manner to precipitation.

From a purely climatological perspective, the following additional features are particularly noteworthy:

(1) The frequency of thunderstorm reports, relative to all precipitation reports (Fig. 21), is strongly region-dependent, even within the tropics. In general, thunderstorm activity is favored within 1000–3000 km of land masses, while being quite rare at greater distances, even within the ITCZ. Satellite-based studies of midnight lightning occurrence (Orville and Henderson 1986; Goodman and Christian 1993) had already revealed a very strong land-ocean contrast in the occurrence of lightning, and Zipser (1994) has specifically focused on the apparent rarity of lightning over the ocean, using shipboard observations taken from the GARP (Global Atmospheric Research Program) Atlantic Tropical Experiment (GATE). All of these studies, however, primarily highlight the sharp gradient in lightning activity that is found in the immediate vicinity of the coastline. The present analyses extends the picture not only by quantifying the relative reporting of oceanic lightning activity on a global basis but also by highlighting the apparently vital influence of land on thunderstorm activity out to considerable distances over the open ocean. It is also interesting to note that even the observations of reduced updraft speeds and modified cloud microphysical properties that Zipser (1994) cited as characterizing over-ocean convective precipitation were nonetheless taken in regions (e.g., near Taiwan, near Darwin, and in the GATE region off the coast of Africa) of comparatively high thunderstorm activity, leading one to wonder what aircraft observations of ITCZ convection near 130°W during September–November might reveal about cloud properties there.

(2) Both the latitudinal frequency of precipitation of all intensities (Figs. 11–13) and the fraction of precipitation that falls as snow (Fig. 19) show very little seasonal variation in the southern hemisphere. The frequency of apparent convective activity (Fig. 14), however, shows considerable seasonal variability, with sharp winter maxima occurring near 38° latitude in both hemispheres.

(3) Drizzle is the preferred form of precipitation in a number of well-defined regions (Fig. 17), most of which coincide with known regions of persistent marine stratus and stratocumulus. Less well-documented, however, is a rather narrow but pronounced tongue of high drizzle occurrence extending westward from South America along the equator during the June–November months. This feature may be associated with colder sea surface temperatures created by coastal and equatorial upwelling.

Since it is believed that some of the climatological characteristics of oceanic precipitation described in this paper have not been fully documented or explained in the past, it is hoped that these results will stimulate new discussion and research regarding the relationship between climate-scale dynamics and the occurrence and character of surface precipitation over the ocean. Future work may include an examination of the relationship between COADS-derived

oceanic precipitation patterns and the phase of the Elño/Southern Oscillation (ENSO). The 2.5° gridded present-weather histogram produced as part of this study has been archived as a computer-readable data file and is available from the author or from the Scientific Computing Division, National Center for Atmospheric Research.

Acknowledgments

The author acknowledges helpful discussions with Carole Hahn (CIRES, Boulder, CO) and Stephen G. Warren (Atmospheric Sciences Department, University of Washington) regarding the analysis of ship present-weather reports. Michael Laing (Weather Bureau, South Africa) and Patrick Haines (Purdue University) were instrumental in obtaining a copy of the weather log from the S.A. Agulhas. Steve Worley (Scientific Computing Division, National Center for Atmospheric Research) is gratefully acknowledged for his assistance in obtaining the COADS data set. Robert Quayle, Alan McNab, Joseph Elms, and Stephen Klein contributed valuable comments and information, as did two anonymous reviewers. This study was supported in part by NASA Grants NAGW-2984 and NAGW-3944.

REFERENCES

Arkin, P.A., and J.E. Janowiak, 1993: Tropical and subtropical precipitation. In *Atlas of Satellite Observations Related to Global Change.* R.J. Gurney, J.L. Foster, and C.L. Parkinsons, Eds., Cambridge University Press, Cambridge, pp. 165–180.

Arkin, P.A., and P. Xie, 1994: The Global Precipitation Climatology Project: First Algorithm Intercomparison Project. *Bull. Amer. Meteor. Soc.,* **75,** 401–419

Barrett, E.C., J. Dodge, M. Goodman, J. Janowiak, and E. Smith, 1994a: The First WetNet Intercomparison Project (PIP-1), *Remote Sens. Rev.,* **11**, ???–???

Barrett, E.C., R.F. Adler, K. Arpe, P. Bauer, W. Berg, A. Chang, R. Ferraro, J. Ferriday, S. Goodman, Y. Hong, J. Janowiak, C. Kidd, D. Kniveton, M. Morrissey, W. Olson, G. Petty, B. Rudolf, A. Shibata, E. Smith, R. Spencer, 1994b: The first WetNet Precipitation Intercomparison Project: Interpretation of results. *Remote Sens. Rev.,* **11**, 303–373

Deser, C., J.J. Bates, and S. Wahl, 1993: The influence of sea surface temperature gradients on stratiform cloudines along the equatorial front in the Pacific Ocean. *J. Climate,* **6,** 1172–1180

Dorman, C.E., and R.H. Bourke, 1979: Precipitation over the Pacific Ocean, 30°S to 60°N. *Mon. Wea. Rev.,* **107,** 896–910.

Dorman, C.E., and R.H. Bourke, 1981: Precipitation over the Atlantic Ocean, 30°S to 70°N. *Mon. Wea. Rev.,* **109,** 554–563

ERL, 1985: *Comprehensive Ocean-Atmosphere Data Set: Release 1.* Available from the Climate Research Program, Environmental Research Laboratory, Boulder, CO.

FMH, 1978: *Federal Meteorological Handbook No. 1. Surface Observations.* Available from the Superintendant of Documents, U.S. Government Printing Office, Washington, D.C. 20402

Goodman, S.J, and H.J Christian, 1993: Global observations of lightning. In *Atlas of Satellite Observations Related to Global Change.* R.J. Gurney, J.L. Foster, and C.L. Parkinsons, Eds., Cambridge University Press, Cambridge, pp. 191–222.

Hahn, C.J., S.G. Warren, and J. London, 1994: *Climatological Data for Clouds Over the Globe from Surface Observations, 1982-1991: The Total Cloud Edition.* NDP026A, Carbon Dioxide Information Analysis Center, Oak Ridge National Laboratory, Oak Ridge, TN. (Also available from the Data Support Section, National Center for Atmospheric Research, Boulder, CO.)

Hahn, C.J., S.G. Warren, and J. London, 1995: The effect of moonlight on observation of cloud cover at night, and application to cloud climatology. In press, *J. Climate*

Huschke, R.E., 1959: *Glossary of Meteorology.* American Meteorological Society, Boston, MA, 638 pp.

Jaeger, L., 1983: Monthly and areal patterns of mean global precipitation. *Variations in the Global Water Budget,* A. Street-Perrott, M. Beran, and R. Ratcliffe, Eds., 129–140.

Legates, D.R., and C.J. Willmott, 1990: Mean seasonal and spatial variability in gauge corrected, global precipitation. *Int. J. Climatol.,* **10,** 111–127.

Orville, R.E., and R.W. Henderson, 1986: Global distribution of midnight lightning: September

1977 to August 1978. *Mon. Wea. Rev.*, **114**, 2640–2653

Quayle, R.G., 1974: A climatic comparison of ocean weather station and transient ship records, NOAA, Environmental Data Service, *Mariners Weather Log, 18,* 307–311.

Reed, R.K, 1979: On the relationship between the amount and frequency of precipitation over the ocean. *J. Appl. Meteor.*, **18,** 692–696.

Reed, R.K, and W.P. Elliott 1979: New precipitation maps for the North Atlantic and North Pacific Oceans. *J. Geophys. Res.*, **84,** 7839–7846.

Simpson, J., R.F. Adler, and G.R. North, 1988: A proposed Tropical Rainfall Measuring Mission (TRMM) satellite. *Bull. Amer. Meteor. Soc.*, **69,** 278–295

Spencer, R.W., 1993: Global oceanic precipitation from the MSU during 1979–91 and comparisons to other climatologies. *J. Climate,* **6,** 1301–1326

Tucker, G.B., 1961: Precipitation over the North Atlantic Ocean, *Quart. J. Royal Met. Soc.*, **87**, 147–158

U.S. Navy, 1974–1979: *Marine Climatic Atlas of the World,* Volumes 1–5. U.S. Government Printing Office.

Warren, S.G., C.J. Hahn, J. London, R.M. Chervin, and R.L. Jenne, 1988: *Global Distribution of Total Cloud Cover and Cloud Type Amounts over the Ocean.* National Center for Atmospheric Research Tech. Note NCAR/TN-317+STR, Boulder, CO.

Wilheit, T.T., 1986: Some comments on passive microwave measurement of rain. *Bull. Amer. Meteor. Soc.*, **67,** 1226–1232

Woodruff, S.D., R.J. Slutz, R.L. Jenne, and P.M. Steuer, 1987: A comprehensive ocean-atmospheric data set. *Bull. Amer. Meteorol. Soc.*, **68,** 1239–1250

World Meteorological Organization, 1974: *Manual on Codes, Volume 1.* (WMO Publ. No. 306), WMO, Geneva.

Zipser, E.J, 1994: Deep cumulonimbus cloud systems in the tropics with and without lightning. *Mon. Wea. Rev.*, **122,** 1837–1851

An Intercomparison of Oceanic Precipitation Frequencies from 10 SSM/I Rain Rate Algorithms and Shipboard Present-Weather Reports (IN PREPARATION – PRELIMINARY DRAFT ONLY)

Grant W. Petty*

Purdue University
West Lafayette, Indiana

Abstract

Ten algorithms submitted to the first Precipitation Intercomparison Project (PIP-1) are evaluated with respect to their ability to reproduce global distributions of oceanic precipitation frequency inferred from ship reports. It is found that, while most algorithms yield distributions in reasonable agreement with the ship-derived climatology at low latitudes, the majority fail to register more than very infrequent (~1%) precipitation at latitudes poleward of about 45°. Only two algorithms, both of which were based on the brightness temperature transformations of Petty (1994), succeeded in generally reproducing global patterns at all latitudes. All algorithms, however, appeared to have difficulty reproducing ship-derived precipitation frequencies in the subtropical trades. This problem is tentatively attributed to the unique physical characteristics of precipitation in those regions.

1 Introduction

Considerable effort has been devoted in recent years to the development and validation of satellite rainfall retrieval techniques. The deployment, beginning in 1987, of several copies of the Special Sensor Microwave Imager (SSM/I) was partly responsible for triggering a flurry of new research into the problem of accurately estimating rain rate from passive microwave radiometers. An additional stimulus has been the increasingly apparent need within the climate modeling and global change communities for an accurate climatology of global precipitation. As a result, there are now a number of distinct national and international research programs in place at least partly for the express purpose of furthering the development, validation, and/or dissemination of satellite-derived precipitation products. Prominent examples include the WMO Global Precipitation Climatology Project (GPCP), which to date has sponsored three Algorithm Intercomparison Projects (AIPs) as well as directing the archival and dissemination of various satellite and ground-truth precipitation data bases; NASA's WetNet project, which has sponsored two Precipitation Intercomparison Projects (PIP-1, Barrett et al. 1994a; and PIP-2, in progress); and the Tropical Rainfall Measuring Mission (TRMM; Simpson et al. 1988), which will launch a dedicated rainfall measuring satellite into orbit in the near future.

The potential for passive microwave techniques in particular to more or less directly sense precipitation, and thus mitigate the severe dearth of surface-based precipitation data over the majority of the world's surface, is well-known. Unfortunately, the same lack of surface data has made it difficult to evaluate the actual global performance of competing algorithms.

Nowhere is the problem more acute than over the world's oceans. Algorithms for the passive microwave retrieval of precipitation must generally be developed separately for over water and over land use, owing to the drastically different microwave emissivity characteristics of the two surface types. Whereas only scattering-based microwave algorithms (typically using the 85.5 GHz channels of the SSM/I and sensitive primarily to ice particles in the upper portions of rain clouds) are of practical value over land, the ocean background admits two additional classes – emission-based and attenuation-based algorithms – which are more directly sensitive to cloud and precipitation liquid water below the freezing level. Consequently, numerous over-water rain rate algorithms now exist whose performance cannot be empirically evaluated by any means other than comparison with over-water precipitation observations of some form.

In this study, it is shown that climatological precipitation frequencies, derived from surface ship reports as described by Petty (1995), can be used

*Corresponding Author Address: Grant W. Petty, Earth and Atmospheric Sciences Dept., West Lafayette, IN, 47907-1397

to evaluate certain aspects of the global quality of oceanic rainfall retrievals from the SSM/I. The algorithms considered here include all ten of those for which latitude-time products (along selected meridians) were submitted to the first Precipitation [algorithm] Intercomparison Project (PIP-1) and for which these products were subsequently released in CD-ROM form to participants and other interested parties. In the short time that has elapsed since the PIP-1 exercise, many of these algorithms have undergone significant modification and many new algorithms have been developed. The results presented here are therefore intended primarily to highlight some of the common strengths and weaknesses of seemingly distinct retrieval strategies, as well as to call attention to the regionally dependent nature of the rainfall retrieval problem. An additional motivation of this study is the desire to provide a degree of empirical corroboration for some of the purported advantages of the author's transformed microwave attenuation and scattering indices (P and S, respectively; Petty 1994a,b) in the context of global over-ocean rainfall estimation.

2 Background

Three organized algorithm intercomparisons to date have attempted some degree of uniform validation of multiple microwave rain rate algorithms over water. The first GPCP Algorithm Intercomparison Project (AIP-1) focused on Japan and its neighboring waters during June–August 1989 (Arkin and Xie 1994), and interested satellite algorithm developers submitted visible, infrared, and/or microwave-based rain rate products for that period. Unfortunately, at that time the SSM/I's 85.5 GHz vertically polarized channel was non-functional, thus handicapping or excluding some otherwise viable microwave algorithms. A second AIP focused mainly on the European continent and surrounding waters during February through early April 1991.

For both AIP-1 and AIP-2, SSM/I products were submitted for a relatively small set of individual data swaths. Over water validation consisted of near-coincident coastal radar data scans, and these were sometimes of questionable quantitative value for the few precipitation events that were distant enough to avoid coastal contamination of the over-water microwave retrievals. As a result, the sample size and quality in both AIPs proved somewhat marginal for evaluation of the over-water submissions.

An additional limitation of both AIPs was that intercomparisons were each restricted to rather narrow geographical regions. Good performance of an algorithm in the context of one or both of these studies could not necessarily be extrapolated to the rest of the world's oceans, owing to expected regional, latitudinal, and seasonal variability in precipitation morphology and microphysics, as well as that of other background variables, such as atmospheric water vapor content.

In light of the above limitations, the first Precipitation Intercomparison Project (PIP-1; Barrett et al. 1994a) was notable for its global scope. For PIP-1, gridded global monthly rainfall estimates, at 0.5° resolution, were solicited from all participants for the months of August–November 1987, and these were intercompared both with surface truth data sets (principally gauges) and with other independent satellite- and model-based rainfall estimates and climatologies.

As was the case for the two AIPs, however, the availability of objective over-water validation data was extremely limited in PIP-1, this time consisting of monthly rain gauge totals from a number of atolls and small islands in the western tropical Pacific. The primary available criteria for evaluating over-water algorithm submissions in PIP-1 were therefore (1) statistical comparisons of monthly gridded satellite estimates with the atoll gauge totals, (2) statistical comparison of individual algorithm estimates at each grid point with the ensemble statistics (e.g., mean, extremes) of all submitted products at that point, and (3) subjective assessment of the "reasonableness" of retrieved global rainfall distributions.

Of the above three criteria, only (1) is a quantitatively useful, objective measure of an algorithm's true performance, albeit for a restricted climate regime. If one specifically considers the correlation coefficient between 2.5° satellite rainfall and atoll gauge total, 8 of the 12 distinct SSM/I algorithms submitted to PIP-1 were statistically indistinguishable in performance, all falling within 2–3% of the top correlation (0.91 for grid boxes containing 3 or more atoll observations). RMS errors varied considerably more, but for those algorithms that had good correlation coefficients, a large RMS error may simply reflect an easily correctable calibration bias, as some newer physically based algorithms were submitted without prior empirical calibration.

Yet the available gauge measurements obviously bear only on the performance of competing algorithms under conditions specific to the western tropical Pacific. Indeed, the impressive (and surprisingly similar) atoll correlation results for many PIP-1 algorithms begin to seem less significant when one considers the disparate *global* distributions of

oceanic rainfall retrieved by the same algorithms (Barrett et al. 1994b). Particularly marked were differences in the precipitation retrieved in two regions for which there was no surface validation data: (1) the "dry" subtropical high pressure zones west of North and South America and South Africa, and (2) the oceans poleward of approximately 45° latitude.

Many of the disparities are manifestly due not only to differences in the retrieved *magnitudes* of rain intensity in individual events, but also to sometimes marked differences in the *frequency* and/or *spatial coverage* of non-zero retrievals. It has previously been argued by the author (Petty 1995) that the ability of a microwave rainfall algorithm to correctly retrieve the areal extent of a precipitation event is an even more direct and fundamental measure of the its global robustness than its ability to correctly estimate the monthly rainfall total for a region, since the former achievement is more strongly dependent on the correct isolation of the rainfall signal from other contaminating variables, of which water vapor and ocean surface emissivity variations are perhaps the two most important (Petty 1994a,b).

Fortunately, rainfall frequencies should be considerably easier to verify over the ocean than rainfall amounts, since only qualitative observations of the presence or absence of rainfall are needed for this purpose, rather than calibrated gauge measurements. Routine synoptic weather observations supplied by oceangoing vessels provide by far the most abundant source of such information.

Petty (1995) undertook a statistical analysis of 34 years of shipboard present-weather observations spanning the period 1958–1991 in order to elucidate regional and seasonal differences in the frequency, character, and phase (e.g., frozen vs. liquid) of surface precipitation over the ocean. Although there are several known factors that could introduce modest systematic biases into quantitative climate statistics derived from synoptic ships reports, there are no known reasons to expect such biases to much exceed, say, O(10%) in relative magnitude. There is therefore no compelling reason to question at least the qualitative picture of rainfall frequencies and other characteristics that emerged in the analysis of Petty (1995).

The following comparison of satellite-derived precipitation frequencies with shipboard precipitation frequencies derived according to the methods of Petty (1995) is therefore believed to offer the most substantive basis to date for assessing at least the qualitative performance of multiple satellite rain rain algorithms over those vast oceanic regions for which neither gauge nor radar rainfall estimates are available.

3 Data

3.1 SSM/I Algorithms and Products

A total of 18 satellite-derived rainfall products were submitted to PIP-1, of which 3 were at least partly based on non-SSM/I rainfall information (infrared satellite data, or data from the Microwave Sounding Unit). The primary product evaluated in PIP-1 consisted of gridded global monthly rainfall estimates at 0.5° resolution for the months of August–November 1987.

A secondary set of products solicited from participants included latitude-time and longitude-time grids of instantaneous rain rate at 0.5° spatial resolution for selected lines of longitude or latitude, respectively (Table 1).

Table 1: Longitude bands

169.5–170.0W
99.5–100.0W
59.5– 60.0W
19.5– 20.0W
25.0– 25.5E
95.0– 95.5E

Table 2: Primary literature references for PIP-1 rainfall algorithms examined in this study.

Algorithm	References
ADL	Adler et al. (1993)
BER	Hollinger (1987), Berg and Chase (1992)
D5K	Kidd and Barrett (1990)
FER	Ferriday and Avery (1994)
GWP	Petty (1994a,b)
SJG	Hollinger (1987)
SMI	Smith and Mugnai (1988), Smith et al. (1992), Mugnai et al. (1993)
SM2	Smith and Mugnai (1988), Smith et al. (1992), Mugnai et al. (1993)
WIL	Wilheit et al. (1977), Wilheit et al. (1991), Wilheit et al. (1994)
WSO	Wilheit et al. (1994), Petty (1994a,b)

These products were submitted for 11 of the participating SSM/I algorithms, of which the over-

water component of two algorithms (D5K and XXX) are identical, leaving a total of 10 distinct over-water products. The 10 algorithms and their primary literature references are listed in Table 2. For more detailed descriptions of the algorithms, see Wilheit et al. (1994) and the references cited in Table 2. Individual algorithms will be referred to hereafter by their 3-letter PIP-1 identifiers.

Because of a programming error that was only detected after PIP-1 algorithms and results were written up by Wilheit et al. (1994), it must be noted here that the GWP product, as submitted to PIP-1, was not derived from the full inversion algorithm described by Petty (1994b) but rather from the first-guess rain rate for that algorithm, which is derived from a much simpler 85.5 GHz scattering-based algorithm. This clarification is important for the correct interpretation of the results described below.

Although both hardcopy and computer-readable copies of the latitude-time and longitude-time products were returned to all participants, no quantitative analysis of these was these was ever undertaken as part of the formal PIP-1 validation exercise. Nevertheless, these products are unique among those submitted to PIP-1 in providing an opportunity to analyze the frequency distributions of instantaneous rainfall yielded by the various algorithms and to compare these distributions with those from surface ship reports.

The latitude-time and longitude-time products spanned the same 122-day period (August–November 1987) as the monthly global total rainfall products, but segregated according to whether the satellite was in its ascending or descending leg on a given day. Thus, a maximum of 244 instantaneous rain rate estimates, at $0.5° \times 0.5°$ spatial resolution, were available for each geographic location included in the profiles. However, because successive SSM/I data swaths are non-overlapping at latitudes equatorward of 57°, the true available sample size decreases from 244 at that latitude to slightly more than half that number at the equator.

The primary emphasis in this study is on the fraction of the valid sample from each gridbox for which an algorithm reported a rain rate exceeding some threshold (most commonly zero). In comparing these with ship-derived precipitation frequencies described below, several qualifications must be kept in mind.

First, the frequency of occurrence of precipitation somewhere within a $0.5° \times 0.5°$ box is expected to be somewhat greater than the point frequency of precipitation at the same location, since it is common for an area of that size to be only partially filled by precipitation. The magnitude of the difference is expected to depend on the characteristic spatial scale of the precipitation, which in turn is known to be strongly regionally dependent, as demonstrated for example by the data of Petty (1995). In particular, it is expected that 0.5°-resolution precipitation frequencies, if perfect, would slightly overestimate the point frequency of the typically widespread oceanic precipitation at high latitudes, while strongly overestimating the point frequency of showery precipitation in the subtropical trade belts. The above behavior notwithstanding, the 0.5°-resolution frequency of rainfall exceeding some relatively high threshold of intensity may be expected to *underestimate* the point frequency of the same intensity, since intense rainfall rarely fills more than a small fraction of a ~50 km box. In summary, the overall effect of spatial averaging of point rainfall distributions is to raise the frequency of non-zero rain rates while reducing the frequency of the most intense rain rates.

Secondly, it is rarely, if ever, claimed that any satellite rainfall technique detects *all* precipitation; rather, it is generally assumed only that rainfall greater than some threshold intensity and covering a significant fraction of the SSM/I's field of view (FOV) will be detected. Consequently, *satellite estimates* of 0.5°-resolution precipitation frequency can be expected *a priori* to underestimate the *true* 0.5°-resolution frequency of all precipation by some amount, the amount depending on the ability of the algorithm to detect the lightest precipitation and/or the smaller sub-FOV scale showers. However, the more extreme the underestimate, the more likely it is that only a small, probably regionally dependent, fraction of the actual rainfall will dominate the satellite determination of total rainfall amounts.

Finally, at latitudes poleward of 57°, the frequency of non-zero satellite precipitation estimates obtained from the PIP-1 latitude-time products must necessarily represent an overestimate of a given algorithm's actual retrieved precipitation frequency, since the PIP-1 frequencies are then based on an average of more than one overpass per grid box. For example, given a true rainfall frequency of ~20%, it is possible in principle for a frequency estimate based on an average of two overpasses per grid box to be as high as 36% (i.e., one minus the square of the no-rain frequency of 80%), or 1.8 times the true value. In practice, of course, the potential size of the error will be greatly reduced by (i) the relatively small degree of overlap between pairs of orbits at all but the highest latitudes and (ii) the expected high temporal autocorrelation of rainfall in a high lati-

tude grid box, relative to the satellite orbital period of 104 minutes.

3.2 Shipboard Rainfall Frequencies

The analysis of shipboard observations of present weather to yield climatological estimates of the frequency and other characteristics of oceanic precipitation is described in some detail by Petty (1995). For the purposes of the present study, it is sufficient to point out that personnel aboard numerous merchant and military vessels worldwide have long routinely reported various facets of the weather experienced at the ship's location, using the shipboard synoptic weather code defined by the World Meteorological Organization (e.g., WMO 1974). One element of that code is used to characterize present weather, the most common examples of which include obstructions to visibility and the various forms and intensities of precipitation. Simple tabulation of the frequency of occurrence of various categories of present weather, relative to all valid present weather reports, permits the climatological frequency of occurrence of that class of weather to be estimated.

Unlike the use of gauges and other instruments to measure rainfall amounts or intensities at sea, the subjective assessment by an observer of whether or not precipitation is occurring at the location of the ship is reasonably robust. Potential systematic biases in the reporting of precipitation are postulated to result primarily from the impact of foul weather on ship routes and speeds. While it is difficult to assess the magnitude of such biases globally, comparisons of cloud reports from moving ships with those from nearby fixed weather ships in the North Atlantic and North Pacific have generally revealed at most modest differences (e.g., Warren et al. 1988).

Less robust, is the subjective classification of precipitation intensity by shipboard observers. While some distinct classes of reportable precipitation (e.g., drizzle, snow grains, etc.) are almost invariably associated with extremely low precipitation intensities (hereafter referred to as "drizzle intensity"), true rain or snow is characterized both by larger hydrometeor sizes and by a very broad range of possible precipitation rates. The available present weather codes usually permit a distinction to be made between rain or snow which is "slight" at the time of observation and that which is "moderate or heavy".

According to the Federal Meteorological Handbook for surface weather observations (FMH 1978), the nominal threshold for reporting at least moderate rain is 2.5 mm h^{-1}. In practice, however, it seems likely that an observer's subjective perception of intensity in a given case is at least partly measured against what that observer has typically experienced in the recent past. Also, the intensity of snowfall is determined often based on visibility rather than accumulation rate, with a threshold of 5/8 statute mile (in the absence of another obstruction to visibility, such as fog or haze) defining the transition from light to moderate intensity. Petty (1995) pointed out that a threshold of 1 mm h^{-1} or less might have to be assumed to bring the high latitude reporting of moderate to heavy precipitation (to which snowfall is a significant contributor) into line with standard climatologies. Such a precipitation rate threshold would seem somewhat inconsistent with either the nominal visibility or intensity thresholds for non-drizzle precipitation. Of course, the reliability of the climatologies themselves in these data sparse regions has never been established beyond doubt.

Despite the greater potential for reporting biases, it will be useful to compare the satellite-derived frequency of precipitation with that of various intensity classes reported by ships, in addition to comparing them with the more robust ship-derived frequencies of all precipitation. The assignment of intensity class to specific present weather codes is described by Petty (1995).

In addition to the occurrence of local precipitation at the actual time of the observation, present weather codes are available for the reporting of (i) precipitation observed in the vicinity of the ship at the time of the observation and (ii) precipitation observed at the ship during the hour preceding the time of the observation. Because precipitation observed during the preceding hour often persists somewhere in the vicinity of the station, both categories may be regarded as reflecting on the probability that precipitation is present not too far from the station at a given point of time. Thus, the inclusion of these reports not only increases the nominal precipitation frequency significantly but may also yield a product more conceptually compatible with the 0.5°-resolution precipitation frequencies represented by the PIP-1 products.

The single more important factor limiting the usefulness of surface ship reports as validation for satellite precipitation frequencies is sample size. While certain regions of the North Atlantic and North Pacific oceans, as well as a few major shipping lanes elsewhere, are heavily sampled in the course of a single year, reports from the majority of the world's ocean areas, particularly the South Pacific and Antarctic oceans, are quite sparse. In such re-

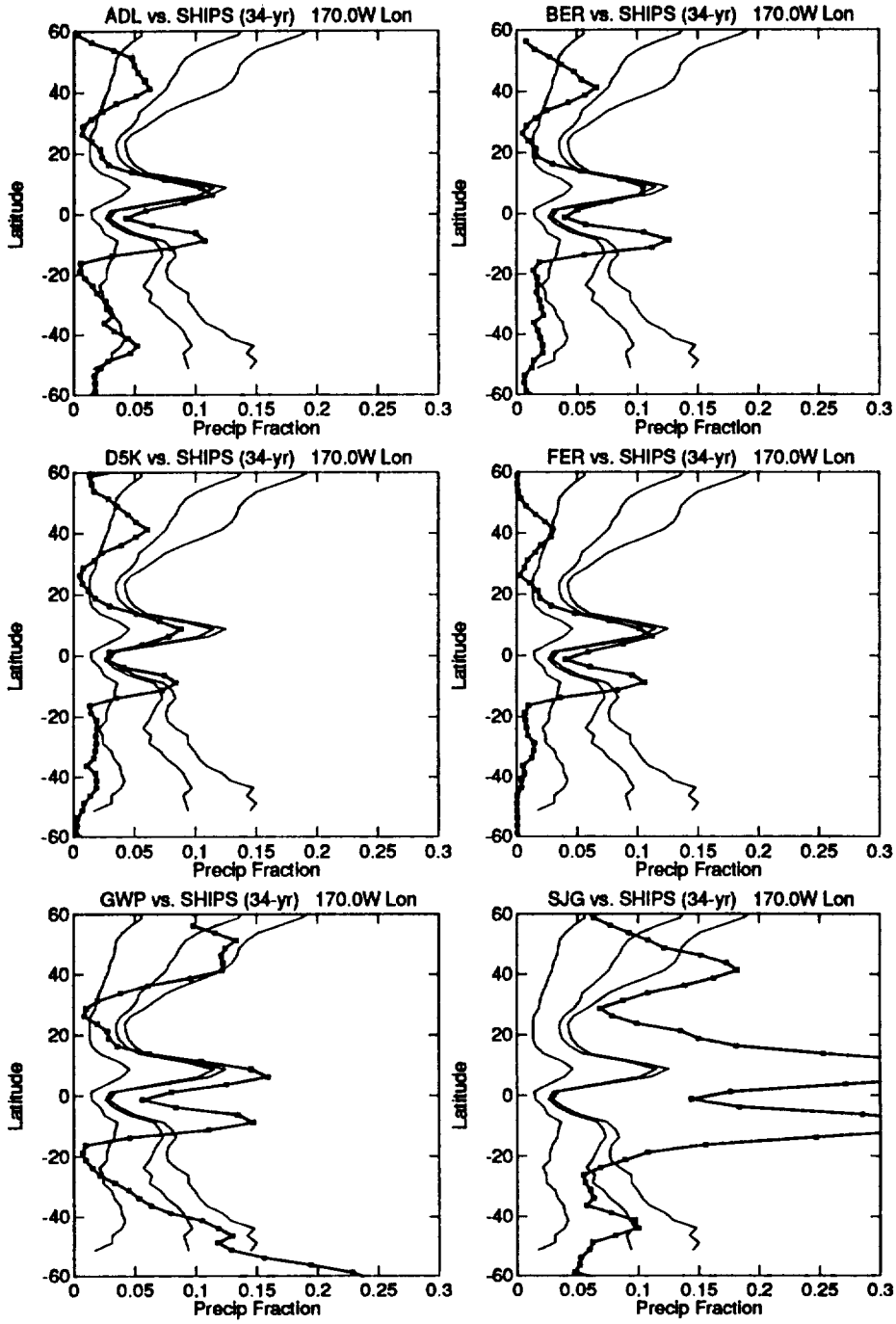

Fig. 1: Latitudinal profiles of precipitation frequency (or fraction) at 170°W longitude for the months of August–November, as derived from SSM/I retrievals submitted to PIP-1 for 1987 (thick line with square markers) and from a 34-year climatology of surface ship present weather reports (thin lines). In order of decreasing fraction, the thin lines represent (1) ship reports indicating local precipitation of any intensity at the time of the observation, (2) precipitation reports of greater than "drizzle" intensity, and (3) precipitation of moderate or heavy intensity.

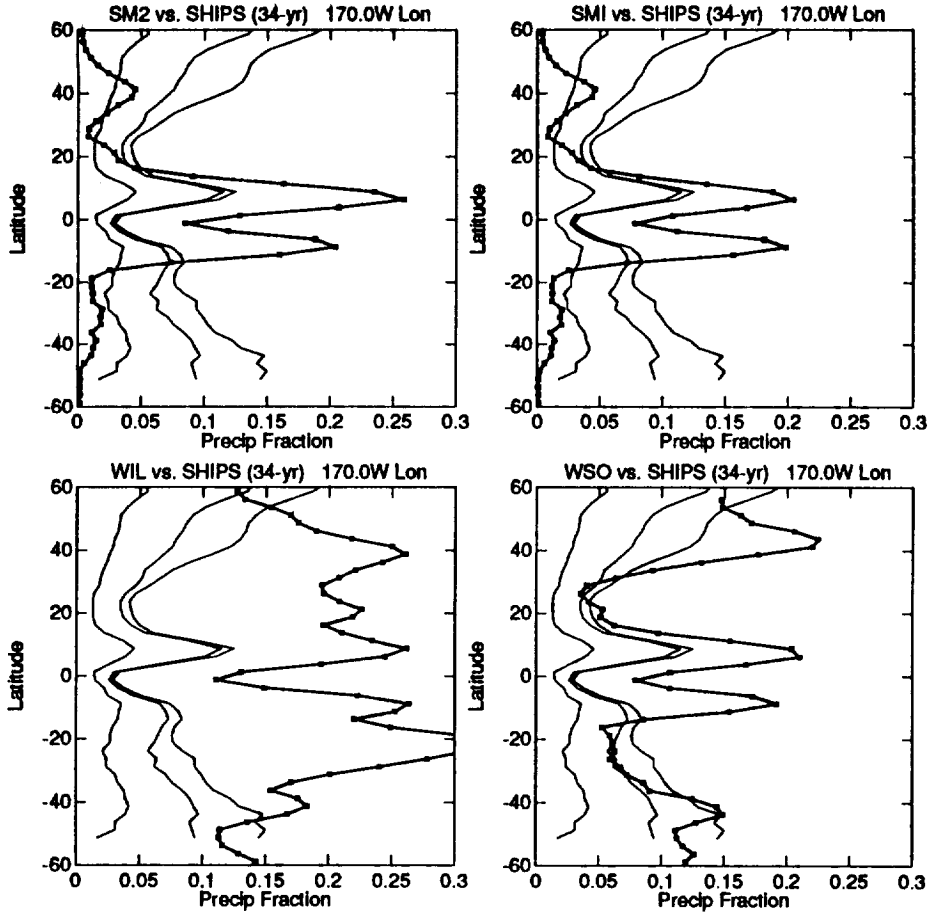

Fig. 1: (continued)

gions, a satisfactory sample size can be achieved only at the expense of spatial and/or temporal resolution.

The approach employed in this study is to average ship-derived precipitation frequencies within boxes of 7.5° latitude × 12.5° longitude, centered on the 0.5°wide latitudinal or longitudinal strips for which the PIP-1 products were derived. The use of a more generous longitudinal averaging dimension is justified by the generally weaker zonal gradients in oceanic precipitation, as contrasted with rather sharp meridional gradients in the vicinity of the Intertropical Convergence Zone (ITCZ) and elsewhere. In addition to averaging spatially, frequencies were averaged for the four calendar months (August–November) employed in the PIP-1 intercomparisons.

Two sets of products were generated according to the above procedures. The first is a climatological precipitation frequency product covering the entire 34-year period of 1958–1991; the second product is limited to the PIP-1 period of August–November 1987. Because of its substantially larger sample size, the climatological product is the most useful one for assessing the general global performance of the satellite algorithms. However, this product cannot resolve interannual variations that might have perturbed local rainfall frequencies way from their climatological means during 1987. The single-year product should capture such anomalies, but can do so only in those heavily trafficked regions for which a ~30-fold reduction in sample size still yields adequate statistics.

In the calculation of precipitation frequencies, the sample was considered adequate if a minimum of 2 instances of the target category appeared in the sample. Based on a confidence limit of 68%, this yields a worst case statistical uncertainty in the estimated frequency of slightly better than a factor of 2, almost independent of total sample size. In any given case, the robustness of the statistics can also be judged from the degree of statistical "noisiness" in the graphically depicted frequency profiles discussed below.

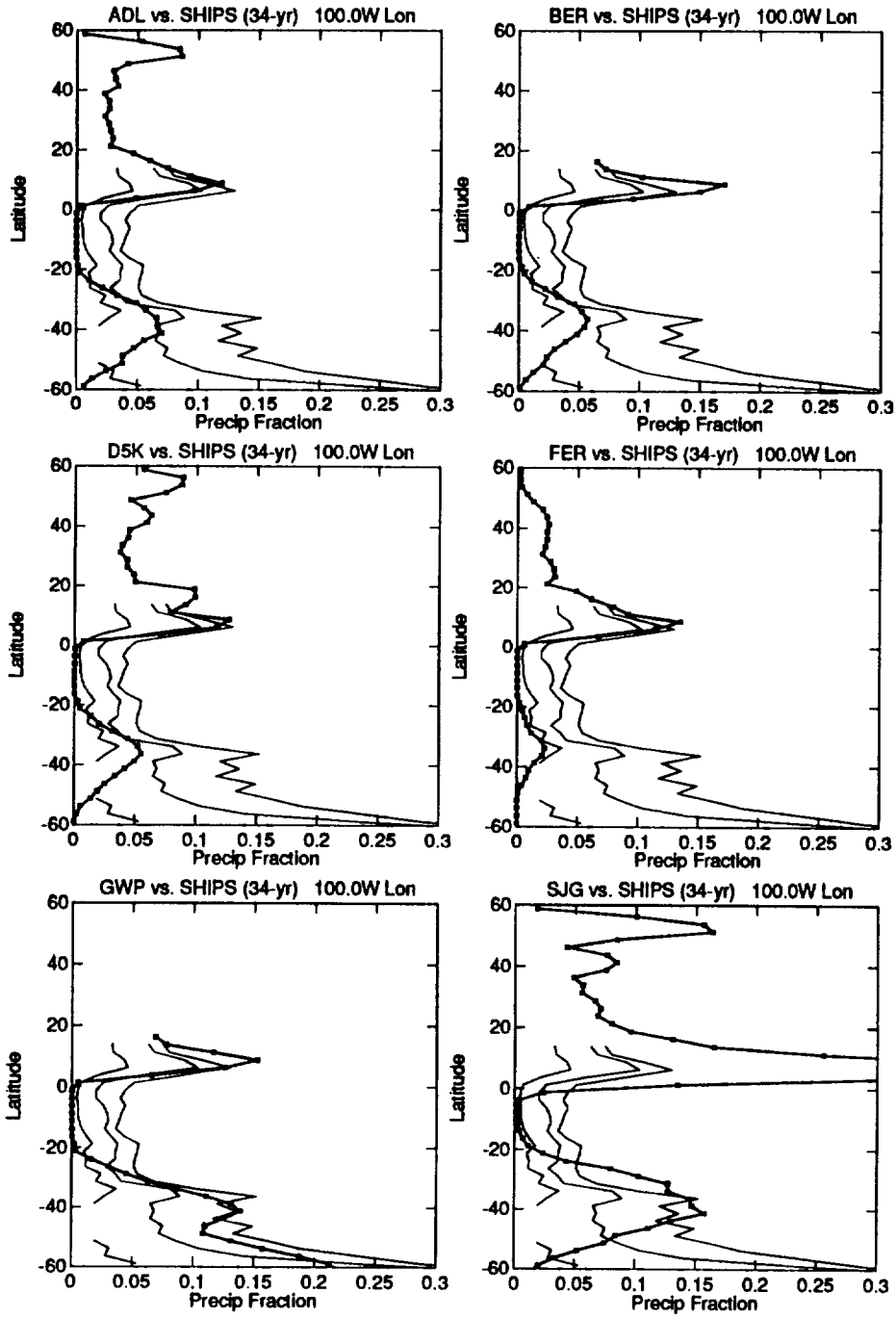

Fig. 2: Same as Fig. 1, except profile is for 100°W longitude

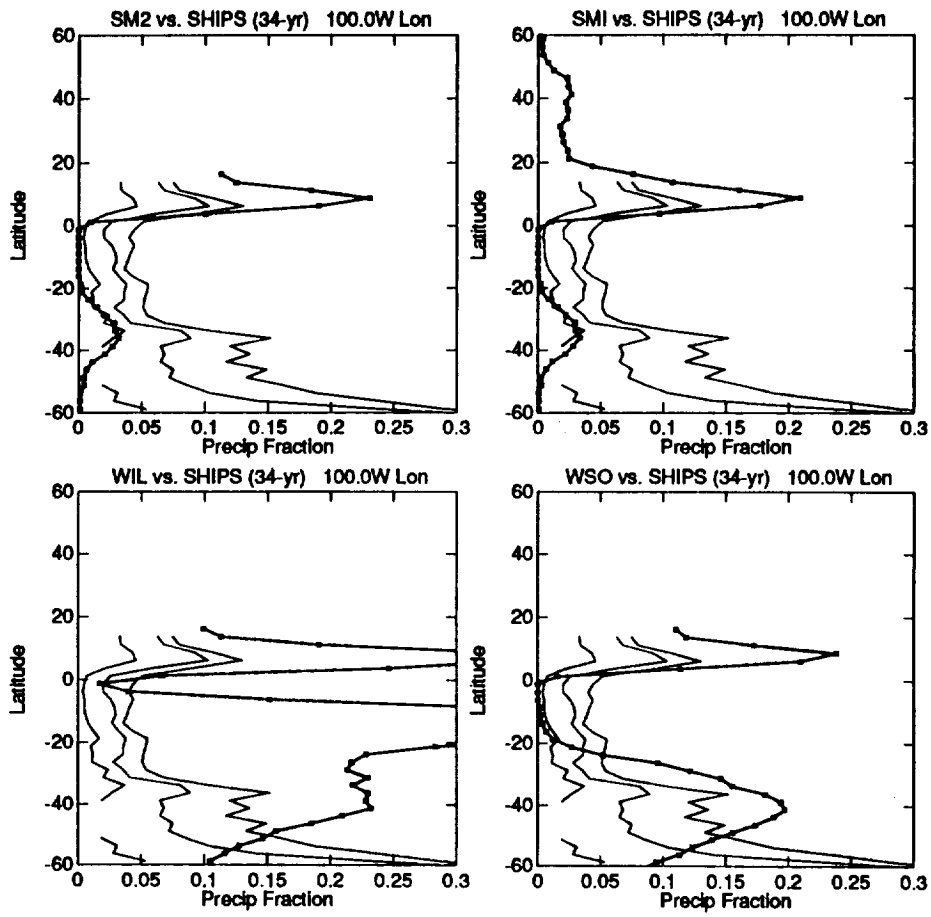

Fig. 2: (continued)

4 Results

4.1 Comparisons with 34-year precipitation frequencies

Figures 1–4 depict profiles of satellite-derived (for ASON 1987) and ship-derived precipitation frequency (ASON, 34-year) as functions of latitude for the 4 meridional stripes that are predominantly over ocean (170W, 100W, 20W, 95E). In each case, the satellite results (heavy lines with markers) are compared with the frequency of ship reports indicating (i) local precipitation of any intensity at the time of the observation, (ii) precipitation of greater than "drizzle" intensity, and (ii) precipitation of moderate or heavy intensity.

It is apparent from all of the above figures that most algorithms capture at least the general shape of the latitudinal distribution of precipitation frequency in the tropics between 10S and 10N latitude, in particular the Intertropical Convergence Zone (ITCZ). Within the ITCZ, the agreement in both shape and magnitude is particularly remarkable for the ADL, BER, D5K, FER algorithms. GWP, SMI, SM2, and WSO also yield reasonable ITCZ shapes, but the overall frequencies are larger, by varying degrees, than those derived from the 34 year record of ship reports. Recall, however, that because of the different interpretations of the satellite and ship-derived frequencies (the first is the frequency in a 0.5° grid box, whereas the latter is a point frequency), perfect agreement is not necessarily to be expected.

The above qualification notwithstanding, two algorithms (WIL and SJG) do appear to grossly overestimate precipitation occurrence in the ITCZ. In addition, WIL exhibits significant problems with the shape of the latitudinal profile, apparently because of a tendency to retrieve very light (<1 mm h^{-1}) rainfall almost continuously over many regions of the ocean. Because of the latter problem, which was already recognized in the course of the PIP-1

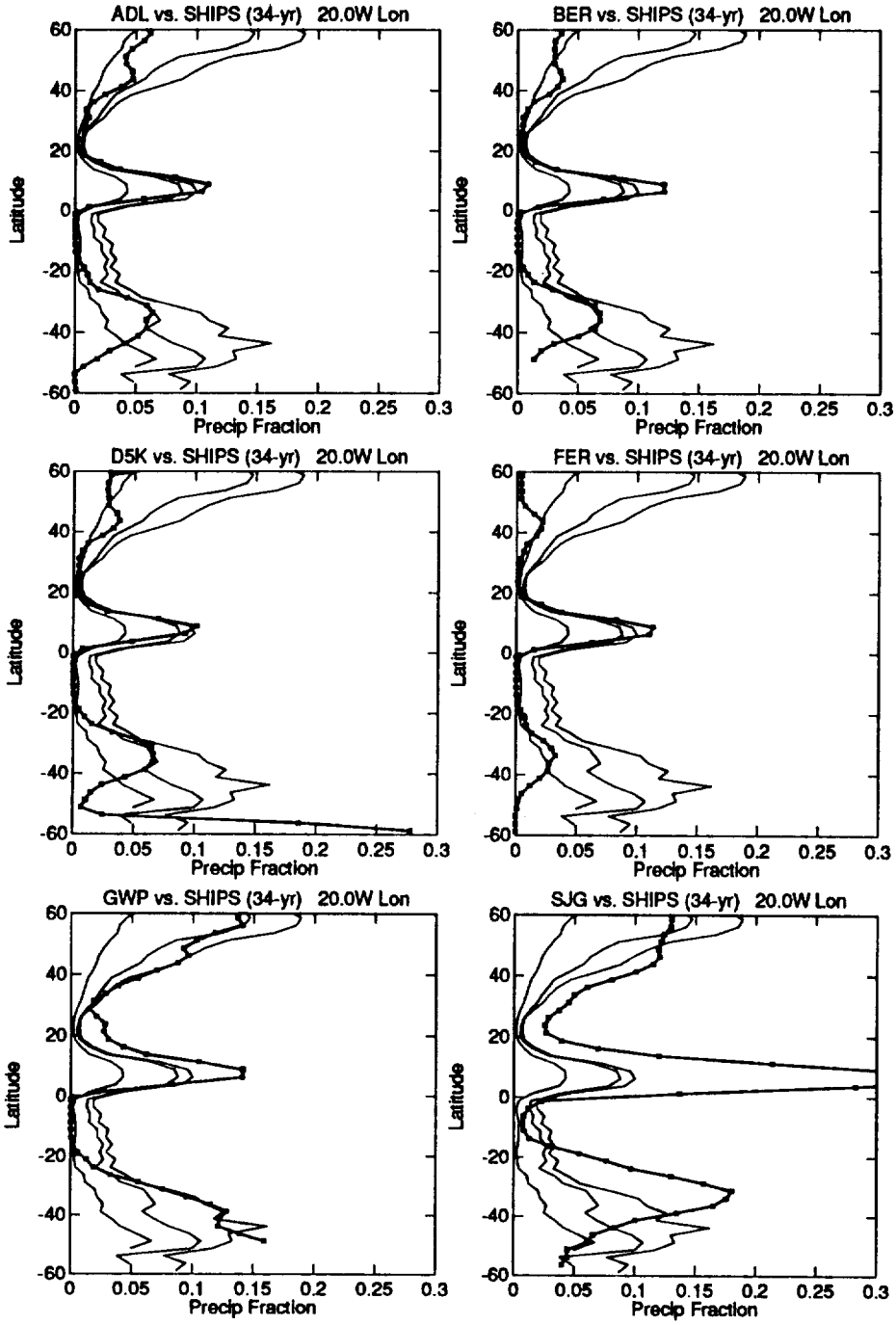

Fig. 3: Same as Fig. 1, except profile is for 20°W longitude

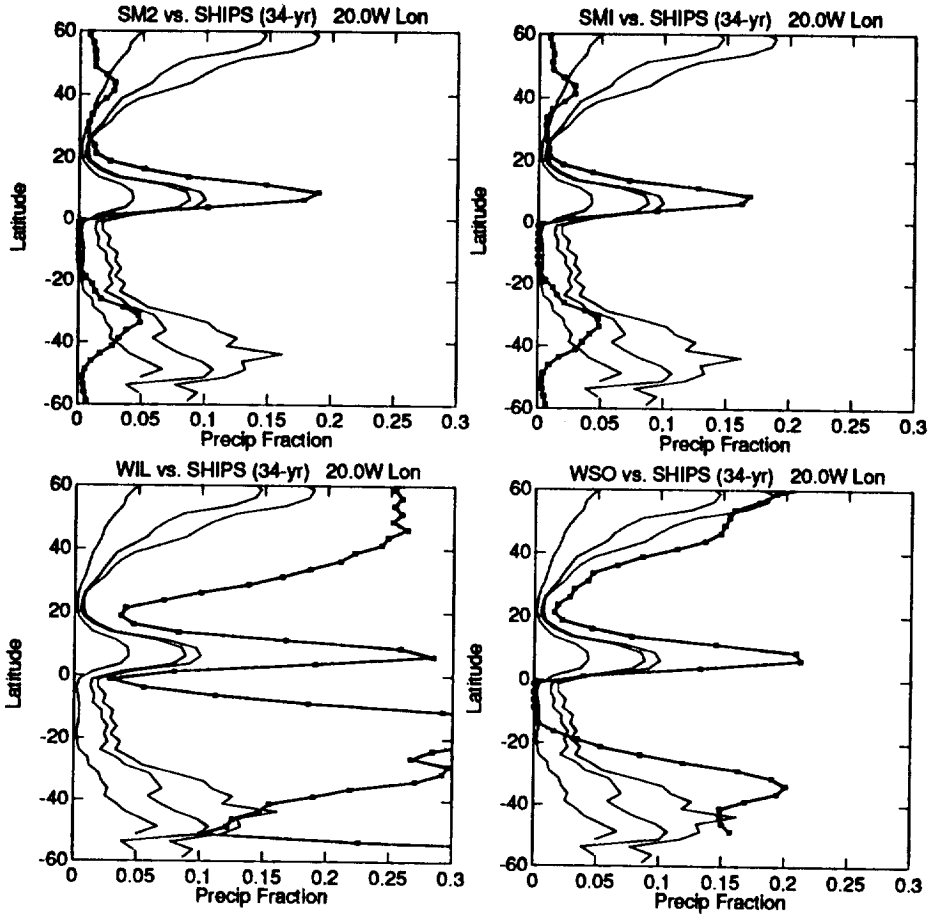

Fig. 3: (continued)

results analysis (Barrett et al. 1994), the rainfall frequency characteristics of the WIL algorithm will not be considered in further detail below.

Despite the large frequencies indicated SJG, the general shape of the profiles is not unreasonable. Nevertheless, it is difficult to explain a factor of 2–3 overestimate of precipitation frequency without concluding that that algorithm may be responding at least partly to microwave signatures other than that of precipitation alone; for example, non-precipitating cloud water or water vapor.

A common feature of all algorithms, other than WIL and SJG, is a nearly complete failure to detect any rainfall whatsoever between the equator and approximately 15S at either 100W (Fig. 2) and 20W (Fig. 3). At both longitudes, the latitude range in question corresponds to the semi-permanent subtropical high pressure zones located to the west of South America and Africa, respectively. In striking contrast to the satellite-derived frequencies, the ship-derived frequencies indicate that precipitation occurs within these regions a significant fraction of the time, with typical frequencies over 34 years being approximately 4–5% for all precipitation, 2–3% for non-drizzle precipitation, and approximately 1% for precipitation of moderate or heavy intensity. While such an apparent discrepancy might be ascribed to interannual variability (i.e., the assumption that ASON 1987 was an anomalously dry period in the region in question, relative to the 34 year climatology), the true explanation appears to lie in the physical and spatial properties of precipitation within those regions. This point will be examined again in a later section.

Also in stark contrast with the precipitation frequencies yielded by most, but not all, algorithms is the tendency of ship-derived precipitation frequencies to increase steadily from the subtropics to the high latitudes. Indeed, the ship climatology indicates that precipitation is more frequent poleward of 40° latitude than it is within the ITCZ. Excluding WIL, only one algorithm (GWP) reproduces

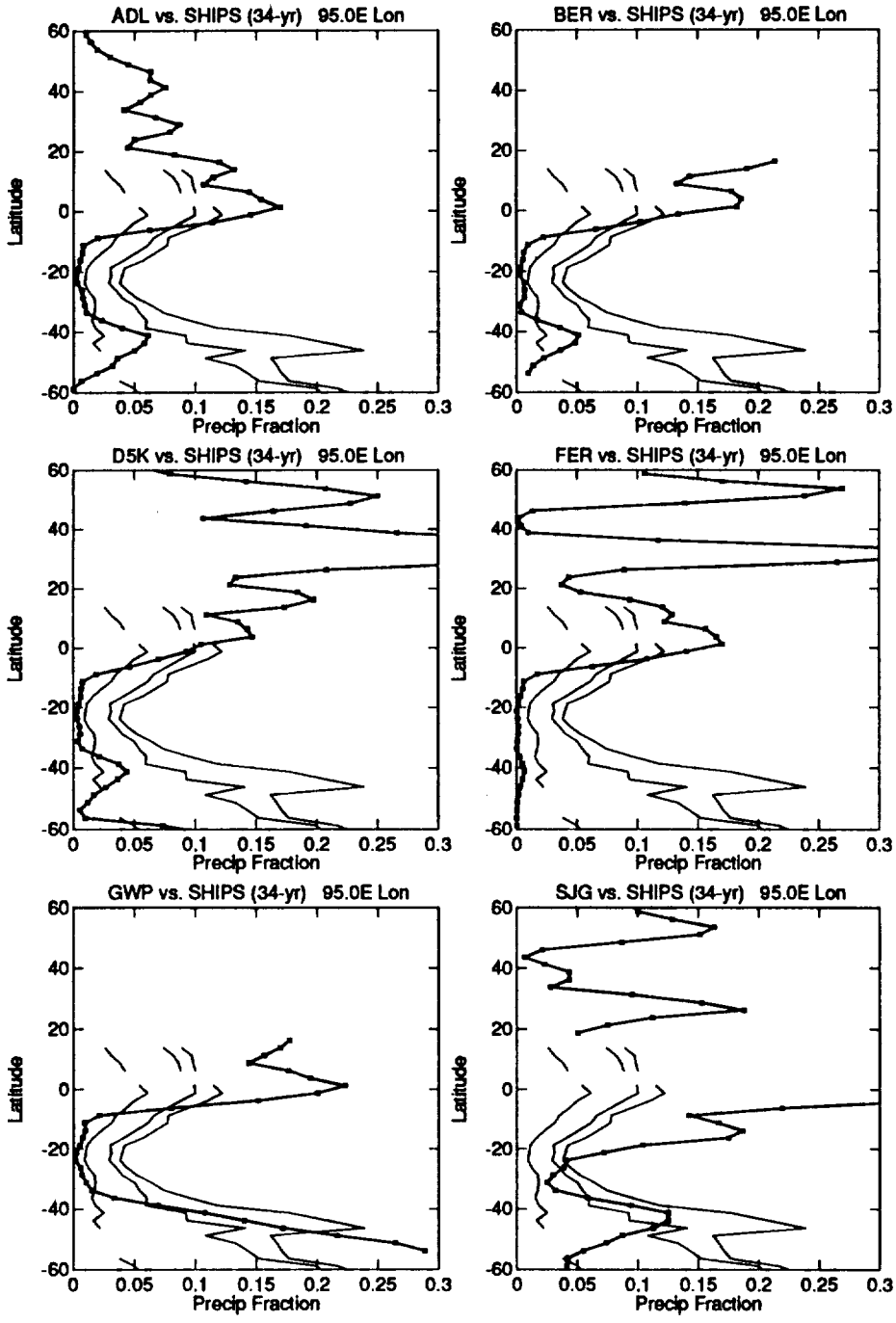

Fig. 4: Same as Fig. 1, except profile is for 95°E longitude

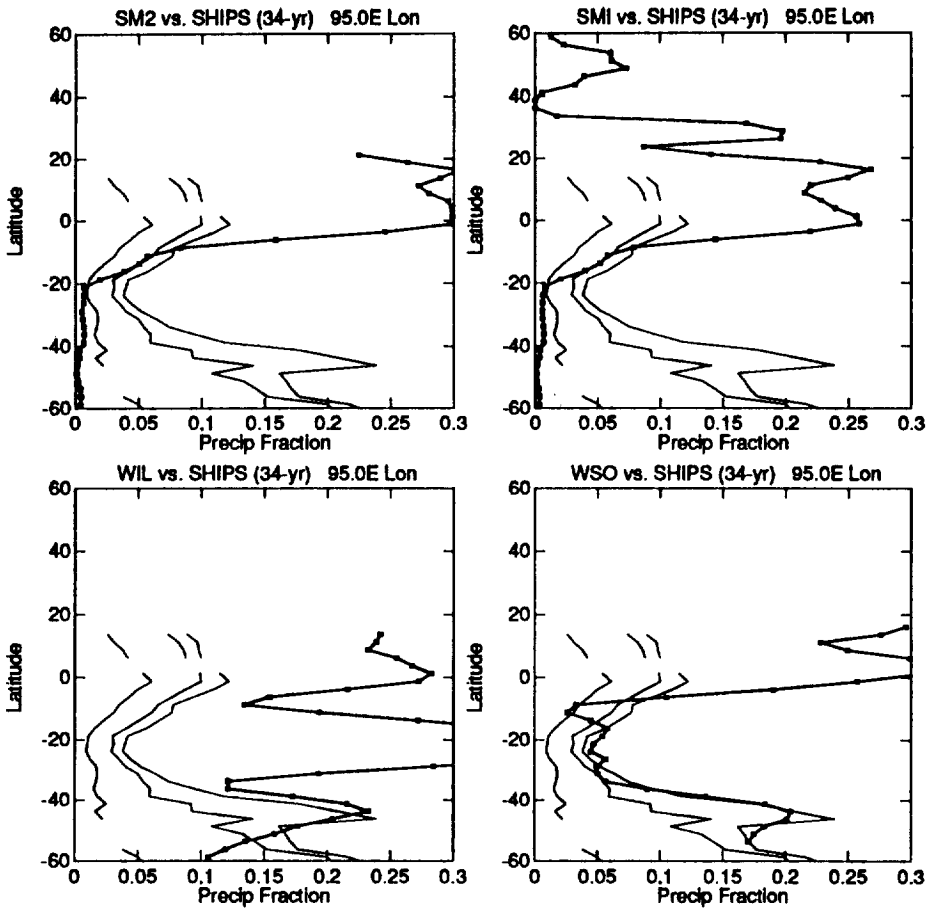

Fig. 4: (continued)

this relationship. General agreement between WSO and the ship-derived frequencies is also good within this latitude belt, although WSO still finds somewhat slightly less precipitation there than in the ITCZ. SJG exhibits reasonable frequencies between 20° and 40° latitude, but this observation must be interpreted cautiously in light of the extreme overestimates made in the ITCZ. Furthermore, SJG yields frequencies that sharply drop off poleward of 40°, a trend that is opposite to that suggested by the ship reports.

All of the remaining algorithms (ADL, BER, D5K, FER, SMI, and SM2) excepting GWP and WSO appear to grossly underestimate the frequency of precipitation of all intensities north of about 40N and south of about 30S. For many of these algorithms, the satellite frequencies are in considerably better agreement with the ship-derived frequency of *moderate to heavy* precipitation. In particular, ADL, BER, and D5K appear to generally reproduce the northern hemisphere frequencies of moderate to heavy precipitation with good accuracy at 20W (Fig. 3), though the agreement elsewhere is less striking.

In general, FER, SMI, and SM2 appear to miss a sizable fraction of even moderate to heavy precipitation at high latitudes. Indeed, these same algorithms find almost no precipitation whatsoever south of 20S at 95E longitude (Fig. 4), despite a significant (2–5%) climatological frequency of moderate to heavy precipitation there.

Overall, only two algorithm – GWP and WSO – stand out in Figs. 1–4 as providing reasonable overall estimates of total precipitation frequency (all intensities) at most latitudes, the only exception being the "dry" subtropical high pressure zones which, as noted, appear to be problematic for all algorithms. Of the two algorithms, WSO appears to be more prone to overestimating precipitation frequencies at some locations. However, it is again difficult to ascribe real significance to the observed differences from climatology, both because of the coarser spatial

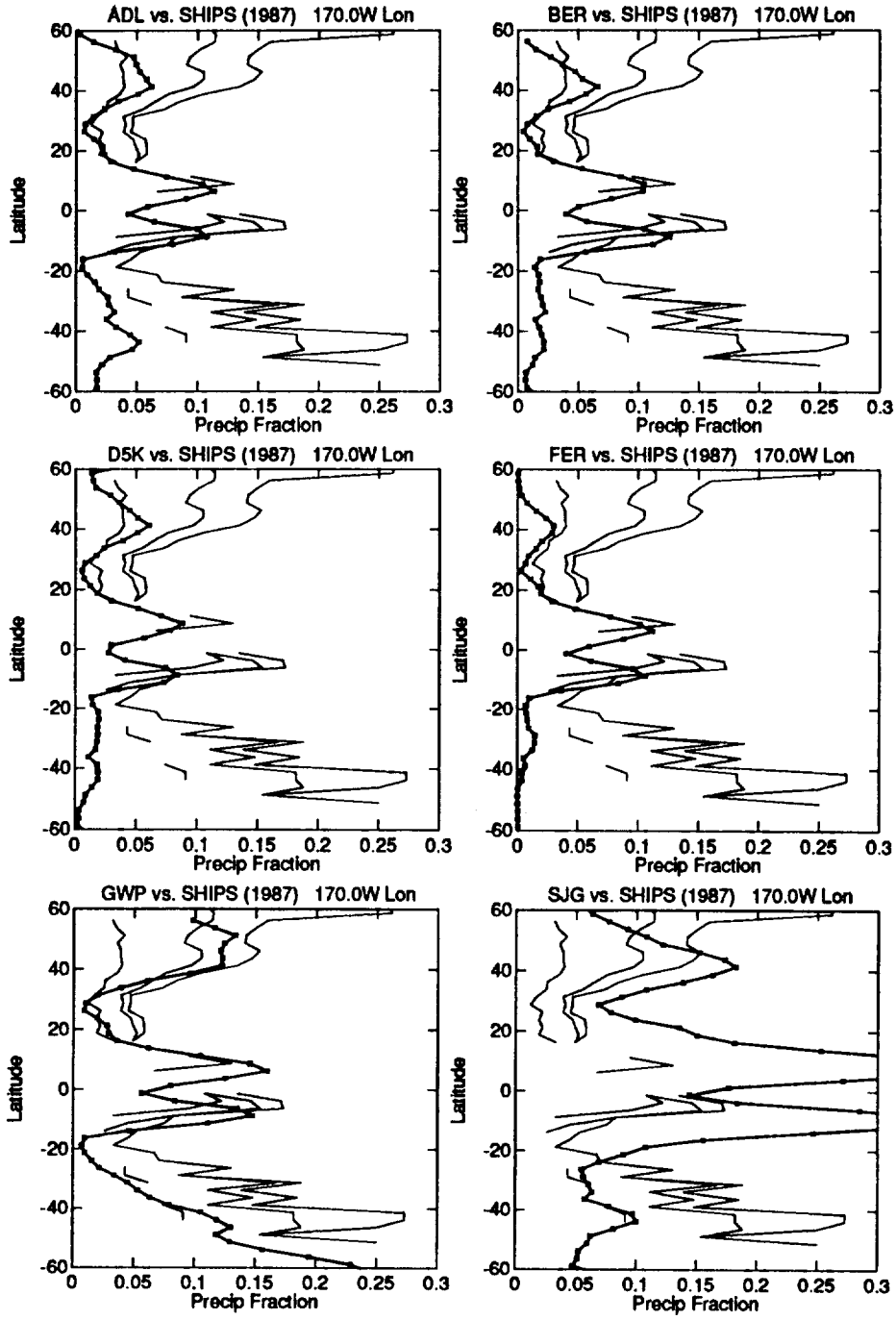

Fig. 5: Same as Fig. 1, except shipboard precipitation frequencies are derived from PIP-1 period during 1987 only.

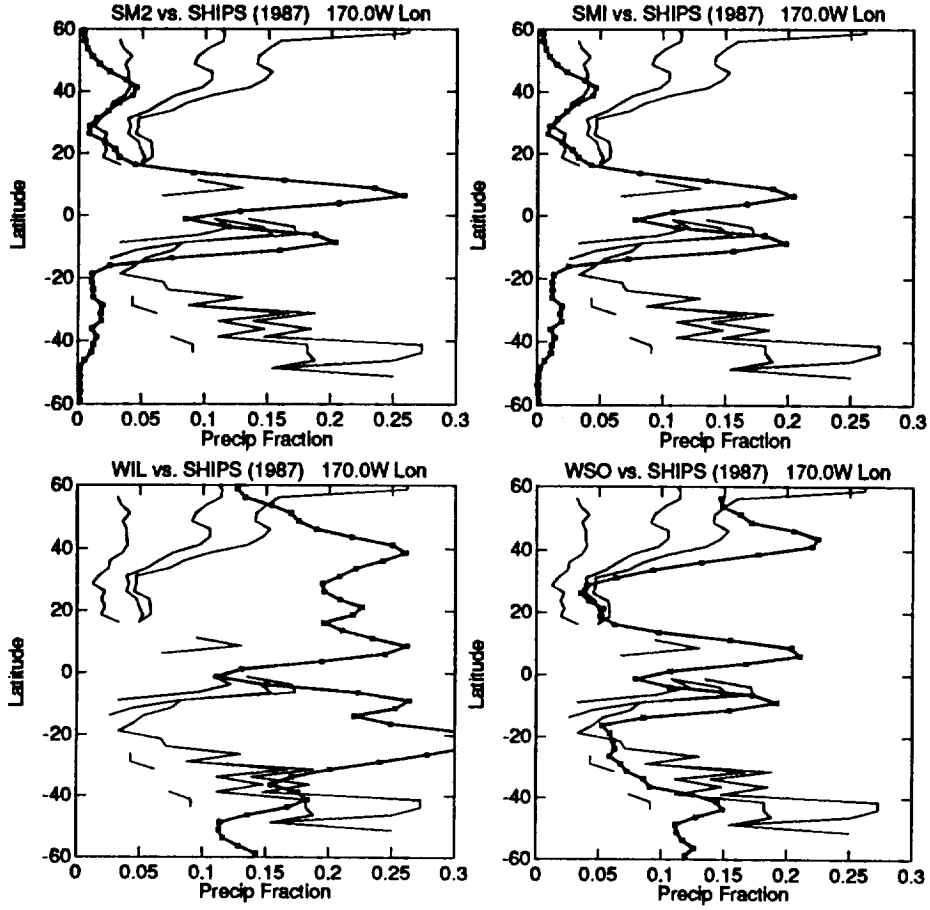

Fig. 5: (continued)

resolution of the satellite frequency estimates and because of the complication introduced by possible interannual variability.

4.2 Comparisons with 1987 precipitation frequencies

Because of the possibility that oceanic precipitation distributions during the period covered by PIP-1 might have been anomalous, relative to the 34 year period covered by the ship climatology, additional precipitation frequency profiles were generated using ship reports from August–November 1987 only. The use of a single 4-month period greatly reduces the area of the ocean over which a useful statistical sample is obtained; consequently, graphical depictions of the latitudinal profiles of shipboard precipitation frequencies are useful only for 170W and 20W (Figs. 5 and 6). Even in these cases, the profiles exhibit greater statistical noisiness than for the 34-year results, though the general trends and magnitudes are still clearly evident.

Despite the less robust statistics, several important differences between the 1987 results and the 34-year results can be discerned. For example, whereas the southern branch of the ITCZ at 170W appears significantly weaker than the northern branch in the 34-year climatology (Fig. 1), the difference between the two branches appears much smaller in the 1987 data (Fig. 5). The overall agreement in shape with all of the algorithm results is thereby improved at this location. Also, the overall frequencies in the ITCZ increase somewhat, favoring those algorithms (GWP, SMI, SM2, and WSO) that previously appeared to slightly overestimate the frequency relative to climatology (Fig. 1). On the other hand, no such improvement is noted in the ITCZ frequencies at 20W (cf. Figs. 3 and 6), though five algorithms (ADL, BER, D5K, FER, and GWP) remain consistent with the shipboard frequencies to well within a factor of two.

More dramatic is the improvement in agreement

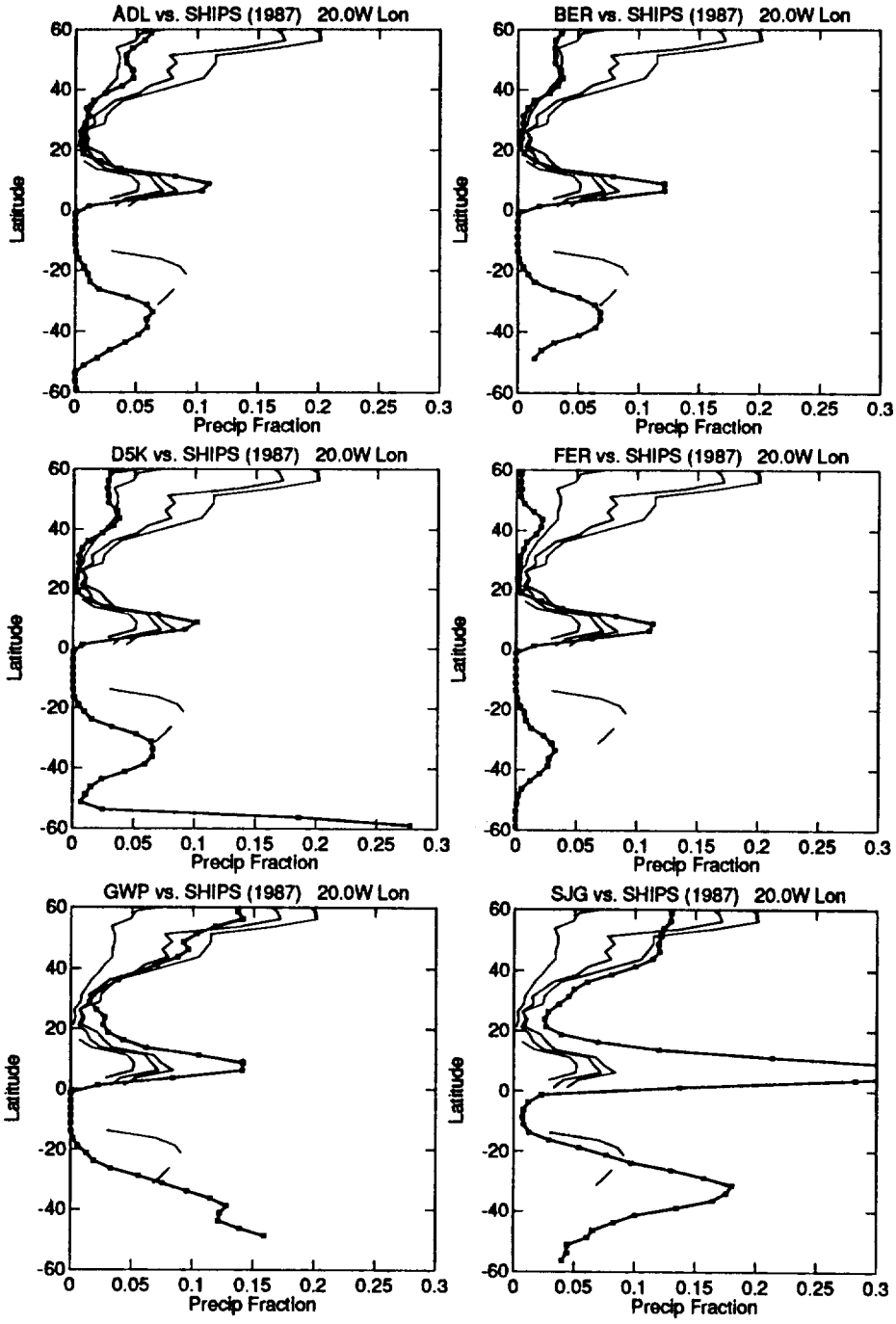

Fig. 6: Same as Fig. 3, except shipboard precipitation frequencies are derived from PIP-1 period during 1987 only.

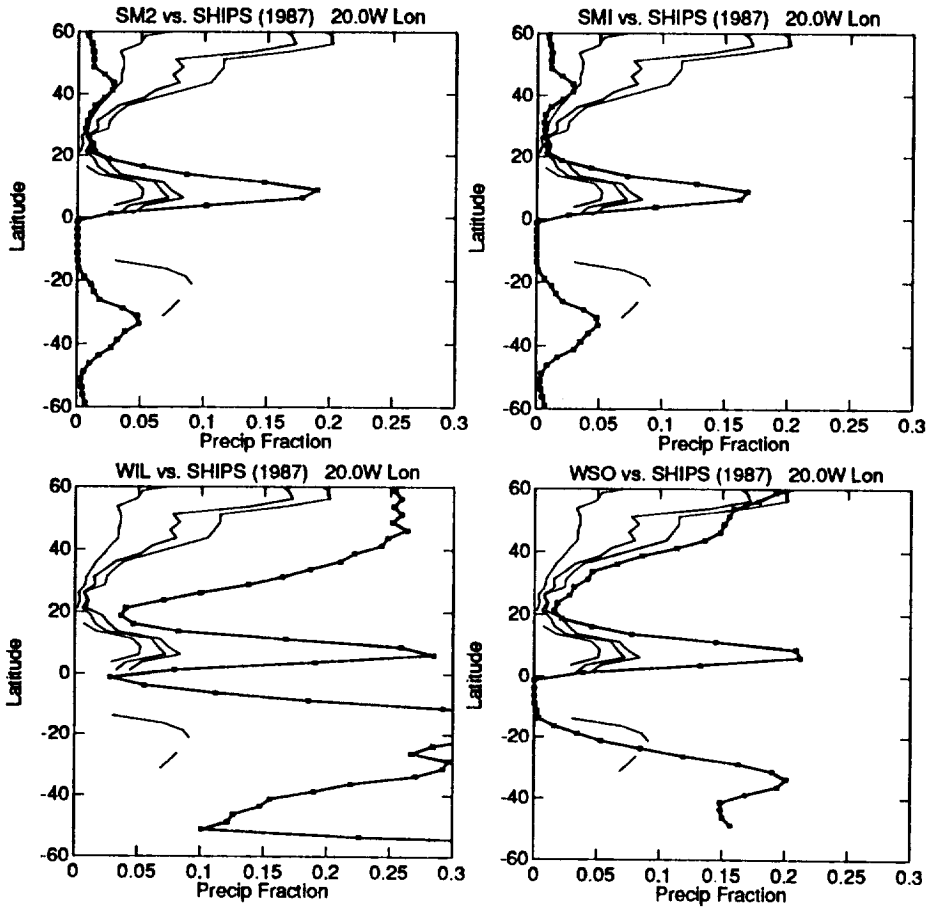

Fig. 6: (continued)

outside the tropics. At both 170W and 20W (Figs. 5 and 6), three algorithms (ADL, BER, and FER) appear to reproduce the latitudinal distribution of moderate to heavy precipitation in the northern extratropics with striking accuracy. In the same latitude belt, GWP and WSO, and to a lesser extent SJG, appear to excel at accurately reproducing the distribution of precipitation of *all* intensities. Although the statistics are noisier in the southern hemisphere, GWP and WSO both appear to be the only algorithms giving a reasonable representation of the distribution of precipitation of all intensities at 170W (Fig. 5), though again WSO shows a tendency to overestimate at some locations.

At 20W, the interpretation of the results in the southern hemisphere is less clear. An acceptable sample of ship reports was found only for the short latitude segment between 15S and 30S. Within this segment, the shape and magnitude of the frequency distribution within this latitude does not appear to be consistent with the results from any algorithm, nor is it consistent with the longer term frequencies in Fig. 3. One plausible explanation is that the feature is just a statistical artifact resulting from the small sample size. Another possibility is that there was indeed an anomalously high frequency of precipitation at that location during 1987, but that it was associated with cumulus-scale tradewind-type showers that are too small to be resolved by the satellite microwave observations (see section 5.2).

4.3 Overall global performance

In order to quantify the degree of global consistency between satellite-derived and ship-derived precipitation frequencies over ocean, pooled comparison statistics were computed for all 6 longitudes in Table 1 (including those not appearing in Figs. 1-6), based on all latitude segments, at each longitude, for which the sample of ship reports was deemed satisfactory according to the criterion given earlier. This was done both for the 34-year (ASON) ship clima-

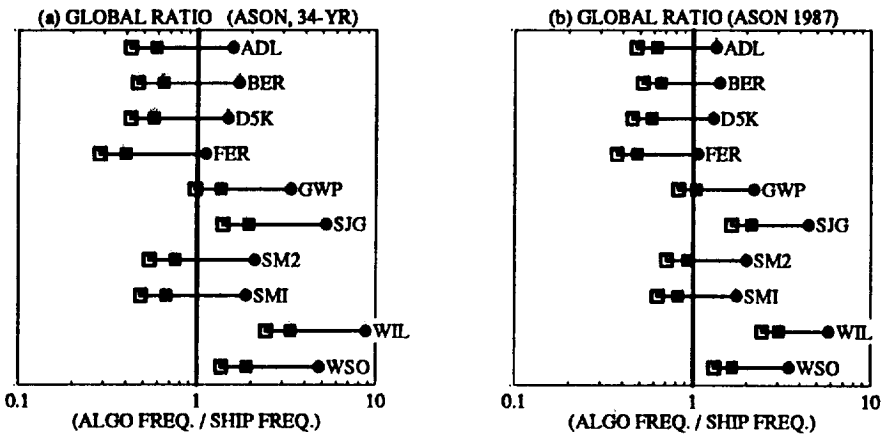

Fig. 7: Ratio of the global frequency of non-zero precipitation rate yielded by each algorithm to the global ship-derived frequencies of (i) all precipitation (left marker), (ii) precipitation of greater than drizzle intensity (middle marker), and (iii) precipitation of moderate to heavy intensity (right marker). (a) Comparison data set corresponds to (a) the 34-year climatology for ASON or (b) ASON 1987 only

tology and for the restricted period of ASON 1987. In the latter case, the comparison sample is much less representative geographically on account of the inadequate sample size over many regions, but this disadvantage is partially offset by the exclusion of interannual variability as a source for some differences.

Figure 7 depicts the ratio of the global frequency of non-zero precipitation rate yielded by each algorithm to the global ship-derived frequencies of (i) all precipitation, (ii) precipitation of greater than drizzle intensity, and (iii) precipitation of moderate to heavy intensity. Consistent with the meridional profiles presented earlier, it is seen that all but 4 algorithms (GWP, SJG, WIL, and WSO) significantly underestimate the overall frequency of precipitation of light intensity. All 10 algorithms, however, yield global frequencies that are at least as large as the global ship-derived frequency of moderate/heavy precipitation. One algorithm however (FER) yields an overall precipitation frequency which is only barely greater than the ship-derived frequency of moderate/heavy precipitation, suggesting that this algorithm misses most light precipitation.

As noted earlier, three algorithms (SJG, WIL, WSO) yield frequencies of non-zero rain rate that exceed even the climatological frequency of drizzle intensity precipitation, implying that these must be frequently finding at least light rain in areas where no rain in fact is present. Only one algorithm (GWP) finds precipitation with a frequency that is very close to the ship-derived frequencies of either drizzle-intensity or light precipitation.

For the three algorithms that appear to overestimate total precipitation frequency, intensity thresholds were found which, when applied to the gridded latitude-time products, reduce the global satellite-derived precipitation frequencies to values approximating the ship-derived frequencies of each intensity class. Similarly, thresholds were found which optimized the agreement between all algorithms and the observed frequency of moderate/heavy precipitation. These thresholds are given in Table 3.

The use of empirically determined thresholds to normalize the global precipitation frequencies from each algorithm to a common value eliminates an important ambiguity in any intercomparison of the satellite-derived precipitation frequencies. In particular, it allows the underlying ability of an algorithm to correctly depict spatial variations in the frequency of precipitation of various intensities to be evaluated without undue sensitivity to either the mean magnitudes of the retrieved rain rates or to problems of the type experienced by the SJG, WIL, and WSO algorithms. Of course, an *a posteriori* threshold applied to the PIP-1 products cannot solve the problem of severe *underestimates* of the frequency of light precipitation, as exhibited by ADL, BER, D5K, FER, SMI, and SM2. It must also be recalled that the above thresholds for normalizing the frequency of retrieved precipitation on a 0.5° grid should not necessarily be equated with optimal thresholds for discriminating rain at the resolution of individual SSM/I pixels. Finally, it is clear from Figs. 1–6 that a threshold that optimizes the global frequency of precipitation for an algorithm may be quite different than one that optimizes the frequency within

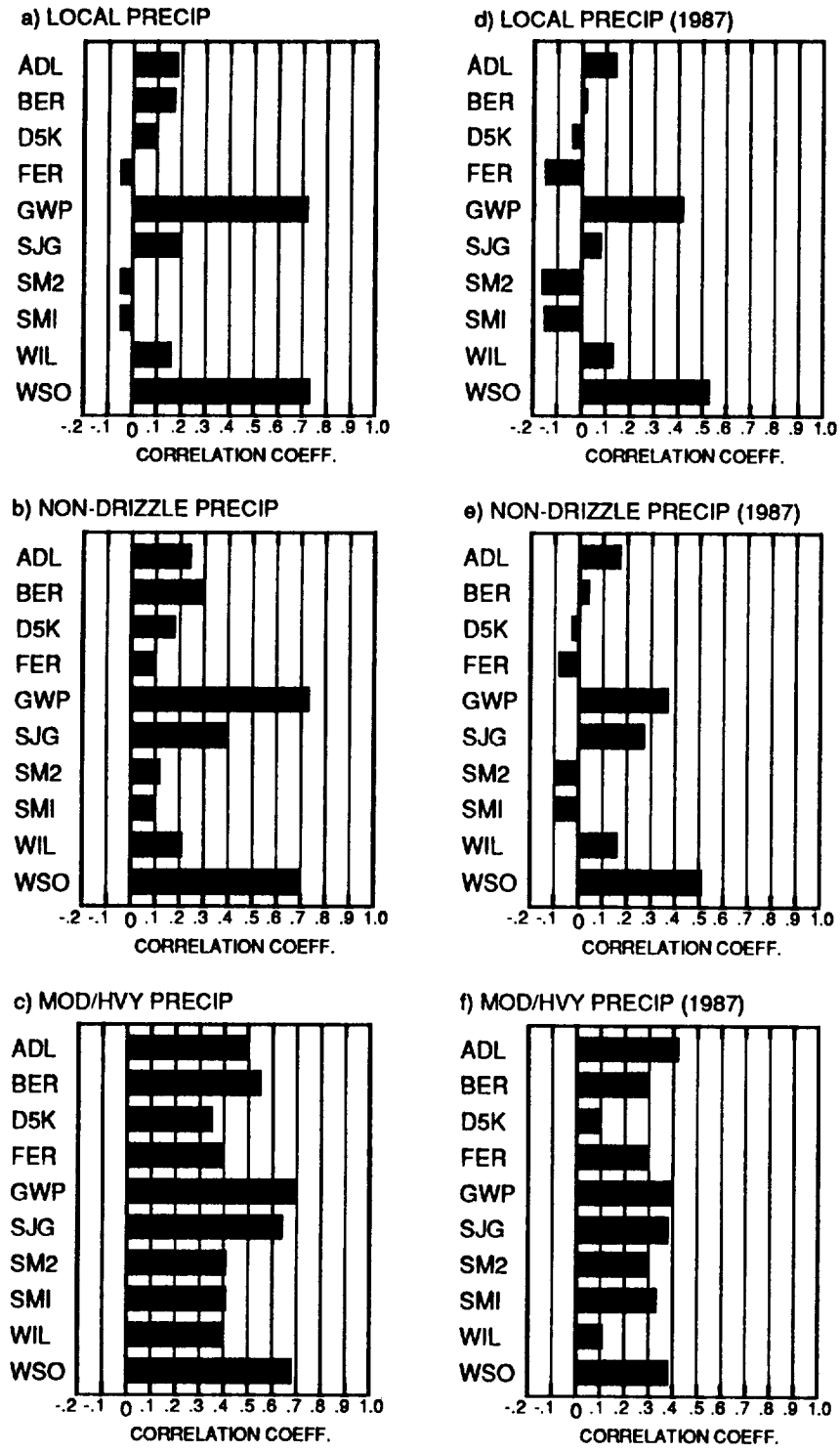

Fig. 8: Correlations between the frequency of thresholded algorithm rainfall and ship-derived precipitation frequencies, pooled over all usable portions of the 6 meridional frequency profiles. Correlation coefficients are presented for both the 34-year period (left column) and for 1987 only (right column).

a specific domain, such as the tropics.

Having normalized, to the extent possible, the global frequencies, an algorithm's ability to correctly reproduce the spatial patterns of oceanic precipitation of various intensities can then be quantified via the spatial correlation coefficient between the algorithm-derived and ship-derived precipitation frequencies, again pooled over all usable portions of the 6 meridional frequency profiles. Correlation coefficients are presented for all algorithms, both for the 34-year period and for 1987 only, in Fig. 8.

With respect to the 34-year climatology, two algorithms — GWP and WSO – stand out as giving the highest correlations, irrespective of intensity threshold. In all cases, both algorithms consistently yield correlation coefficients of $r \approx 0.7$, even for the lightest precipitation intensities (Figs. 8a and 8b), for which all other algorithms give quite poor correlation coefficients. The correlations for all of the latter algorithms improve significantly as the precipitation intensity threshold increases. Nevertheless, even for moderate/heavy precipitation (Fig. 8c), only SJG achieves a correlation coefficient ($r = 0.64$) approaching that of WSO and GWP, while all other algorithms fall in the range $0.35 < r < 0.5$.

With respect to the single-year shipboard precipitation frequencies, overall correlations are invariably lower for all algorithms, probably due both to the greater statistical noisiness of the shipboard frequencies and to the smaller geographic range of usable data. Nevertheless, the difference between GWP and WSO and their nearest competitors remains rather striking for lighter precipitation rates (Figs. 8d and 8e). For these cases, WSO takes the lead with $r \approx 0.5$, while for GWP $r \approx 0.4$. Five algorithms (BER, D5K, FER, SMI, and SM2) yield near-zero or even negative correlations at lighter intensities. For moderate/heavy precipitation, the distinction between ADL, GWP, SJG, and WSO essentially vanishes, as all four algorithms yield $r \approx 0.4$.

5 Discussion

The comparison between satellite and ship precipitation frequencies highlights a two issues that merit further examination: (1) the failure of most algorithms to detect precipitation in the subtropical dry zones, in contrast to the information from the ship-derived climatology suggesting that precipitation does regularly occur there; and (2) the failure of most algorithms to make reasonable estimates of precipitation fraction at high latitudes. These will be considered in turn.

5.1 Lack of high-latitude precipitation

The observed differences in correlation between algorithm precipitation frequencies and shipboard precipitation frequencies are easily explained by the clear failure (Figs. 1–6) of most algorithms to find much precipitation at high latitudes, even precipitation of moderate or greater intensity. The reasons for this failure, and the fact that two algorithms – GWP and WSO – do not appear to share this problem, both merit examination.

Several factors relevant to passive microwave remote sensing distinguish high latitude precipitation from precipitation in middle and low latitudes. The most obvious of these are (1) low total precipitable water, (2) low average freezing level, and (3) the higher likelihood of frozen precipitation at the surface. All of these of course are related to the general cold temperatures associate with polar air masses.

The first of these (low water vapor content) is important because of the influence of water vapor on SSM/I brightness temperatures. Model calculations reveal that the difference between 10 mm of total water vapor at high latitudes and 60 mm of total water vapor in the tropics implies a brightness temperature difference of approximately 39, 60, 73, 25, 45, 41, and 82 K for the 19V, 19H, 22V, 37V, 37H, 85V, and 85H channels of the SSM/I respectively. Regardless of which channels are used in an algorithm, such differences are likely to be significant relative to the signature of light precipitation. If an algorithm has been tuned to retrieve light precipitation in the humid zones of the world, it is not unlikely that it will overlook lighter precipitation at high latitudes, unless the algorithm explicitly accounts for the variable contribution of water vapor to the observed brightness temperatures.

The second and third factors (low freezing level and/or frozen precipitation at the surface) are mainly of importance to those algorithms that depend on an emission signature of precipitation, since it is primarily liquid water that provides this signature, and the vertically integrated liquid water path seen by the SSM/I will be small when the freezing level (and thus the approximate geometric upper limit to the liquid precipitation layer) is low or even at the surface. Thus, an algorithm that relies entirely on emission may fail to see shallow rain in a cold air mass, unless it accounts both for weakness of the water vapor contribution and for the reduced liquid water layer depth.

A scattering-based algorithm might not be expected to suffer from the same problem, since it is predominately sensing the presence of precipitation

size ice particles (grauple, snow aggregates) above the freezing level. Nevertheless, some scattering-based algorithms (e.g., ADL) rely on emission signatures from liquid water at 37 GHz, or some other lower frequency channel, in order to distinguish cold 85.5 GHz brightness temperatures due to the open ocean surface from cold brightness temperatures due to scattering by ice. Therefore, even these algorithms may have difficulty registering the type of shallow, light precipitation that predominates at high latitudes, notwithstanding the possible presence of sufficient ice aloft.

The key factors that are believed to distinguish the GWP and WSO algorithms from the other SSM/I algorithms considered here are that both explicitly compensate for the effects of water vapor on SSM/I brightness temperatures *and* both rely in part on a polarization-corrected 85.5 GHz brightness temperature depression (similar to that of Spencer et al. 1989) that allows scattering by ice to be distinguished even in the absence of significant liquid precipitation.

5.2 Rainfall in subtropical dry zones

Apart from the failure of many algorithms to register much precipitation at high latitudes, the most notable discrepancy between *all* algorithms (except those which registered excessive precipitation virtually everywhere) and the shipboard precipitation climatology was the failure of the former to retrieve any precipitation whatsoever in the subtropical dry zones. By contrast, the ship climatology suggests that, over the 34 year period in question, light (non-drizzle) intensity precipitation occurs in these areas ~3% of the time (e.g., Fig. 2), and even moderate to heavy precipitation is observed ~1% of the time. At the particular longitudes of the PIP-1 latitude-time products, the ship sample is too sparse to permit a direct comparison to be be made for only ASON 1987; however, an examination of neighboring regions within the dry zones (e.g., along the Panama–Punta Arenas shipping lane), for which sampling was adequate, reveals that 1987 was not an anomalously dry year relative to the climatology.

It is significant, however, that the large majority of reports of precipitation in these regions refer not to precipitation at the ship at the time of the observation, but rather to precipitation observed reaching the surface *near* the ship or to rainfall at the ship during the hour preceding the observation time. The implication is that precipitation occurs predominantly in the form of widely scattered, brief showers that are far more likely to be observed in the neighborhood of a ship at a given point in time than to actually be affecting the ship directly. The low-etage cloud type codes most often reported together with past or nearby precipitation are 2, 3, and 8; corresponding (respectively) to cumulus congestus, cumulonimbus calvus (a cumulonimbus tower without a well-defined cirriform top or anvil), and cumulus appearing together with stratocumulus.

Assuming that the above interpretation is correct, it is not surprising that SSM/I rainfall algorithms have difficulty detecting these showers, as the latter's spatial dimensions are undoubtedly much smaller than the 30–60 km resolution of those SSM/I channels used in most emission- or attenuation-based algorithms. Furthermore, neither a scattering-based microwave algorithm nor an infrared satellite technique is likely to respond to the relatively warm tops expected with these showers.

If there is any hope at all of directly sensing precipitation from tradewind cumulus clouds with the SSM/I, it probably lies with the use of the 85.5 GHz channels in an emission- or attenuation-type algorithm, as these channels have both the finest resolution and the highest sensitivity to liquid water, provided only that levels of precipitable water not excessive.

The one algorithm known to the author that uses 85.5 GHz information in anything other than a scattering mode is that of Petty (1994b). Unfortunately, as noted earlier, the GWP product submitted to PIP-1 was based on the first-guess (scattering-based) rain rate field only. It is therefore not yet known whether the full physical algorithm of Petty (1994b) would have had better success at detecting some of the warm-rain showers that appear to predominate in the trade belts.

Acknowledgments

This study was supported by NASA Grant NAGW-3944.

REFERENCES

Arkin, P.A., and P. Xie, 1994: The Global Precipitation Climatology Project: First Algorithm Intercomparison Project. *Bull. Amer. Meteor. Soc.*, **75**, 401–419

Adler, R.F., A.J. Negri, P.R. Keehn, and I.M. Hakkarinen, 1993: Estimation of monthly rainfall over Japan and surrounding waters from a combination of low-orbit microwave and geosynchronous IR data. *J. Appl. Meteor.*, **32**,

335–356

Barrett, E.C., J. Dodge, M. Goodman, J. Janowiak, and E. Smith, 1994a: The First WetNet Intercomparison Project (PIP-1), *Remote Sens. Rev.*, **11**, 49–60

Barrett, E.C., R.F. Adler, K. Arpe, P. Bauer, W. Berg, A. Chang, R. Ferraro, J. Ferriday, S. Goodman, Y. Hong, J. Janowiak, C. Kidd, D. Kniveton, M. Morrissey, W. Olson, G. Petty, B. Rudolf, A. Shibata, E. Smith, R. Spencer, 1994b: The first WetNet Precipitation Intercomparison Project: Interpretation of results. *Remote Sens. Rev.*, **11**, 303–373

Berg, W., and R. Chase, 1992: Determination of mean rainfall from the special sensor microwave/imager (SSM/I) using a mixed lognormal distribution. *J. Atmos. Ocean. Tech.*, **9**, 129–141.

Ferriday, J.G., and S.K. Avery, 1994: Passive microwave remote sensing of rainfall with SSM/I: Algorithm development and implementation. *J. Appl. Meteor.*, **33**, 1587–1596

Hollinger, J., P. Lo, G. Poe, R. Savage, and J. Pierce, 1987: *Special Sensor Microwave/Imager User's Guide,* Naval Research Laboratory, 120 pp.

Kidd, C., and E.C. Barrett, 1990: The use of passive microwave imagery in rainfall monitoring. *Remote Sensing Reviews*, **4**, 415–450

Mugnai, A., E.A. Smith, G.J. Tripoli, 1993: Foundations for physical-statistical precipitation retrieval from passive microwave satellite measurements. Part II: Emission source and generalized weighting function properties of a time dependent cloud-radiation model. *J. Appl. Meteor.*, **23**, 17–39

Petty, G.W., 1994a: Physical retrievals of over-ocean rain rate from multichannel microwave imagery. Part I: Theoretical characteristics of normalized polarization and scattering indices. *Meteorol. Atmos. Phys.*, **54**, 79–100

Petty, G.W., 1994b: Physical retrievals of over-ocean rain rate from multichannel microwave imagery. Part II: Algorithm implementation. *Meteorol. Atmos. Phys.*, **54**, 101–122

Petty, G.W., 1995: Frequencies and characteristics of global oceanic precipitation from shipboard present-weather reports. *Bull. Amer. Meteor. Soc.* (in press)

Simpson, J., R.F. Adler, and G.R. North, 1988: A proposed Tropical Rainfall Measuring Mission (TRMM) satellite. *Bull. Amer. Meteor. Soc.*, **69**, 278–295

Smith, E.A., and A. Mugnai, 1988: Radiative transfer to space through a precipitating cloud at multiple microwave frequencies. Part II: Results and analysis. *J. Appl. Meteor.*, **27**, 1074–1091

Smith, E.A., A. Mugnai, H.J. Cooper, G.J. Tripoli, and X. Xiang, 1992: Foundations for statistical-physical precipitation retrieval from passive microwave satellite measurements. Part I: Brightness-temperature properties of a time-dependent cloud model. *J. Appl. Meteor.*, **31**, 506–531.

Spencer, R.W., H.M. Goodman, and R.E. Hood 1989: Precipitation retrieval over land and ocean with the SSM/I: Identification and characteristics of the scattering signal. *J. Atmos. Ocean. Tech.*, **6**, 254–273

Warren, S.G., C.J. Hahn, J. London, R.M. Chervin, and R.L. Jenne, 1988: *Global Distribution of Total Cloud Cover and Cloud Type Amounts over the Ocean.* National Center for Atmospheric Research Tech. Note NCAR/TN-317+STR, Boulder, CO.

Wilheit, T.T., A.T.C. Chang, M.S.V. Rao, E.B. Rodgers, and J.S. Theon, 1977: A satellite technique for quantitatively mapping rainfall rates over the oceans. *J. Appl. Meteor.*, **16**, 551–560

Wilheit, T.T., A.T.C. Chang, L.S. Chiu, 1991: Retrieval of monthly rainfall indices from microwave radiometric measurements using probability distribution functions. *J. Atmos. Ocean. Tech.*, **8**, 118–136

Wilheit, T., R. Adler, S. Avery, E. Barrett, P. Bauer, W. Berg, A. Chang, J. Ferriday, N. Grody, S. Goodman, C. Kidd, D. Kniveton, C. Kummerow, A. Mugnai, W. Olson, G. Petty, A. Shibata, E. Smith, R. Spencer, 1994: Algorithms for the retrieval of rainfall from passive microwave measurements. *Remote Sens. Rev.*, **11**, 163–194

World Meteorological Organization, 1974: *Manual on Codes, Volume 1.* (WMO Publ. No. 306), WMO, Geneva.

Table 3: Precipitation intensity thresholds (mm h^{-1}) used to match algorithm precipitation frequencies with ship-derived precipitation frequencies for various intensity classes. A missing value implies that the algorithm underestimated the frequency of the class in question, even with a zero intensity threshold.

Algorithm	drizzle	light	moderate/heavy
ADL	-	-	0.6
BER	-	-	1.8
D5K	-	-	0.2
FER	-	-	0.1
GWP	0.0	0.1	1.0
SJG	0.1	0.3	0.9
SMI	-	-	0.4
SM2	-	-	0.9
WIL	0.5	0.8	1.9
WSO	0.2	0.4	1.0